


 Cite this: *RSC Adv.*, 2022, 12, 21621

Design, synthesis, bio-evaluation, and *in silico* studies of some N-substituted 6-(chloro/nitro)-1*H*-benzimidazole derivatives as antimicrobial and anticancer agents†

 Em Canh Pham,^a Tuong Vi Thi Le^b and Tuyen Ngoc Truong^{b,c*}

A new series of 6-substituted 1*H*-benzimidazole derivatives were synthesized by reacting various substituted aromatic aldehydes with 4-nitro-*o*-phenylenediamine and 4-chloro-*o*-phenylenediamine through condensation using sodium metabisulfite as the oxidative reagent. The N-substituted 6-(chloro/nitro)-1*H*-benzimidazole derivatives were prepared from the 6-substituted 1*H*-benzimidazole derivatives and substituted halides using potassium carbonate by conventional methods as well as by exposure to microwave irradiation. Seventy-six 1*H*-benzimidazole derivatives have been synthesized in moderate to excellent yields with the microwave-assisted method (40 to 99%). Compounds **1d**, **2d**, **3s**, **4b**, and **4k** showed potent antibacterial activity against *Escherichia coli*, *Streptococcus faecalis*, MSSA (methicillin-susceptible strains of *Staphylococcus aureus*), and MRSA (methicillin-resistant strains of *Staphylococcus aureus*) with MIC (the minimum inhibitory concentration) ranging between 2 and 16 $\mu\text{g mL}^{-1}$ as compared to ciprofloxacin (MIC = 8–16 $\mu\text{g mL}^{-1}$), in particular compound **4k** exhibits potent fungal activity against *Candida albicans* and *Aspergillus niger* with MIC ranging between 8 and 16 $\mu\text{g mL}^{-1}$ compared with the standard drug fluconazole (MIC = 4–128 $\mu\text{g mL}^{-1}$). In addition, compounds **1d**, **2d**, **3s**, **4b**, and **4k** also showed the strongest anticancer activity among the synthesized compounds against five tested cell lines with IC₅₀ (half-maximal inhibitory concentration) ranging between 1.84 and 10.28 $\mu\text{g mL}^{-1}$, comparable to paclitaxel (IC₅₀ = 1.38–6.13 μM). Furthermore, the five most active compounds showed a good ADMET (absorption, distribution, metabolism, excretion, and toxicity) profile in comparison to ciprofloxacin, fluconazole, and paclitaxel as reference drugs. Molecular docking predicted that dihydrofolate reductase protein from *Staphylococcus aureus* is the most suitable target for both antimicrobial and anticancer activities, and vascular endothelial growth factor receptor 2 and histone deacetylase 6 are the most suitable targets for anticancer activity of these potent compounds.

 Received 6th June 2022
 Accepted 20th July 2022

DOI: 10.1039/d2ra03491c

[rsc.li/rsc-advances](https://rsc-advances.rsc.li)

1. Introduction

Benzimidazole is a naturally occurring bicyclic compound consisting of fused benzene and imidazole rings and is an integral part of the structure of vitamin B12. It is a cyclic ring that has two nitrogens as heteroatoms and is called a heterocyclic aromatic compound. In addition, benzimidazole is a remarkable scaffold of medicinal importance possessing

promising pharmacological activities like anticancer,^{1–4} antimicrobial,^{5–7} anti-inflammation,⁸ antiviral,⁹ anti-hypertensive,¹⁰ antihistamine,¹¹ antitubercular,¹² antiulcer,¹³ analgesic,¹⁴ anthelmintic,¹⁵ antiprotozoal,¹⁶ antiamebic,¹⁷ anticonvulsant,¹⁸ and antiparasitic.¹⁹

Moreover, many important drugs used therapeutically in the research area contain a benzimidazole ring such as antiulcer (omeprazole, lansoprazole, rabeprazole, pantoprazole), antihistamines (astemizole, clemizole, and emedastine), antihypertensives (telmisartan, candesartan, and azilsartan), anthelmintics (thiabendazole, parbendazole, mebendazole, albendazole, cambendazole, and flubendazole), antiviral (maribavir), antidiabetic (rivoglitazone), analgesic (clonitazene), especially antifungal (systemic fungicide, *e.g.* benomyl) and anticancer (antimitotic agent, *e.g.* nocodazole, PAR inhibitor, *e.g.* veliparib) (Fig. 1).²⁰ In addition, the potency of drugs like carbendazim, and dovitinib containing benzimidazole moiety

^aDepartment of Medicinal Chemistry, Faculty of Pharmacy, Hong Bang International University, 700000 Ho Chi Minh City, Vietnam. E-mail: canhem112009@gmail.com; empc@hiu.vn

^bDepartment of Pharmacology – Clinical Pharmacy, Faculty of Pharmacy, City Children's Hospital, 700000 Ho Chi Minh City, Vietnam

^cDepartment of Organic Chemistry, Faculty of Pharmacy, University of Medicine and Pharmacy at Ho Chi Minh City, 700000 Ho Chi Minh City, Vietnam. E-mail: truongtuyen@ump.edu.vn

† Electronic supplementary information (ESI) available: ADMET and Docking Information, and NMR spectra. See <https://doi.org/10.1039/d2ra03491c>



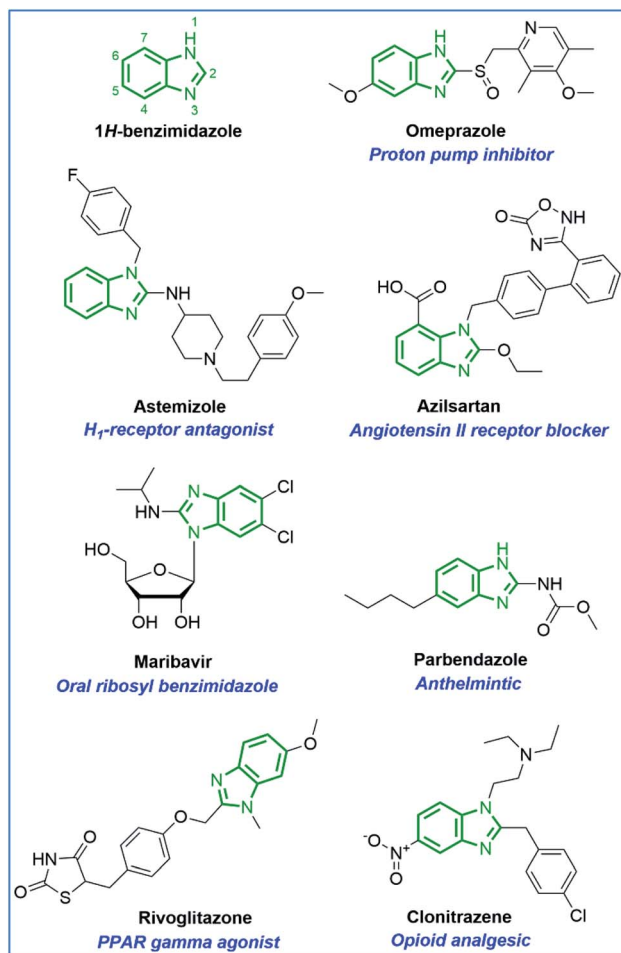


Fig. 1 Marketed 1*H*-benzimidazole ring containing drug compounds.

has been recognized against various types of cancer cell lines.^{21,22}

There are many different synthetic pathways to build the 1*H*-benzimidazole structures with different substituents at positions C-2 and C-5/6. However, the simplest synthesis pathway is the condensation of *o*-phenylenediamines and carboxylic acids (or their derivatives such as nitriles, chlorides, and orthoesters) in the presence of an acid or aldehydes using sodium metabisulfite ($\text{Na}_2\text{S}_2\text{O}_5$).^{3,4} In addition, the N-1 derivatives were synthesized using 1*H*-benzimidazole derivatives and substituted halides in the presence of a base.²³ The highlight of our study is the application of microwaves in the whole synthesis process of 1*H*-benzimidazole derivatives. This is a green chemical method that contributes to environmental protection.

Rationale and structure-based design as antimicrobial and anticancer agents: Structure–activity relationship studies of benzimidazole ring system suggested the N-1, C-2, C-6 positions are very much important for the pharmacological effect.^{24,25} Especially, the N-1 position can increase chemotherapeutic activity when attached to different substituents, for example, benzyl groups similar to clemizole and candesartan drugs. Since N-substitutions in benzimidazole exhibit biologically

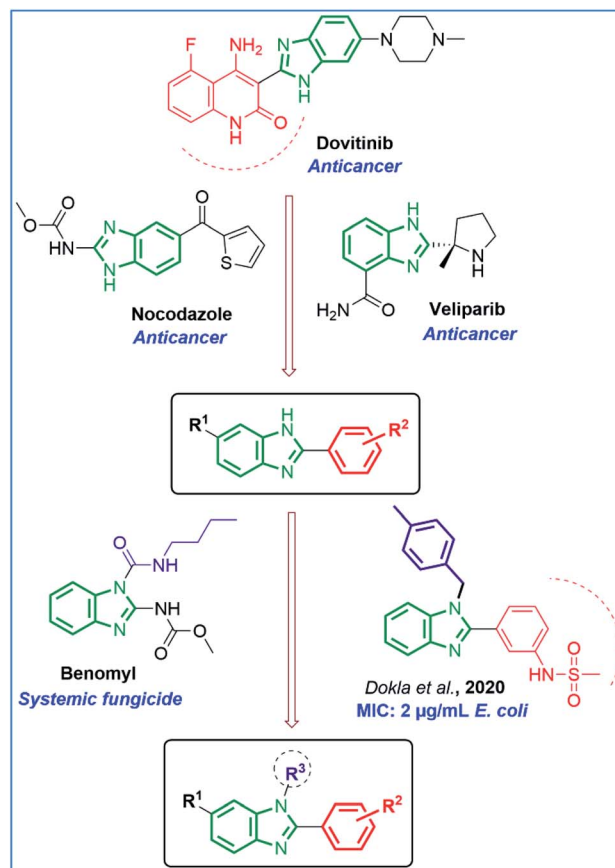


Fig. 2 Rational study design, illustrating the structure of the newly designed N-substituted 6-(chloro/nitro)-1*H*-benzimidazole derivatives with representative examples for antibacterial, antifungal, and anticancer drugs (MIC – minimal inhibitory concentration).

active compounds,^{23,26} we were interested in designing compounds containing them (Fig. 2). Our designed derivatives and anticancer drug dovitinib, antifungal drug benomyl, and antibacterial derivatives of Dokla *et al.*, 2020 (minimal inhibitory concentration (MIC) on *E. Coli* strain at $2 \mu\text{g mL}^{-1}$)²⁷ share three common essential structural features (i) a planar benzimidazole moiety. (ii) Aromatic ring with different substituted groups at the C-2 position. (iii) The different substituted groups at the N-1 position. Moreover, the C-6 position with different substituents such as $-\text{Cl}$ and $-\text{NO}_2$ were designed in order to examine their effects on antimicrobial and anticancer activities.

The mechanism of action of one pharmacological activity is expressed through one or more different receptors.^{28,29} Furthermore, a receptor may also exhibit more than one pharmacological activity. A good example is dihydrofolate reductase (DHFR) which is a potential receptor for both antitumor and antimicrobial activities.^{20,30} Therefore, the *in silico* studies were the potential approach to confirm the ligand–target interaction in many different receptors. In recent years there has been significant progress to improve the receptor flexibility in docking,^{31–33} *in silico* studies are able to rank the compound potency or precisely predict the target after having experimental *in vitro* results.



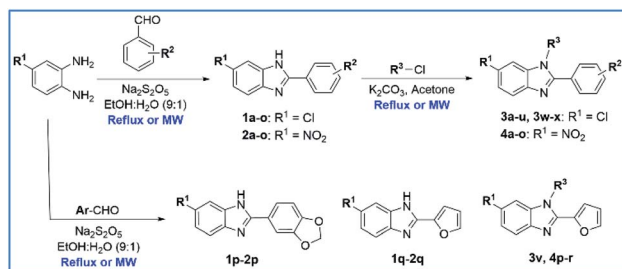
Amoxicillin, norfloxacin, and ciprofloxacin are the most commonly used antibacterial drugs, as well as docetaxel, cyclophosphamide, 5-fluorouracil, and epirubicin are the most commonly used anticancer drugs but are related to severe side effects. Besides, the continued increase in the number of infections caused by bacteria resistant to one or multiple antibiotic classes and cancer resistance is a significant threat and can lead to treatment failure and complications. This has resulted in research and development in search of new antibiotics and anticancer drugs to maintain an effective drug supply at all times.³⁴ It is important to find out newer, safer, and more effective antibiotics and anticancer drugs with multiple effects, especially showing both good anticancer and anti-microbial activities. This is very beneficial for cancer patients due to their weakened immunity and susceptibility to microbial attack.

Therefore, the purpose of this study is to synthesize novel N-substituted 6-(chloro/nitro)-1*H*-benzimidazole derivatives with various substituents at positions N-1, C-2, and C-6, and evaluation of their antibacterial, antifungal, and anticancer activities. The synthesized derivatives will be investigated *in silico* to understand the potential for drug-receptor interaction.

2. Results and discussion

2.1. Chemistry

The benzene-1,2-diamine derivatives with a 4-Cl or 4-NO₂ group are the starting material for the preparation of N-substituted 6-(chloro/nitro)-1*H*-benzimidazole derivatives. The process of synthetic research consists of two steps (Scheme 1). Firstly, a series of 6-substituted 1*H*-benzimidazole derivatives (**1a–1q** and **2a–2q**) have been synthesized by condensing benzene-1,2-diamine derivatives with substituted aromatic aldehydes using conventional heating and microwave-assisted methods. Thirty-four derivatives have been synthesized in good to excellent yields with the reflux method (70 to 91%) and excellent yields with the microwave-assisted method (90 to 99%). The reaction time has been dramatically reduced, as using conventional heating the reaction is carried out in 6–12 h compared with 10–15 min heating in the microwave. In addition, the reaction yield has increased ranging between 7 to 22% with microwave assistance (Table 1). Secondly, a series of N-substituted 6-(chloro/nitro)-1*H*-benzimidazole derivatives (**3a–3x** and **4a–4r**) have been synthesized by reacting 6-substituted 1*H*-benzimidazole derivatives with substituted halides using



Scheme 1 Construction of N-substituted 6-(chloro/nitro)-1*H*-benzimidazole derivatives (MW: microwave irradiation, EtOH: ethanol).

conventional heating and microwave-assisted methods. Compounds **3a–3x** and **4a–4r** showed nearly identical reaction yields. Forty-two derivatives have been synthesized in moderate yields with the reflux method (26 to 43%) and moderate to excellent yields with the microwave-assisted method (40 to 50%). The reaction time also has been dramatically reduced, as using conventional heating the reaction is carried out in 12–24 h compared with 20–60 min heating in the microwave. Furthermore, the reaction yield has increased ranging between 7 to 15% with microwave assistance (Table 2). All compounds have physical-chemical properties of fragments ($M_w < 500$) or lead-like ($M_w < 350$) that follow Lipinski's rules which could lead to potent compounds for further development.^{35,36} Especially, twenty-nine derivatives (**3** and **4**) are new compounds.

IR, ¹H NMR, ¹³C NMR, and mass spectra of the synthesized compounds are in accordance with the assigned structures. The IR spectra of all the synthesized displayed a medium absorbance band in the ν 1535–1374 cm⁻¹ region which is distinctive of the aromatic ring as well as a strong absorbance band in the ν 1646–1505 cm⁻¹ region characteristic of imine (C=N) of imidazole nucleus of 1*H*-benzimidazole derivatives. Compounds **4a–4r** displayed a strong absorbance band in the ν 1355–1215 cm⁻¹ region which is distinctive of the NO₂ group. In addition, ¹H NMR spectra of compounds **1** and **2** indicated the characteristic NH protons of 1*H*-benzimidazole as a singlet in the δ 13.92–12.71 ppm region, as well as the distinctive aromatic proton in the δ 9.00–6.72 ppm region. On the other hand, ¹H NMR spectra of compounds **3** and **4** revealed the appearance of a singlet in the 5.90–4.70 ppm region of methylene (–CH₂–) moiety of allyl (–CH₂–CH=CH₂), 1-(2-ethoxy-2-oxoethyl) (–CH₂COOC₂H₅), and arylmethyl (–CH₂–Ar) groups, as well as the distinctive aromatic proton in the δ 8.80–6.65 ppm region. Furthermore, the C=N group (δ 164.0–145.0 ppm), C_{Ar} (δ 171.5–101.5 ppm), and the methylene moiety of allyl, 1-(2-ethoxy-2-oxoethyl), and arylmethyl groups (δ 57.1–46.1 ppm) were identified in the ¹³C NMR spectrum of compounds **3** and **4**. The molecular ion peak M (m/z) of compounds **1–4** was observed in the mass spectrum, confirming the hypothesized structure.

2.2. *In vitro* antibacterial and antifungal activities

Antimicrobial activities (exhibited by MIC values) including antibacterial activities at two strains of Gram-negative (EC – *Escherichia coli* and PA – *Pseudomonas aeruginosa*) and three strains of Gram-positive (SF – *Streptococcus faecalis*, MSSA, MRSA) and antifungal activities (CA – *Candida albicans* and AN – *Aspergillus niger*) of all synthesized compounds are summarized in Table 3 and 4.

With antimicrobial activities of a series of 6-substituted 1*H*-benzimidazole derivatives, all compounds are totally inactive at the Gram-negative strain PA (MIC $\geq 1024 \mu\text{g mL}^{-1}$). Compounds **1a**, **1c**, **1e–1p**, **2a**, **2c** and **2e–2p** showed weak to moderate activities at 4 strains of bacteria (EC, SF, MSSA, and MRSA) and 2 strains of fungi (MIC $\geq 32 \mu\text{g mL}^{-1}$). Compounds **1b** (6-chloro, 4-chlorophenyl), **1d** (6-chloro, 3,4-dichlorophenyl), **1q** (6-chloro, furan-2-yl), **2d** (6-nitro, 3,4-dichlorophenyl) showed potent antibacterial activities against the Gram-positive



Table 1 Yields and physicochemical parameters of 6-substituted 1*H*-benzimidazole derivatives (1a–1q and 2a–2q)^a

Entry	R group		Code	Physicochemical parameters	Yield		
	R ¹	R ²			Re	MW	
1	6-Cl	2-Cl	1a	<i>M_w</i> : 263.12 NHA: 1 NHD: 1	NRB: 1 LogP: 3.96 TPSA: 28.68	87	96
2	6-Cl	4-Cl	1b	<i>M_w</i> : 263.12 NHA: 1 NHD: 1	NRB: 1 LogP: 4.01 TPSA: 28.68	91	99
3	6-Cl	2,4-Cl ₂	1c	<i>M_w</i> : 297.57 NHA: 1 NHD: 1	NRB: 1 LogP: 4.46 TPSA: 28.68	77	90
4	6-Cl	3,4-Cl ₂	1d	<i>M_w</i> : 297.57 NHA: 1 NHD: 1	NRB: 1 LogP: 4.51 TPSA: 28.68	81	91
5	6-Cl	2-Cl, 6-F	1e	<i>M_w</i> : 281.11 NHA: 2 NHD: 1	NRB: 1 LogP: 4.33 TPSA: 28.68	78	92
6	6-Cl	3,4-(OCH ₃) ₂	1f	<i>M_w</i> : 288.73 NHA: 3 NHD: 1	NRB: 3 LogP: 3.40 TPSA: 47.14	75	90
7	6-Cl	4-OC ₂ H ₅	1g	<i>M_w</i> : 272.73 NHA: 2 NHD: 1	NRB: 3 LogP: 3.80 TPSA: 37.91	76	90
8	6-Cl	3-OC ₂ H ₅ , 4-OH	1h	<i>M_w</i> : 288.73 NHA: 3 NHD: 2	NRB: 3 LogP: 3.40 TPSA: 58.14	79	93
9	6-Cl	4-F	1i	<i>M_w</i> : 246.67 NHA: 2 NHD: 1	NRB: 1 LogP: 3.79 TPSA: 28.68	82	94
10	6-Cl	3-OH	1j	<i>M_w</i> : 244.68 NHA: 2 NHD: 2	NRB: 1 LogP: 3.07 TPSA: 48.91	76	95
11	6-Cl	3-OCH ₃	1k	<i>M_w</i> : 258.70 NHA: 2 NHD: 1	NRB: 2 LogP: 3.47 TPSA: 37.91	75	90
12	6-Cl	3-OH, 4-OCH ₃	1l	<i>M_w</i> : 274.70 NHA: 3 NHD: 2	NRB: 2 LogP: 3.04 TPSA: 58.14	90	98
13	6-Cl	3-NO ₂	1m	<i>M_w</i> : 273.67 NHA: 3 NHD: 1	NRB: 2 LogP: 2.86 TPSA: 74.50	81	97
14	6-Cl	4-NO ₂	1n	<i>M_w</i> : 273.67 NHA: 3 NHD: 1	NRB: 2 LogP: 2.86 TPSA: 74.50	79	96
15	6-Cl	4-N(CH ₃) ₂	1o	<i>M_w</i> : 271.74 NHA: 1 NHD: 1	NRB: 2 LogP: 3.47 TPSA: 31.92	81	93
16	6-Cl		1p	<i>M_w</i> : 272.69 NHA: 3 NHD: 1	NRB: 1 LogP: 3.29 TPSA: 47.14	80	90
17	6-Cl		1q	<i>M_w</i> : 218.64 NHA: 2 NHD: 1	NRB: 1 LogP: 2.82 TPSA: 41.82	83	91
18	6-NO ₂	2-Cl	2a	<i>M_w</i> : 273.67 NHA: 3 NHD: 1	NRB: 2 LogP: 2.90 TPSA: 74.50	84	93
19	6-NO ₂	4-Cl	2b	<i>M_w</i> : 273.67 NHA: 3 NHD: 1	NRB: 2 LogP: 2.94 TPSA: 74.50	88	95
20	6-NO ₂	2,4-Cl ₂	2c	<i>M_w</i> : 308.12 NHA: 3 NHD: 1	NRB: 2 LogP: 3.32 TPSA: 74.50	82	91



Table 1 (Contd.)

Entry	R group		Code	Physicochemical parameters	Yield		
	R ¹	R ²			Re	MW	
21	6-NO ₂	3,4-Cl ₂	2d	M _w : 308.12 NHA: 3 NHD: 1	NRB: 2 LogP: 3.46 TPSA: 74.50	85	96
22	6-NO ₂	2-Cl, 6-F	2e	M _w : 291.66 NHA: 4 NHD: 1	NRB: 2 LogP: 3.23 TPSA: 74.50	81	90
23	6-NO ₂	3,4-(OCH ₃) ₂	2f	M _w : 299.28 NHA: 5 NHD: 1	NRB: 4 LogP: 2.26 TPSA: 92.96	82	97
24	6-NO ₂	4-OC ₂ H ₅	2g	M _w : 283.28 NHA: 4 NHD: 1	NRB: 4 LogP: 2.71 TPSA: 83.73	74	90
25	6-NO ₂	3-OC ₂ H ₅ , 4-OH	2h	M _w : 299.28 NHA: 5 NHD: 2	NRB: 4 LogP: 2.09 TPSA: 103.96	70	92
26	6-NO ₂	4-F	2i	M _w : 257.22 NHA: 4 NHD: 1	NRB: 2 LogP: 2.72 TPSA: 74.50	83	93
27	6-NO ₂	3-OH	2j	M _w : 255.23 NHA: 4 NHD: 2	NRB: 2 LogP: 1.82 TPSA: 94.73	76	94
28	6-NO ₂	3-OCH ₃	2k	M _w : 269.26 NHA: 4 NHD: 1	NRB: 3 LogP: 2.37 TPSA: 83.73	75	92
29	6-NO ₂	3-OH, 4-OCH ₃	2l	M _w : 285.25 NHA: 5 NHD: 2	NRB: 3 LogP: 1.74 TPSA: 103.96	78	90
30	6-NO ₂	3-NO ₂	2m	M _w : 284.23 NHA: 5 NHD: 1	NRB: 3 LogP: 1.64 TPSA: 120.32	83	95
31	6-NO ₂	4-NO ₂	2n	M _w : 284.23 NHA: 5 NHD: 1	NRB: 3 LogP: 1.65 TPSA: 120.32	86	95
32	6-NO ₂	4-N(CH ₃) ₂	2o	M _w : 282.30 NHA: 3 NHD: 1	NRB: 3 LogP: 2.41 TPSA: 77.74	74	91
33	6-NO ₂		2p	M _w : 283.24 NHA: 5 NHD: 1	NRB: 2 LogP: 2.17 TPSA: 92.96	77	92
34	6-NO ₂		2q	M _w : 229.19 NHA: 4 NHD: 1	NRB: 2 LogP: 1.77 TPSA: 87.64	80	91

^a Re and MW – yields of conventional heating (or reflux) and microwave-assisted method (%), Re – reflux, MW – microwave, M_w – molecular weight, NHA – number of hydrogen bond acceptor, NHD – number of hydrogen bond donor, NRB – number rotatable bond, PSA – polar surface area (Angstroms squared).

strains SF, MSSA and MRSA with MIC ranging between 4 to 8 µg mL⁻¹ as compared to ciprofloxacin (Cipro, MIC = 8–16 µg mL⁻¹), but showed moderate activities at the fungi strains CA, and AN (MIC 32–64 µg mL⁻¹) as compared to fluconazole (Flu, MIC of 4 µg mL⁻¹ at CA and 128 µg mL⁻¹ at AN). In addition, these compounds also showed good antibacterial activities against the Gram-negative strain EC with MIC ranging between 8 to 16 µg mL⁻¹. Compound **2b** (6-nitro, 4-chlorophenyl), **2q** (6-nitro, furan-2-yl) showed good antibacterial activities against EC, SF, MSSA, and MRSA with MIC ranging between 8 to 16 µg mL⁻¹ as compared to Cipro and moderate fungal activities

against CA and AN (MIC 32–64 µg mL⁻¹) as compared to Flu. The results suggested that the 4-chloro and 3,4-dichloro groups of the aromatic ring and furan nucleus at position 2 of the 1*H*-benzimidazole scaffold enhanced antibacterial activities against EC, SF, MSSA, and MRSA strains.

With antimicrobial activities of a series of N-substituted 6-(chloro/nitro)-1*H*-benzimidazole derivatives, compounds **3a**, **3e**, **3g–3i**, **3k–3m**, **3o–3q**, **3t–3w**, **4a**, **4c–4e**, **4g–4j** and **4l–4r** showed weak to moderate activities at 5 strains of bacteria and 2 strains of fungi (MIC ≥ 32 µg mL⁻¹). Compounds **3b** (6-chloro, 4-chlorophenyl, *N*-allyl), **3c** (6-chloro, 2,4-dichlorophenyl, *N*-allyl),



Table 2 Yields and physicochemical parameters of N-substituted 6-(chloro/nitro)-1*H*-benzimidazole derivatives (3a–3x and 4a–4r)^a

Entry	R group			Code	Physicochemical parameters	Yield		
	R ¹	R ²	R ³			Re	MW	
1	6-Cl	2-Cl	Allyl	3a	<i>M_w</i> : 303.19 NHA: 1 NHD: 0	NRB: 3 LogP: 4.58 TPSA: 17.82	31	43
2	6-Cl	4-Cl	Allyl	3b	<i>M_w</i> : 303.19 NHA: 1 NHD: 0	NRB: 3 LogP: 4.58 TPSA: 17.82	35	46
3	6-Cl	2,4-Cl ₂	Allyl	3c	<i>M_w</i> : 337.63 NHA: 1 NHD: 0	NRB: 3 LogP: 5.11 TPSA: 17.82	30	41
4	6-Cl	3,4-Cl ₂	Allyl	3d	<i>M_w</i> : 337.63 NHA: 1 NHD: 0	NRB: 3 LogP: 5.11 TPSA: 17.82	36	45
5	6-Cl	3,4-(OCH ₃) ₂	Allyl	3e	<i>M_w</i> : 328.79 NHA: 3 NHD: 0	NRB: 5 LogP: 4.01 TPSA: 36.28	27	40
6	6-Cl	4-OC ₂ H ₅	Allyl	3f	<i>M_w</i> : 312.79 NHA: 2 NHD: 0	NRB: 5 LogP: 4.37 TPSA: 27.05	29	42
7	6-Cl	4-F	Allyl	3g	<i>M_w</i> : 286.73 NHA: 2 NHD: 0	NRB: 3 LogP: 4.36 TPSA: 17.82	36	48
8	6-Cl	3-NO ₂	Allyl	3h	<i>M_w</i> : 313.74 NHA: 3 NHD: 0	NRB: 4 LogP: 3.42 TPSA: 63.64	34	41
9	6-Cl	4-NO ₂	Allyl	3i	<i>M_w</i> : 313.74 NHA: 3 NHD: 0	NRB: 4 LogP: 3.45 TPSA: 63.64	42	50
10	6-Cl	2-Cl	Benzyl	3j	<i>M_w</i> : 353.24 NHA: 1 NHD: 0	NRB: 3 LogP: 5.22 TPSA: 17.82	31	40
11	6-Cl	4-Cl	Benzyl	3k	<i>M_w</i> : 353.24 NHA: 1 NHD: 0	NRB: 3 LogP: 5.30 TPSA: 17.82	41	49
12	6-Cl	2,4-Cl ₂	Benzyl	3l	<i>M_w</i> : 387.69 NHA: 1 NHD: 0	NRB: 3 LogP: 5.78 TPSA: 17.82	35	44
13	6-Cl	3,4-Cl ₂	Benzyl	3m	<i>M_w</i> : 387.69 NHA: 1 NHD: 0	NRB: 3 LogP: 5.79 TPSA: 17.82	38	47
14	6-Cl	3,4-(OCH ₃) ₂	Benzyl	3n	<i>M_w</i> : 378.85 NHA: 3 NHD: 0	NRB: 5 LogP: 4.68 TPSA: 36.28	26	41
15	6-Cl	4-OC ₂ H ₅	Benzyl	3o	<i>M_w</i> : 362.85 NHA: 2 NHD: 0	NRB: 5 LogP: 5.07 TPSA: 27.05	34	43
16	6-Cl	4-F	Benzyl	3p	<i>M_w</i> : 336.79 NHA: 2 NHD: 0	NRB: 3 LogP: 5.08 TPSA: 17.82	33	46
17	6-Cl	3-NO ₂	Benzyl	3q	<i>M_w</i> : 363.80 NHA: 3 NHD: 0	NRB: 4 LogP: 4.15 TPSA: 63.64	37	48
18	6-Cl	4-NO ₂	Benzyl	3r	<i>M_w</i> : 363.80 NHA: 3 NHD: 0	NRB: 4 LogP: 4.13 TPSA: 63.64	40	50
19	6-Cl	4-N(CH ₃) ₂	Benzyl	3s	<i>M_w</i> : 361.87 NHA: 1 NHD: 0	NRB: 4 LogP: 4.76 TPSA: 21.06	27	40
20	6-Cl	4-Cl	2-Chlorobenzyl	3t	<i>M_w</i> : 387.69 NHA: 1 NHD: 0	NRB: 3 LogP: 5.73 TPSA: 17.82	29	42

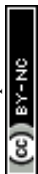


Table 2 (Contd.)

Entry	R group			Code	Physicochemical parameters	Yield		
	R ¹	R ²	R ³			Re	MW	
21	6-Cl	3,4-Cl ₂	4-Chlorobenzyl	3u	<i>M_w</i> : 422.13 NHA: 1 NHD: 0 LogP: 6.29 TPSA: 17.82	NRB: 3	40	49
22	6-Cl		4-Chlorobenzyl	3v	<i>M_w</i> : 343.21 NHA: 2 NHD: 0 LogP: 4.58 TPSA: 30.96	NRB: 3	43	50
23	5-Cl	4-Cl	Benzyl	3w	<i>M_w</i> : 378.85 NHA: 3 NHD: 0 LogP: 4.69 TPSA: 36.28	NRB: 5	35	47
24	5-Cl	3,4-(OCH ₃) ₂	4-Chlorobenzyl	3x	<i>M_w</i> : 387.69 NHA: 1 NHD: 0 LogP: 5.76 TPSA: 17.82	NRB: 3	39	46
25	6-NO ₂	2,4-Cl ₂	Allyl	4a	<i>M_w</i> : 348.18 NHA: 3 NHD: 0 LogP: 3.94 TPSA: 63.64	NRB: 4	35	45
26	6-NO ₂	3,4-Cl ₂	Allyl	4b	<i>M_w</i> : 348.18 NHA: 3 NHD: 0 LogP: 3.99 TPSA: 63.64	NRB: 4	42	49
27	6-NO ₂	3,4-(OCH ₃) ₂	Allyl	4c	<i>M_w</i> : 339.35 NHA: 5 NHD: 0 LogP: 2.90 TPSA: 82.10	NRB: 6	40	48
28	6-NO ₂	4-OC ₂ H ₅	Allyl	4d	<i>M_w</i> : 323.35 NHA: 4 NHD: 0 LogP: 3.24 TPSA: 72.87	NRB: 6	40	47
29	6-NO ₂	4-F	Allyl	4e	<i>M_w</i> : 297.28 NHA: 4 NHD: 0 LogP: 3.22 TPSA: 63.64	NRB: 4	32	44
30	6-NO ₂	4-N(CH ₃) ₂	Allyl	4f	<i>M_w</i> : 322.36 NHA: 3 NHD: 0 LogP: 2.77 TPSA: 66.88	NRB: 5	38	46
31	6-NO ₂	3,4-Cl ₂	4-Chlorobenzyl	4g	<i>M_w</i> : 432.69 NHA: 3 NHD: 0 LogP: 5.10 TPSA: 63.64	NRB: 4	39	49
32	6-NO ₂	3,4-(OCH ₃) ₂	4-Chlorobenzyl	4h	<i>M_w</i> : 423.85 NHA: 5 NHD: 0 LogP: 4.01 TPSA: 82.10	NRB: 6	40	49
33	6-NO ₂	3-OC ₂ H ₅ , 4-OH	4-Chlorobenzyl	4i	<i>M_w</i> : 423.85 NHA: 5 NHD: 1 LogP: 3.92 TPSA: 93.10	NRB: 6	35	43
34	6-NO ₂	3-OH	4-Chlorobenzyl	4j	<i>M_w</i> : 379.80 NHA: 4 NHD: 1 LogP: 3.55 TPSA: 83.87	NRB: 4	32	44
35	6-NO ₂	4-N(CH ₃) ₂	4-Chlorobenzyl	4k	<i>M_w</i> : 406.86 NHA: 3 NHD: 0 LogP: 4.05 TPSA: 66.88	NRB: 5	38	49
36	6-NO ₂	4-Cl	#	4l	<i>M_w</i> : 359.76 NHA: 5 NHD: 0 LogP: 2.85 TPSA: 89.94	NRB: 6	37	46
37	6-NO ₂	4-N(CH ₃) ₂	#	4m	<i>M_w</i> : 368.39 NHA: 5 NHD: 0 LogP: 2.39 TPSA: 93.18	NRB: 7	35	48
38	6-NO ₂	4-F	#	4n	<i>M_w</i> : 343.31 NHA: 6 NHD: 0 LogP: 2.60 TPSA: 89.94	NRB: 6	37	47
39	6-NO ₂	3-O#, 4-OCH ₃	#	4o	<i>M_w</i> : 457.43 NHA: 9 NHD: 0 LogP: 2.51 TPSA: 134.70	NRB: 12	40	48
40	6-NO ₂		Allyl	4p	<i>M_w</i> : 269.26 NHA: 4 NHD: 0 LogP: 2.28 TPSA: 76.78	NRB: 4	36	45



Table 2 (Contd.)

Entry	R group			Code	Physicochemical parameters	Yield		
	R ¹	R ²	R ³			Re	MW	
41	6-NO ₂		4-Chlorobenzyl	4q	M _w : 353.76 NHA: 4 NHD: 0	NRB: 4 LogP: 3.41 TPSA: 76.78	36	48
42	6-NO ₂		#	4r	M _w : 315.28 NHA: 6 NHD: 0	NRB: 6 LogP: 1.72 TPSA: 103.08	37	48

^a (#) - 1-(2-ethoxy-2-oxoethyl) (-CH₂COOC₂H₅), Re and MW - yields of conventional heating (or reflux) and microwave-assisted method (%), Re - reflux, MW - microwave, M_w - molecular weight, NHA - number of hydrogen bond acceptor, NHD - number of hydrogen bond donor, NRB - number rotatable bond, PSA - polar surface area (Angstroms squared).

Table 3 Antimicrobial (MIC, μg mL⁻¹) and anticancer (IC₅₀, μM) activities of synthesized compounds **1a–1q** and **2a–2q**^a

Entry	Code	Antibacterial				Antifungal			Anticancer				RMS
		EC	PA	SF	MSSA	MRSA	CA	AN	HepG2	MDA-MB-231	MCF7	C26	
1	1a	64	—	128	64	128	—	—	73.19 ± 3.71	52.28 ± 2.66	47.89 ± 2.92	37.45 ± 3.03	33.41 ± 2.44
2	1b	16	—	8	8	8	64	64	19.56 ± 1.24	10.32 ± 1.60	17.04 ± 1.71	7.35 ± 0.88	8.33 ± 1.07
3	1c	64	—	64	64	128	512	512	36.74 ± 2.42	30.24 ± 2.70	18.53 ± 1.62	35.29 ± 2.54	19.36 ± 1.72
4	1d	8	—	8	4	8	32	32	5.75 ± 0.83	5.91 ± 0.71	5.05 ± 0.60	8.33 ± 0.75	6.45 ± 0.69
5	1e	128	—	128	64	128	—	—	51.34 ± 3.36	29.70 ± 1.73	>100	35.82 ± 2.35	38.91 ± 2.40
6	1f	64	—	128	128	256	512	512	15.72 ± 1.23	12.09 ± 0.94	17.54 ± 1.15	10.46 ± 0.85	13.60 ± 1.03
7	1g	256	—	256	128	256	—	—	21.68 ± 1.49	23.05 ± 1.21	>100	36.44 ± 2.52	31.37 ± 2.73
8	1h	64	—	64	32	32	512	512	46.51 ± 2.35	40.24 ± 2.19	52.34 ± 2.79	41.23 ± 2.38	35.48 ± 1.99
9	1i	64	—	64	64	128	512	512	64.63 ± 3.02	81.29 ± 3.50	34.73 ± 2.48	75.20 ± 3.84	28.17 ± 1.45
10	1j	64	—	64	32	64	256	256	29.04 ± 1.78	22.39 ± 1.32	34.59 ± 1.93	22.18 ± 1.65	31.07 ± 1.95
11	1k	128	—	128	128	256	256	256	17.89 ± 1.92	10.44 ± 1.64	37.55 ± 2.39	14.62 ± 1.75	23.84 ± 1.79
12	1l	64	—	64	64	128	512	512	28.09 ± 2.53	37.46 ± 2.97	44.81 ± 3.03	32.73 ± 1.95	41.43 ± 2.21
13	1m	128	—	128	32	64	—	—	55.08 ± 3.12	>100	26.36 ± 1.70	64.47 ± 2.67	28.82 ± 1.50
14	1n	64	—	64	32	64	256	256	8.91 ± 1.02	7.37 ± 1.41	10.22 ± 0.98	8.16 ± 1.14	11.92 ± 1.05
15	1o	64	—	64	64	128	128	128	18.50 ± 1.43	10.61 ± 1.34	12.78 ± 1.01	20.38 ± 1.76	16.04 ± 1.65
16	1p	128	—	64	64	128	512	512	56.11 ± 3.02	62.35 ± 2.81	33.47 ± 3.23	63.34 ± 3.01	36.60 ± 2.92
17	1q	8	—	8	4	8	32	32	52.63 ± 2.43	74.62 ± 2.53	54.65 ± 3.35	28.39 ± 2.17	47.05 ± 2.28
18	2a	64	—	128	64	64	—	—	63.24 ± 3.19	36.88 ± 2.74	>100	55.73 ± 3.41	42.03 ± 2.54
19	2b	16	—	16	8	8	32	32	16.64 ± 1.36	11.25 ± 1.52	41.68 ± 3.83	8.04 ± 0.84	9.87 ± 1.19
20	2c	64	—	64	64	128	256	256	25.05 ± 1.87	33.50 ± 1.69	30.08 ± 1.78	16.78 ± 0.98	22.74 ± 1.95
21	2d	8	—	8	8	8	32	32	5.32 ± 0.80	3.64 ± 0.68	6.41 ± 0.57	7.36 ± 0.79	6.02 ± 0.66
22	2e	64	—	128	64	128	512	512	51.34 ± 3.36	29.70 ± 1.73	>100	>100	38.91 ± 2.40
23	2f	64	—	128	128	128	512	512	23.86 ± 1.62	>100	36.64 ± 1.56	27.94 ± 1.44	30.39 ± 2.22
24	2g	256	—	256	128	256	—	—	24.93 ± 1.38	29.70 ± 1.51	>100	44.63 ± 2.83	34.74 ± 1.96
25	2h	64	—	64	64	64	256	256	66.28 ± 3.12	52.84 ± 2.10	>100	42.78 ± 2.77	47.66 ± 2.08
26	2i	64	—	64	64	128	—	—	28.36 ± 1.35	31.32 ± 1.33	44.16 ± 1.94	38.49 ± 1.87	40.27 ± 1.74
27	2j	64	—	64	32	32	128	128	42.56 ± 1.76	>100	49.91 ± 2.03	36.27 ± 1.43	31.13 ± 1.85
28	2k	128	—	128	128	256	256	256	64.53 ± 2.24	>100	84.91 ± 4.31	26.12 ± 1.38	55.49 ± 2.63
29	2l	64	—	64	64	128	256	256	76.85 ± 3.16	>100	>100	>100	47.79 ± 2.44
30	2m	128	—	64	32	64	512	512	58.91 ± 2.65	>100	83.57 ± 4.08	13.44 ± 0.89	34.09 ± 1.98
31	2n	64	—	64	32	64	512	512	8.91 ± 1.02	7.37 ± 1.41	10.22 ± 0.98	8.16 ± 1.14	11.92 ± 1.05
32	2o	64	—	64	32	64	128	128	23.45 ± 1.84	47.02 ± 2.60	10.36 ± 1.25	19.53 ± 1.58	21.09 ± 1.36
33	2p	128	—	64	64	128	—	—	64.25 ± 3.50	66.22 ± 2.77	41.83 ± 3.05	68.20 ± 2.71	39.53 ± 2.85
34	2q	16	—	8	8	16	64	64	90.14 ± 4.07	>100	>100	>100	87.42 ± 4.21
35	Cipro	16	16	8	8	16	ND	ND	ND	ND	ND	ND	ND
36	Flu	ND	ND	ND	ND	ND	4	128	ND	ND	ND	ND	ND
37	PTX	ND	ND	ND	ND	ND	ND	ND	4.75 ± 0.67	1.38 ± 0.42	2.35 ± 0.51	6.13 ± 0.83	3.32 ± 0.55

^a -: MIC ≥ 1024 μg mL⁻¹, ND - not determined, EC - *Escherichia coli* ATCC 25922, PA - *Pseudomonas aeruginosa* ATCC 27853, SF - *Streptococcus faecalis* ATCC 29212, MSSA - Methicillin-susceptible strains of *Staphylococcus aureus* ATCC 29213, MRSA - Methicillin-resistant strains of *Staphylococcus aureus* ATCC 43300, CA - *Candida albicans* ATCC 10321, AN - *Aspergillus niger* ATCC 16404, Cipro - ciprofloxacin, Flu - fluconazole, MIC (μg mL⁻¹) ± 0.5 μg mL⁻¹, PTX - paclitaxel, HepG2 - human hepatocyte carcinoma cell line, MDA-MB-231 - human breast adenocarcinoma cell line, MCF7 - human breast cancer cell line, C26 - colon carcinoma cell line, RMS - human rhabdomyosarcoma cell line. IC₅₀ ± SEM (μM, SEM - standard error of the mean). The values in bold highlight the best compounds with the best MIC and IC₅₀ values compared to positive controls.



Table 4 Antimicrobial (MIC, $\mu\text{g mL}^{-1}$) and anticancer (IC₅₀, μM) activities of synthesized compounds **3a–3x** and **4a–4r**^a

Entry	Code	Antibacterial				Antifungal			Anticancer				
		EC	PA	SF	MSSA	MRSA	CA	AN	HepG2	MDA-MB-231	MCF7	C26	RMS
1	3a	128	—	128	32	64	512	512	25.92 ± 2.13	25.33 ± 1.91	21.27 ± 1.63	33.50 ± 2.30	65.50 ± 3.04
2	3b	16	—	16	16	32	64	64	35.59 ± 2.74	32.52 ± 1.96	54.24 ± 2.35	9.59 ± 0.82	11.17 ± 2.62
3	3c	8	512	16	16	16	64	64	35.03 ± 1.48	30.44 ± 2.21	22.68 ± 1.86	10.68 ± 0.84	66.35 ± 3.18
4	3d	16	256	16	8	8	32	32	32.40 ± 1.71	48.52 ± 1.80	61.78 ± 3.12	35.86 ± 1.93	51.11 ± 2.55
5	3e	128	—	64	64	64	256	256	44.59 ± 2.78	28.15 ± 1.44	47.03 ± 2.36	26.14 ± 1.51	32.26 ± 1.62
6	3f	16	—	16	8	8	32	32	25.58 ± 1.53	28.91 ± 1.76	40.64 ± 2.38	47.60 ± 2.29	16.76 ± 0.99
7	3g	128	512	128	128	256	256	256	25.63 ± 1.46	22.60 ± 1.37	58.11 ± 2.71	30.54 ± 1.84	51.95 ± 2.20
8	3h	128	—	64	64	64	512	512	68.37 ± 3.49	29.98 ± 1.60	25.89 ± 1.65	34.67 ± 1.77	32.49 ± 2.33
9	3i	64	—	64	32	64	128	128	12.91 ± 0.62	13.26 ± 0.58	10.48 ± 0.56	8.65 ± 0.70	9.73 ± 0.53
10	3j	16	512	16	16	16	64	64	48.86 ± 2.24	27.74 ± 1.74	31.16 ± 2.03	9.86 ± 0.89	35.22 ± 1.66
11	3k	64	—	128	32	32	—	—	30.87 ± 2.38	29.07 ± 1.63	>100	42.43 ± 1.87	43.77 ± 2.78
12	3l	64	512	64	64	64	256	256	32.16 ± 1.38	24.33 ± 1.31	29.63 ± 1.65	21.49 ± 1.82	20.65 ± 1.43
13	3m	64	—	64	32	32	128	128	36.77 ± 2.40	48.77 ± 3.34	23.22 ± 1.37	26.99 ± 1.56	57.39 ± 3.29
14	3n	16	256	16	4	8	64	64	26.60 ± 1.36	19.19 ± 1.42	23.19 ± 2.38	14.91 ± 0.88	28.16 ± 2.43
15	3o	64	—	64	64	64	—	—	42.76 ± 2.58	46.65 ± 3.06	29.19 ± 1.30	38.16 ± 2.41	36.60 ± 1.47
16	3p	64	256	64	32	64	32	32	25.25 ± 1.65	24.60 ± 2.09	37.84 ± 1.78	28.97 ± 1.68	52.86 ± 3.23
17	3q	64	—	64	32	64	—	—	86.12 ± 3.67	79.77 ± 4.02	27.35 ± 1.59	23.39 ± 1.61	>100
18	3r	64	—	64	16	32	256	256	18.74 ± 1.47	22.61 ± 1.13	17.36 ± 1.52	14.05 ± 0.92	16.34 ± 1.07
19	3s	8	128	8	4	4	32	32	6.85 ± 0.88	6.45 ± 1.23	10.09 ± 0.97	5.50 ± 1.01	3.68 ± 0.95
20	3t	64	—	64	64	64	64	64	87.74 ± 3.11	51.01 ± 2.45	47.45 ± 1.96	15.77 ± 1.33	68.33 ± 2.36
21	3u	64	128	64	32	64	128	128	61.25 ± 3.36	54.06 ± 2.91	44.38 ± 2.67	34.62 ± 3.55	32.79 ± 3.02
22	3v	128	—	128	128	128	256	256	53.27 ± 2.45	48.06 ± 3.79	31.23 ± 1.75	26.93 ± 1.80	34.65 ± 2.03
23	3w	64	—	64	32	32	512	512	39.32 ± 1.48	36.29 ± 1.51	40.27 ± 2.11	34.70 ± 1.69	30.09 ± 1.46
24	3x	16	128	16	8	8	32	32	40.94 ± 1.63	31.55 ± 1.24	38.42 ± 2.04	29.85 ± 1.72	32.32 ± 1.52
25	4a	32	—	32	32	32	64	64	37.48 ± 2.37	33.61 ± 1.59	>100	37.19 ± 1.36	31.90 ± 1.33
26	4b	16	—	16	8	8	32	32	7.97 ± 0.78	8.58 ± 0.76	10.28 ± 1.22	9.25 ± 0.87	9.88 ± 0.84
27	4c	128	—	64	64	128	512	512	67.98 ± 3.14	59.05 ± 2.87	>100	42.81 ± 2.25	46.11 ± 2.35
28	4d	64	—	64	32	64	—	—	36.48 ± 2.47	40.32 ± 1.90	47.58 ± 2.34	89.91 ± 3.79	54.02 ± 2.22
29	4e	128	—	128	128	256	256	256	39.36 ± 2.47	30.16 ± 1.54	25.96 ± 1.18	43.38 ± 2.01	26.97 ± 1.60
30	4f	32	—	32	16	32	64	64	13.32 ± 0.85	15.90 ± 1.04	18.92 ± 1.37	10.98 ± 0.94	11.83 ± 0.94
31	4g	64	128	64	32	64	128	128	65.32 ± 2.95	47.24 ± 2.68	51.23 ± 2.37	29.71 ± 1.76	23.31 ± 1.80
32	4h	64	—	64	64	64	256	256	33.84 ± 1.96	39.01 ± 1.60	40.18 ± 2.03	25.40 ± 1.70	27.73 ± 2.23
33	4i	64	—	64	64	64	256	256	48.64 ± 1.83	27.43 ± 1.47	21.04 ± 1.21	41.12 ± 2.33	32.73 ± 1.39
34	4j	64	—	64	64	64	512	512	53.09 ± 2.31	36.42 ± 1.77	28.13 ± 1.34	26.85 ± 2.04	37.54 ± 1.55
35	4k	4	64	4	2	4	8	16	1.84 ± 0.62	3.11 ± 0.58	4.10 ± 0.56	3.74 ± 0.70	2.45 ± 0.53
36	4l	128	—	128	128	256	512	512	65.97 ± 3.65	>100	54.88 ± 2.35	60.05 ± 3.14	56.38 ± 2.47
37	4m	32	—	64	32	64	256	256	78.83 ± 3.13	>100	46.73 ± 2.33	53.49 ± 2.08	49.50 ± 2.26
38	4n	128	—	128	128	256	—	—	88.05 ± 3.49	>100	73.25 ± 3.29	58.37 ± 1.86	45.58 ± 2.36
39	4o	64	—	128	64	128	512	512	>100	>100	78.34 ± 3.51	61.78 ± 3.42	64.45 ± 3.30
40	4p	64	—	128	64	128	256	256	42.33 ± 1.77	33.64 ± 1.65	49.10 ± 2.42	74.19 ± 2.47	37.62 ± 1.81
41	4q	64	—	64	64	128	256	256	39.17 ± 1.24	42.90 ± 1.98	>100	>100	31.25 ± 1.84
42	4r	64	—	128	64	128	512	512	>100	>100	80.11 ± 3.64	56.88 ± 3.35	67.72 ± 3.57
43	Cipro	16	16	8	8	16	ND	ND	ND	ND	ND	ND	ND
44	Flu	ND	ND	ND	ND	ND	4	128	ND	ND	ND	ND	ND
45	PTX	ND	ND	ND	ND	ND	ND	ND	4.75 ± 0.67	1.38 ± 0.42	2.35 ± 0.51	6.13 ± 0.83	3.32 ± 0.55

^a -: MIC $\geq 1024 \mu\text{g mL}^{-1}$, ND - not determined, EC - *Escherichia coli* ATCC 25922, PA - *Pseudomonas aeruginosa* ATCC 27853, SF - *Streptococcus faecalis* ATCC 29212, MSSA - Methicillin-susceptible strains of *Staphylococcus aureus* ATCC 29213, MRSA - Methicillin-resistant strains of *Staphylococcus aureus* ATCC 43300, CA - *Candida albicans* ATCC 10321, AN - *Aspergillus niger* ATCC 16404, Cipro - ciprofloxacin, Flu - fluconazole, MIC ($\mu\text{g mL}^{-1}$) $\pm 0.5 \mu\text{g mL}^{-1}$. PTX - paclitaxel, HepG2 - human hepatocyte carcinoma cell line, MDA-MB-231 - human breast adenocarcinoma cell line, MCF7 - human breast cancer cell line, C26 - colon carcinoma cell line, RMS - human rhabdomyosarcoma cell line. IC₅₀ \pm SEM (μM , SEM - standard error of the mean). The values in bold highlight the best compounds with the best MIC and IC₅₀ values compared to positive controls.

3j (6-chloro, 2-chlorophenyl, *N*-benzyl) **3r** (6-chloro, 4-nitrophenyl, *N*-benzyl), and **4f** (6-nitro, *N,N*-dimethylaminophenyl, *N*-allyl) showed good antibacterial activities against Gram-positive strain MSSA with MIC of $16 \mu\text{g mL}^{-1}$ but showed weak to moderate activities at PA, CA and AN with MIC $\geq 32 \mu\text{g mL}^{-1}$. Compounds **3c** and **3j** also showed good antibacterial

activities against three bacteria strains EC, SF, and MRSA with MIC ranging between 8 to $16 \mu\text{g mL}^{-1}$ as compared to Cipro. Compounds **3b** showed good antibacterial activities against EC with MIC of $16 \mu\text{g mL}^{-1}$ while showed moderate antibacterial activities against MRSA with MIC of $32 \mu\text{g mL}^{-1}$. Besides, compounds **3d** (6-chloro, 3,4-dichlorophenyl, *N*-allyl), **3f** (6-



chloro, 4-ethoxyphenyl, *N*-allyl), **3n** (6-chloro, 3,4-dimethoxyphenyl, *N*-benzyl), **3x** (5-chloro, 3,4-dimethoxyphenyl, *N*-(4-chlorobenzyl)), and **4b** (6-nitro, 3,4-dichlorophenyl, *N*-allyl) showed good antibacterial activities at Gram-positive strains MSSA and MRSA with MIC ranging between 4 to 8 $\mu\text{g mL}^{-1}$, strains EC and SF with MIC value at 16 $\mu\text{g mL}^{-1}$, and strain AN with MIC value at 32 $\mu\text{g mL}^{-1}$. However, these compounds showed weak to moderate activities at PA and CA (MIC \geq 32 $\mu\text{g mL}^{-1}$) as compared to Cipro and Flu. Moreover, compounds **3s** (6-chloro, *N,N*-dimethylaminophenyl, *N*-benzyl), and **4k** (6-chloro, *N,N*-dimethylaminophenyl, *N*-(4-chlorobenzyl)) exhibited the strongest activity among the synthesized compounds against the Gram-positive strains MSSA and MRSA with MIC ranging between 2 to 4 $\mu\text{g mL}^{-1}$ and strains EC and SF with MIC ranging between 4 to 8 $\mu\text{g mL}^{-1}$ as compared to Cipro (MIC = 8–16 $\mu\text{g mL}^{-1}$), but showed weak activity at PA. In particular, compound **4k** also showed potent fungal activities against CA and AN with MIC of 8 and 16 $\mu\text{g mL}^{-1}$, respectively as compared to Flu (MIC of 4 $\mu\text{g mL}^{-1}$ at CA and 128 $\mu\text{g mL}^{-1}$ at AN). From the structure–activity relationship (SAR), the presence of the *N,N*-dimethylamino ($-\text{N}(\text{CH}_3)_2$) group in the aromatic ring at position 2 and chloro/nitro group at position 6 of the 1*H*-benzimidazole scaffold is more desirable for enhanced antibacterial and antifungal activities in **3s** and **4k** (Fig. 3).

In published studies, the 5,6-dichloro-1*H*-benzimidazole derivative with 4-fluoro and 4-chloro substituent on the phenyl ring or *N*-cyclopentyl and 4-benzyloxy on the phenyl ring exhibited the potent antibacterial activity with MIC 3.12 mg mL^{-1} against *S. aureus*.⁵ In addition, the 1*H*-benzimidazole-5-carbohydrazide derivative with a 4-nitro substituent on the phenyl ring showed good inhibitory activity against lanosterol 14 α -demethylase (CYP51) with IC_{50} value at 0.19 $\mu\text{g mL}^{-1}$ compared to fluconazole as reference IC_{50} value at 0.62 $\mu\text{g mL}^{-1}$.³⁷ The pyridin-3-yl-1*H*-benzimidazole-5-carboxylate derivative was found to be the potent active with MIC of 0.112 μM against *Mycobacterium tuberculosis* H37Rv and 6.12 μM against INH-resistant *Mycobacterium tuberculosis*, respectively.³⁸ Especially, the 6-fluoro-1*H*-benzimidazole derivative showed potent antibacterial activities against the Gram-positive strains MSSA and MRSA with MIC of 4 and 2–8 $\mu\text{g mL}^{-1}$, respectively.⁷ Some of our synthesized compounds (**3s** and **4k**) also exhibited potential antibacterial activity with MICs of 2–4 $\mu\text{g mL}^{-1}$ against MSSA and MRSA when compared with compounds of Tunçbilek *et al.* (2009) and Malasala *et al.* (2021).^{5,7} This may be due to the

structure of compound **3s** and **4k** with the presence of *N,N*-dimethylamino group at position 4 on the phenyl ring of the 1*H*-benzimidazole nucleus has shown a similar role to the 4-chloro/4-nitro group that of Tunçbilek *et al.* (2009) and Morcoss *et al.* (2020).^{5,37}

2.3. Anticancer activity

The synthesized compounds **1a–1q**, **2a–2q**, **3a–3x**, and **4a–4r** were also tested for their potent anticancer activity using MTT assay against hepatocellular carcinoma cell line (HepG2), human breast cancer cell line (MDA-MB-231 and MCF7), colon carcinoma cell line (C26) and the aggressive and highly malignant rhabdomyosarcoma cell line (RMS) using paclitaxel (PTX) as a non-selective positive control. The results are summarized in Table 3 and 4

In both series of 1*H*-benzimidazole derivatives, fifty-six compounds **1a**, **1c**, **1e**, **1g–1j**, **1l–1m**, **1p–1q**, **2a**, **2c**, **2e–2l**, **2p–2q**, **3a**, **3d–3h**, **3k–3m**, **3o–3q**, **3t–3x**, **4a**, **4c–4j**, and **4l–4r** exhibited moderate activity (IC_{50} = 15.0–50.0 μM) or weak activity (IC_{50} > 50 μM) toward HepG2, MDA-MB-231, MCF7, RMS, and C26. Compounds **1b**, **1f**, and **2b** showed good anticancer activity against the MDA-MB-231, C26, and RMS cell lines with IC_{50} ranging between 7.35 to 13.60 μM as compared to PTX (IC_{50} = 1.38–6.13 μM) and weak to moderate anticancer activities against HepG2 and MCF7 cell lines (IC_{50} > 15.0 μM). Compound **1k** showed good anticancer activity against the MDA-MB-231 and C26 cell lines with IC_{50} values at 10.44 and 14.62 μM , respectively but exhibited weak moderate anticancer activities against HepG2, MCF7, and RMS cell lines (IC_{50} = 17.89–37.55 μM). Compound **1o** showed good anticancer activity against the MDA-MB-231 and MCF7 cell lines with IC_{50} values at 10.61 and 12.78 μM , respectively, and weak moderate anticancer activities against HepG2, C26, and RMS cell lines with IC_{50} ranging between 16.04 to 20.38 μM . Besides, compound **3b** showed good anticancer activity against the C26 and RMS cell lines with IC_{50} values at 9.59 and 11.17 μM , respectively but exhibited weak moderate anticancer activities against HepG2, MDA-MB-231, and MCF7 cell lines (IC_{50} = 32.52–54.24 μM). On the other hand, some compounds showed good anticancer activity at only one cell line such as compounds **2m**, **3c**, **3j**, **3n**, and **3r** against C26 and **2o** against MCF7 with IC_{50} ranging between 9.86 to 14.91 μM as compared to PTX. Particularly, eight compounds **1d** (6-chloro, 3,4-dichlorophenyl), **1n** (6-chloro, 4-nitrophenyl), **2d** (6-nitro, 3,4-dichlorophenyl), **2n** (6-nitro, 4-nitrophenyl), **3i** (6-chloro, 4-nitrophenyl, *N*-allyl), **3s** (6-chloro, *N,N*-dimethylaminophenyl, *N*-benzyl), **4b** (6-nitro, 3,4-dichlorophenyl, *N*-allyl), and **4k** (6-chloro, *N,N*-dimethylaminophenyl, *N*-(4-chlorobenzyl)) showed the strongest anticancer activity among the synthesized compounds against all tested cell lines with IC_{50} ranging between 1.84 to 13.26 $\mu\text{g mL}^{-1}$ comparable to PTX (IC_{50} = 1.38–6.13 μM). Moreover, compound **4k** showed the strongest anticancer activity among all active compounds against HepG2, MDA-MB-231, MCF7, RMS, and C26 with IC_{50} of 1.84, 3.11, 4.10, 3.74, and 2.45 μM , respectively as compared to PTX. Compound **4k** exhibited a weaker anticancer activity than PTX on the MCF7 cell line but exhibited

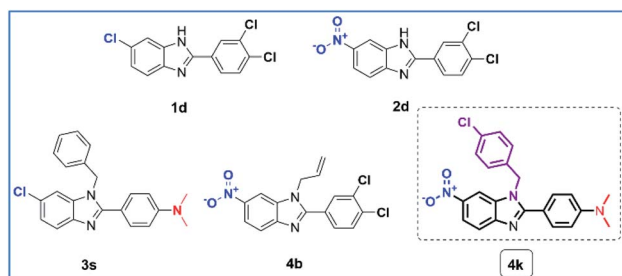


Fig. 3 The structure of potentially active 1*H*-benzimidazole derivatives.



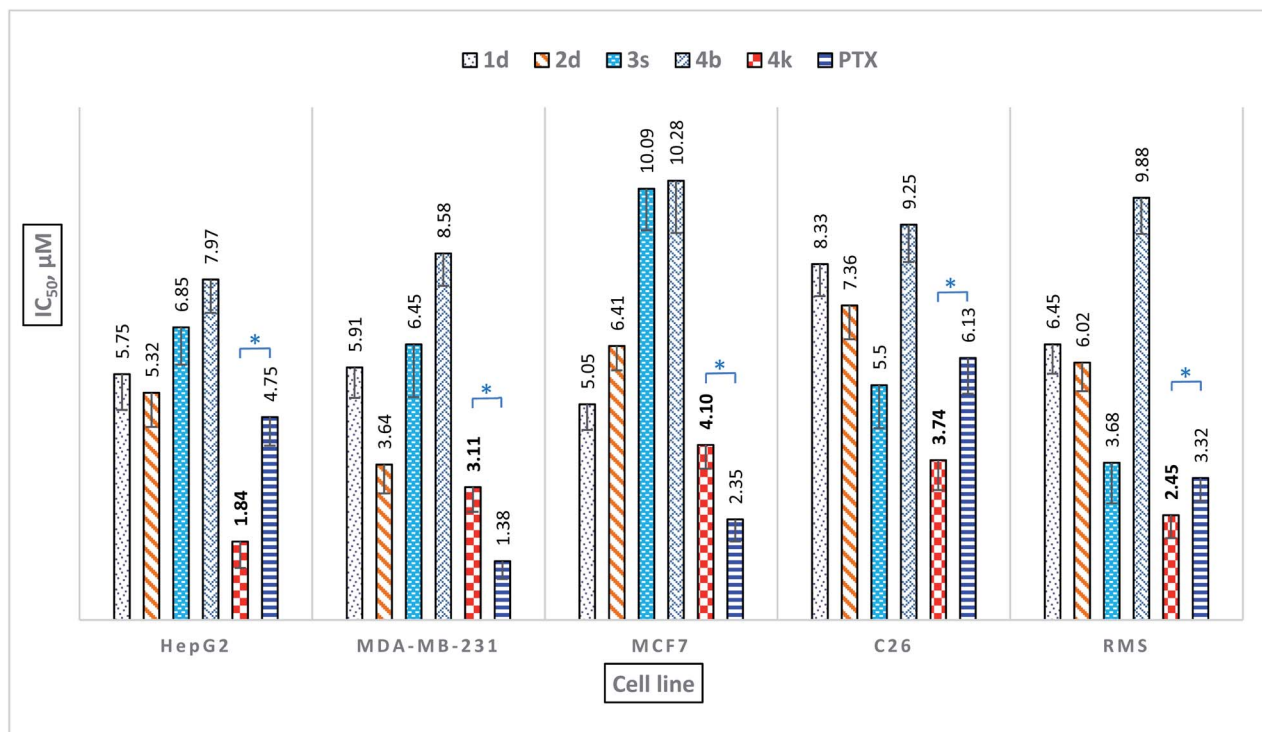


Fig. 4 Comparison of anticancer activity (IC_{50} values) between standard and synthesized compounds. (PTX – paclitaxel, HepG2 – human hepatocyte carcinoma cell line, MDA-MB-231 – human breast adenocarcinoma cell line, MCF7 – human breast cancer cell line, C26 – colon carcinoma cell line, RMS – human rhabdomyosarcoma cell line, (*) – significantly different compared with IC_{50} of 4k and paclitaxel with $p < 0.05$).

better anticancer activity than PTX on HepG2, MDA-MB-231, C26, and RMS cell lines (Fig. 4), and especially also showed the strongest antimicrobial activities (Table 4). Target engagement with electron-donating substituent 4- $N(CH_3)_2$ on the phenyl ring and N -(4-chlorobenzyl) substituent of 1*H*-benzimidazole scaffold may be responsible for its anticancer activity as compared to other compounds.

In published studies with similar structures, the 6-benzoyl-1*H*-benzimidazole derivative with a 3-hydroxy substituent on the phenyl ring was found to be a potent multi-cancer inhibitor against human lung adenocarcinoma epithelial (A549), MDA-MB-231, and human prostate cancer (PC3) cell lines with IC_{50} values 4.47, 4.68, and 5.50 $\mu g mL^{-1}$, respectively.⁴ Besides, the 2,6-disubstituted benzoimidazolyl quinazolinamine derivative with a 4-fluoro substituent on the phenyl ring was found to be potent against tyrosine-protein kinase Met (c-Met) and vascular endothelial growth factor receptor 2 (VEGFR-2) with IC_{50} of 0.05 μM and 0.02 μM respectively.³⁹ In addition, the 2,6-disubstituted benzimidazole-oxindole conjugate derivative with 3,5-difluoro substituent on the phenyl ring showed 43.7% and 64.8% apoptosis against MCF-7, respectively, at 1 and 2 μM concentrations.⁴⁰ The presence of the halogen groups of our active 1*H*-benzimidazole derivatives (1d, 2d, and 4b) is the similarity to the reported potent compounds.

On the other hand, the N ,2,5-trisubstituted 1*H*-benzimidazole derivative with N -phenyl group and 4-dimethylamino on the phenyl ring showed Sirtuins inhibitory activity for SIRT1 ($IC_{50} = 54.21 \mu M$) and for SIRT2 ($IC_{50} = 26.85 \mu M$). Cell

proliferation assay demonstrated that this compound had pronounced antitumor activity against three different types of cancer cells (breast MDA-MB-468, colon HCT-116, and blood-leukemia CCRF-CEM).⁴¹ Moreover, the N ,2,5-trisubstituted 1*H*-benzimidazole derivative with N -(3-phenylpropyl) group showed good antitumor activity against MCF7 cell line with IC_{50} value at $5.73 \pm 0.95 \mu M$ and induces obvious autophagy in MCF7 cells by fluorescence microscope assays and western blot analysis.⁴² The 5-chloro- N -benzyl-1*H*-benzimidazole also showed potent antitumor activity with an IC_{50} of $7.01 \pm 0.20 \mu M$ and arresting MCF-7 cell growth at the G2/M phase and S phase.⁴³ Compounds 3s and 4k have similarities to the active compound of Yoon *et al.* (2014) with the $-N(CH_3)_2$ group at position 4 on the 2-phenyl ring and the N -aryl group at position 1 of the 1*H*-benzimidazole nucleus. However, compound 4k exhibited more potential antitumor activity against five different types of cancer cells when compared with compounds of Yoon *et al.* (2014) and Zhang *et al.* (2017).^{41,42} This may be due to the structure of 4k having the presence of a 4- $N(CH_3)_2$ substituent on the phenyl ring, 6-nitro, and N -(4-chlorobenzyl) groups on the 1*H*-benzimidazole scaffold.

2.4. *In silico* ADMET profile

In the present study, a computational study of the five most active compounds was conducted to determine the surface area and other physicochemical properties according to the directions of Lipinski's rule.²⁸ Lipinski suggested that the absorption capacity of a compound is much better if the molecule achieves



Table 5 *In silico* molecular docking results of active compounds and standard drugs^a

Co.	DHFR-B		GytB		DHFR-F		NMT		VEGFR-2		FGFR-1		HDAC6	
	a	b	a	b	a	b	a	b	a	b	a	b	a	b
1d	-8.6	1, THR121*	-7.4	2, GLU58, GLY85	-7.7	0	-10.1	1, HIS227	-9.7	2, ASP1046, GLU885	-8.2	1, LYS514*	-7.4	1, HIS232*
2d	-8.9	2, ASN18, ILE14	-7.7	0	-8.4	5, ALA11, ILE19, VAL10 [#] , GLY114 [#] , THR147*	-10.1	1, HIS227	-9.1	3, ASP1046, GLU885, LYS868	-8.1	3, ASP641, PHE642, LYS514*	-8.1	3, HIS192, HIS193, LYS330*
3s	-9.2	1, ASN18 [#]	-7.7	1, ASP81 [#]	-8.4	0	-9.6	0	-9.4	1, VAL914 [#]	-9.6	1, GLU531 [#]	-7.6	1, SER150
4b	-9.2	1, GLN95	-7.6	1, ASN54 [#]	-7.7	3, GLY23, GLY114 [#] , THR147*	-9.9	1, HIS227	-7.5	3, ASP1046, ILE1025 [#] , HIS1026 [#]	-8.0	1, GLY567 [#]	-7.8	5, HIS192, HIS193, SER150, TYR363, GLY361*
4k	-9.4	3, ALA7, ASP120 [#] , THR121*	-8.0	1, ASN54 [#]	-8.2	1, TYR118	-9.9	1, ASP110 [#]	-9.6	3, HIS1026 [#] , VAL914 [#]	-8.5	1, LYS514*	-8.6	5, HIS192, HIS193, SER150, TYR363, GLY361*
Cipro	-9.1	1, SER49	-7.3	2, ASP81, SER55	-	-	-	-	-	-	-	-	-	-
Flu	-	-	-	-	-7.0	4, ALA115, GLU116, LYS57	-7.9	1, TYR225	-	-	-	-	-	-
PTX	-10.0	3, LEU20, SER49, THR121	-7.8	5, ASN54, ARG84, GLY85, THR173	-8.5	2, ARG28	-11.4	1, GLY213	-7.8	1, GLY1048	-10.5	3, ASN628, GLU486, THR658	-8.8	4, LYS330, SER150, VAL151

^a Co. - compound. The bacterial targets consist of DHFR-B: Dihydrofolate Reductase-Bacteria, GytB: Gyrase B. The fungal targets consist of DHFR-F: Dihydrofolate Reductase-Fungi, NMT: N-myristoyl Transferase. The cancer targets include all seven receptors. Hydrogen bonds include conventional (not a symbol), carbon ([#]), and π -donor (*) categories. Cipro: ciprofloxacin, Flu: fluconazole, PTX: paclitaxel. a: affinity (Kcal mol⁻¹), b: hydrogen bond (number, position).

at least three out of four of the following rules: (i) HB donor groups ≤ 5 ; (ii) HB acceptor groups ≤ 10 ; (iii) M_w less than 500; (iv) logP less than 5. In this study, compounds **1d**, **2d**, **3s**, **4b**, and **4k** follow all Lipinski's rules. All the highest active derivatives have a number of hydrogen bonding acceptor groups ranging between 1 to 3, and hydrogen bonding donor groups ranging between 0 to 1. Also, molecular weights ranging from 297.57 to 406.86, and logP values ranging between 3.46 to 4.76, and all these values agree with Lipinski's rules.

After assessing ADMET profiles of active compounds (Table 5), we can suggest that these derivatives have the advantage of better intestinal absorption in humans than Cipro, Flu, and PTX, as all compounds showed Caco-2 permeability higher than the control drugs and higher than -5.15 log unit. Besides, compounds **2d**, **3s**, **4b**, and **4k** showed high passive MDCK permeability ($>20 \times 10^{-6} \text{ cm s}^{-1}$) as compared to the reference drugs. This preference may attribute to the superior lipophilic of the designed ligands, which would facilitate passage along different biological membranes.²⁸ Accordingly, they may have remarkably good bioavailability after oral administration. Compounds **3s**, **4b**, and **4k** are highly likely to be Pgp-inhibitor similar to the PTX reference drug. This is a therapeutic approach for overcoming multidrug resistance in cancer. In addition, all compounds showed good plasma protein binding capacity with PPB $> 98.5\%$ as compared to Cipro (PPB = 37%), Flu (PPB = 62%), and PTX (95%). Studying the BBB (Blood-Brain Barrier) permeability, compounds **3s** and **4b** demonstrated the best ability to penetrate the BBB as compared to Flu, while other compounds, Cipro and PTX are unable to penetrate. Therefore, the treatment of brain tumors and brain infections is a great advantage of compounds **3s** and **4b** compared with reference drugs.

The less skin permeant is the molecule, the more negative the log Kp (with Kp in cm s^{-1}). Therefore, all active compounds (log Kp in the range of -5.03 to -4.54) showed better skin permeation than Cipro (log Kp at -9.09) and Flu (log Kp -7.92). The cytochrome enzymes could be moderate to strong inhibited under the effect of active compounds especially CYP1A2, CYP2C19, CYP2C9, and CYP2D6, while Cipro and Flu couldn't. Compounds **2d**, **3s**, **4b**, and **4k** also showed the effect of CYP3A4 inhibition compared with PTX.

The CL (clearance) is a significant parameter in deciding dose intervals as a tool for the assessment of excretion. Compounds **3s** and **4k** ($6.55\text{--}7.91 \text{ mL min}^{-1} \text{ kg}^{-1}$) and Flu (CL = $5.69 \text{ mL min}^{-1} \text{ kg}^{-1}$) was classified as a moderate clearance level ranging between 5 to $15 \text{ mL min}^{-1} \text{ kg}^{-1}$. In contrast, compounds **1d** ($4.89 \text{ mL min}^{-1} \text{ kg}^{-1}$), **2d** ($3.98 \text{ mL min}^{-1} \text{ kg}^{-1}$), and **4b** ($4.48 \text{ mL min}^{-1} \text{ kg}^{-1}$), Cipro ($3.21 \text{ mL min}^{-1} \text{ kg}^{-1}$) and PTX ($3.42 \text{ mL min}^{-1} \text{ kg}^{-1}$) showed lower CL values and were classified as low clearance levels (CL $< 5 \text{ mL min}^{-1} \text{ kg}^{-1}$).

Toxicity is the last parameter examined in the ADMET profile. All the new ligands did not show H-HT (human hepatotoxicity), rat oral acute toxicity, skin sensitization, and eye corrosion. However, all the new ligands showed eye irritation, and the maximum recommended daily dose similar to the reference drug. In particular, the most potent compounds **3s** and **4k** showed lower carcinogenicity than the reference drug

Cipro and lower respiratory toxicity than the reference drug PTX. Moreover, compound **4k** exhibited good "Tox21 pathway" and "Toxicophore rules" profiles as compared to the reference drug PTX.

2.5. *In silico* molecular docking studies

After ADMET profiling, docking studies were carried out to predict the most suitable binding pose and inhibition mechanism of good active compounds. Based on the principle that similar compounds tend to bind to the same proteins, we predicted several reported protein targets against reference compounds (Cipro – ciprofloxacin, Flu – fluconazole, and PTX – paclitaxel) and docked our active compounds against them. Four different target proteins were selected for antimicrobial activity including dihydrofolate reductase (DHFR-F) and *N*-myristoyl transferase (NMT) from *Candida albicans* as fungal targets together with dihydrofolate reductase (DHFR-B) and gyrase B (GyrB) from *Staphylococcus aureus* as bacterial targets.²⁸ Both seven target proteins were selected for anticancer activity including DHFR-B, GyrB, DHFR-F, NMT, vascular endothelial growth factor receptor 2 (VEGFR-2), fibroblast growth factor receptor 1 (FGFR-1), and histone deacetylase 6 (HDAC6). The protein–ligand complex is formed through the electrostatic interactions of the binding interface including hydrogen bonds (both from side chains and backbones), salt bridges, and π – π stacking. Hydrogen bonding provides stability to protein molecules and selected protein–ligand interactions, thus being one of the most important for biological macromolecule interactions. In addition, hydrogen bonds are divided into different types such as conventional, carbon, and π -donor, in which conventional hydrogen bonds are the strongest interactions.

Among all these seven proteins, two proteins (DHFR-B and NMT) as both antimicrobial and antitumor targets presented good binding affinity with a higher affinity than $-8.6 \text{ Kcal mol}^{-1}$.⁴⁴ On the other hand, two proteins (VEGFR-2 and HDAC6) as antitumor targets presented good interactions with affinity in the range of -7.4 to $-9.7 \text{ Kcal mol}^{-1}$ compared with reference drug PTX ($-7.8 \text{ Kcal mol}^{-1}$ at VEGFR-2 and $-8.8 \text{ Kcal mol}^{-1}$ at HDAC6), while FGFR-1 showed weaker interactions with affinity in the range of -8.0 to $-9.6 \text{ Kcal mol}^{-1}$ compared with PTX ($-10.5 \text{ Kcal mol}^{-1}$) (Table 5).

On the DHFR-B receptor, compounds **3s** and **4b** established one hydrogen bond with the affinity of $-9.2 \text{ Kcal mol}^{-1}$. Compound **4b** established a conventional hydrogen bond (2.05 \AA) with GLN95 amino acid but compound **3s** only established a carbon–hydrogen bond (3.52 \AA) with ASN18 amino acid. In particular, compound **4k** being the most potent antimicrobial and antitumor agent against DHFR-B displayed the highest negative affinity of $-9.4 \text{ Kcal mol}^{-1}$ which is comparable to Cipro ($-9.1 \text{ Kcal mol}^{-1}$) and PTX ($-10.0 \text{ Kcal mol}^{-1}$). Besides, compound **4k** established three hydrogen bonds that were similar to PTX with ALA7 (conventional), ASP120 (carbon), and THR121 (π -donor) amino acids with bond lengths of 2.46, 3.57, and 2.98 \AA , respectively. On the other hand, compound **4k** showed hydrophobic interactions (π - σ , alkyl, π -alkyl) with LEU20, LYS45, ILE14, and ALA7 with the crucial residue of the



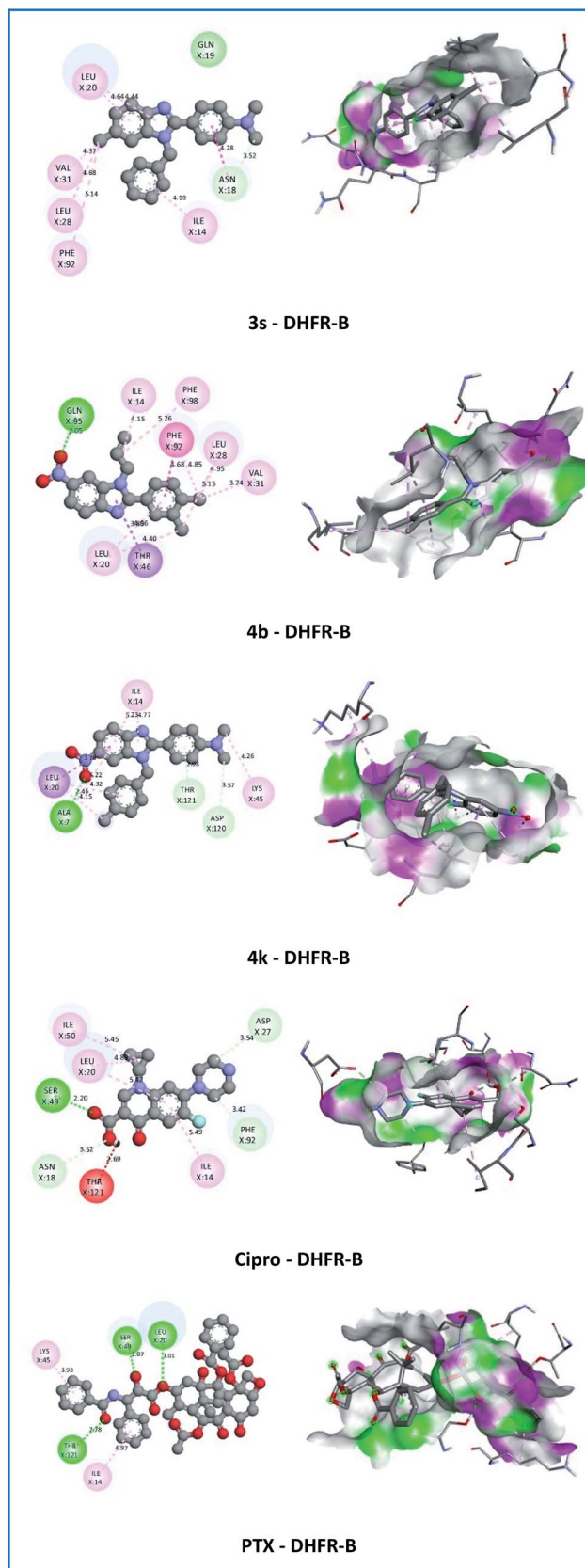


Fig. 5 2D and 3D representation of the interaction of the synthesized molecules **3s**, **4b**, **4k**, ciprofloxacin (Cipro), and paclitaxel (PTX) with dihydrofolate reductase from *S. aureus* (unit of interaction distance – Å).

DHFR-B protein from *S. aureus* that resembles the co-crystallization ligand, Cipro, and PTX. As illustrated in Fig. 5, the *N,N*-dimethylamino ($-N(CH_3)_2$) group in the 2-phenyl ring of a 1*H*-benzimidazole nucleus of compound **4k** were engaged in the formation of carbon–hydrogen bond with ASP120 and alkyl interactions with LYS45 amino acid with a bond length of 4.26 Å. Moreover, the *N*-(4-chlorobenzyl) group and 1*H*-benzimidazole nucleus displayed π - σ , alkyl, and π -alkyl interactions with the crucial residue LEU20, ILE14, and ALA7 of the target protein with a bond length in the range of 3.78–5.23 Å. These results have demonstrated that compound **4k** has the most potential *in vitro* antibacterial and antitumor activities.

On the GyrB receptor, all active compounds showed good interactions with affinity in the range of -7.4 to -8.0 Kcal mol $^{-1}$ compared with the standard drug Cipro (-7.3 Kcal mol $^{-1}$) and PTX (-7.8 Kcal mol $^{-1}$) but showed less hydrogen bonding. Similarly, all active compounds also showed good interactions with affinity in the range of -7.7 to -8.4 Kcal mol $^{-1}$ compared with the standard drug Flu (-7.0 Kcal mol $^{-1}$) and PTX (-8.5 Kcal mol $^{-1}$) on DHFR-F receptor, but compounds **1d**, **3s**, **4b**, and **4k** have not formed or have formed hydrogen bonds in lesser quantities at amino acid sites other than the reference drug Flu. However, compound **2d** displayed the best negative affinity of -8.4 Kcal mol $^{-1}$ with five hydrogen bonds (2.13–3.62 Å) with ALA11, ILE19, VAL10, GLY114, and THR147 amino acids.

On the NMT receptor, compounds **1d**, **2d**, and **4b** established one conventional hydrogen bond (2.30–2.44 Å) with a good affinity (-9.9 to -10.1 Kcal mol $^{-1}$) with HIS227 amino acid compared with Flu (-7.9 Kcal mol $^{-1}$), PTX (-11.4 Kcal mol $^{-1}$). On the contrary, compound **3s** did not establish hydrogen bonds with affinity at -9.6 Kcal mol $^{-1}$ and compound **4k** only establish one carbon–hydrogen bond with a bond length of 3.79 Å with a good affinity of -9.9 Kcal mol $^{-1}$.

On the VEGFR-2 receptor, compounds **1d**, **2d**, **3s**, and **4k** showed stronger interactions with the affinity between -9.1 and -9.7 Kcal mol $^{-1}$ compared with reference drug PTX (-7.8 Kcal mol $^{-1}$). Compounds **2d**, **4b**, and **4k** established three hydrogen bonds with bond lengths in the range of 1.87–3.75 Å. However, compounds **1d** and **4k** showed the strongest interactions with the affinity of -9.7 and -9.6 Kcal mol $^{-1}$, respectively. Compound **1d** established two conventional hydrogen bonds (1.97–2.29 Å) with ASP1046 and GLU885 amino acids, electrostatic (π -cation) interactions with bond lengths in the range of 4.33 to 4.50 Å with LYS868 amino acid. In particular, compound **4k** established three carbon–hydrogen bonds (3.29–3.65 Å) at 6-nitro and *N,N*-dimethylamino groups with HIS1026 and VAL914 amino acids. Besides, compound **4k** showed electrostatic (π -cation) interactions with LYS868 and HIS1026 amino acids with bond lengths in the range of 4.45 to 4.49 Å and electrostatic (π -anion) interactions with GLU885 amino acid with a bond length of 3.67 Å. In addition, compound **4k** showed hydrophobic interactions (π - σ , π - π T-shaped, alkyl, π -alkyl) with LEU889, VAL899, HIS1026, LYS868, VAL916, ILE892, LEU1019, and ILE888 amino acids with bond lengths in the range of 3.79 to 5.44 Å (Fig. 6).



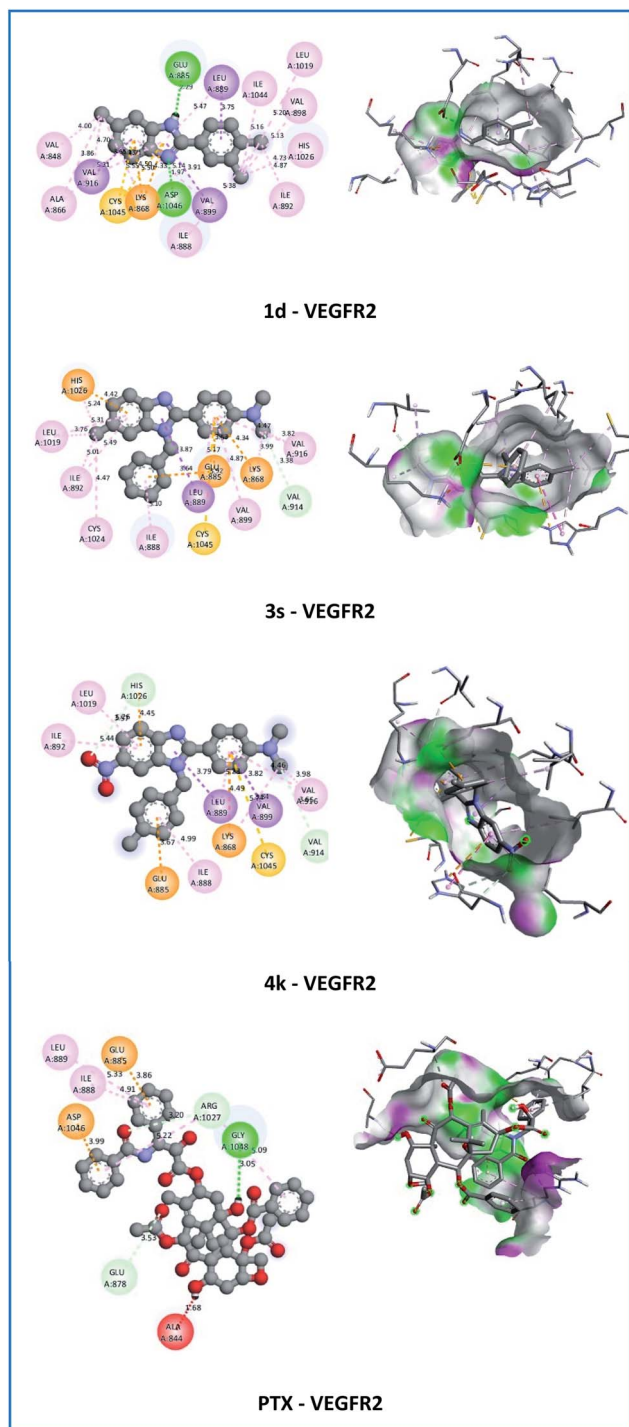


Fig. 6 2D and 3D representation of the interaction of the synthesized molecules **1d**, **3s**, **4k**, and paclitaxel (PTX) with vascular endothelial growth factor receptor 2 (unit of interaction distance – Å).

On the FGFR-1 receptor, all active compounds established one π -donor hydrogen or carbon–hydrogen bond (3.00–3.66 Å) except for **2d** established three hydrogen bonds (2.17–3.01 Å) with ASP641, PHE642, and LYS514 amino acids. In addition, these compounds showed weaker interactions with the affinity between -8.0 and -9.6 Kcal mol $^{-1}$ compared with the reference drug PTX (-10.5 Kcal mol $^{-1}$). Compound **3s** displayed the

highest negative affinity of -9.6 Kcal mol $^{-1}$ among active compounds against FGFR-1. Moreover, compound **3s** established one carbon–hydrogen bond with a bond length of 3.20 Å with GLU531 amino acid, electrostatic (π -anion) interaction with a bond length of 4.54 Å with ASP641 amino acid.

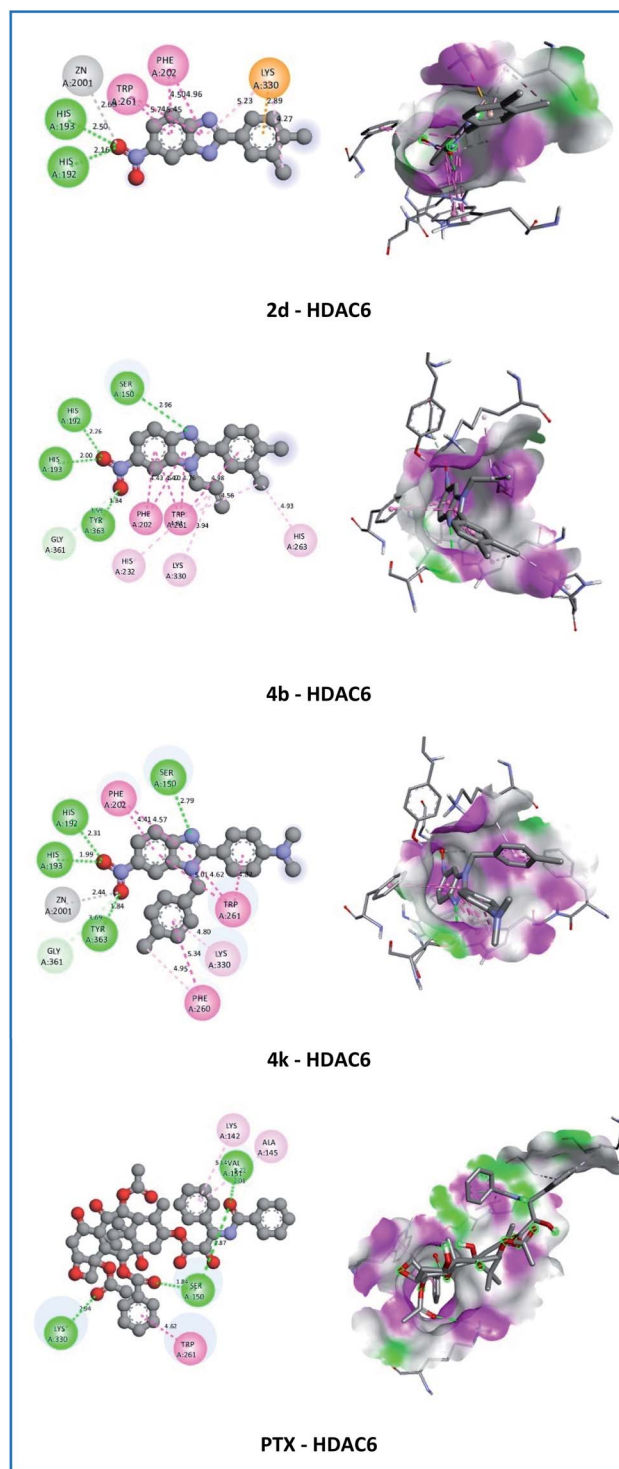


Fig. 7 2D and 3D representation of the interaction of the synthesized molecules **2d**, **4b**, **4k**, and paclitaxel (PTX) with histone deacetylase 6 (unit of interaction distance – Å).



Compound **3s** also showed hydrophobic interactions (π - σ , π - π T-shaped, alkyl, π -alkyl) with LEU889, VAL899, HIS1026, LYS868, VAL916, ILE892, LEU1019, and ILE888 amino acids with bond lengths in the range of 3.79 to 5.44 Å.

On the HDAC6 receptor, all active compounds showed weaker interactions with the affinity between -7.4 and -8.6 Kcal mol $^{-1}$ compared with the reference drug PTX (-8.8 Kcal mol $^{-1}$). However, compounds **4b** and **4k** exhibited more hydrogen bonds than PTX (Fig. 7). These compounds established four conventional hydrogen bonds (1.84–2.96 Å) with SER150, HIS192, HIS193, and TYR363 amino acids and one carbon–hydrogen bond (3.59–3.69 Å) with GLY361 amino acid at the nitro group and 1*H*-imidazole nucleus. In particular, compound **4k** demonstrated the strongest affinity (-8.6 Kcal mol $^{-1}$) among all active derivatives against HDAC6. In addition, compound **4k** showed metal–acceptor interaction with ZN2001 with a bond length of 2.44 Å and hydrophobic interactions (π - π stacked, π - π T-shaped, π -alkyl) with PHE202, PHE260, TRP261, and LYS330 amino acids with bond lengths in the range of 4.16 to 5.34 Å at the aromatic rings. Hydrophobic interaction with TRP261 of **4k** compound is similar to that of PTX. These results suggested that HDAC6 also are the most likely target for the anticancer activity of the **4k** compound.

In summary, from the *in silico* molecular docking study results, it can be concluded that compound **4k** is considered the best dock conformation in antibacterial and antitumor targets such as DHFR-B, VEGFR-2, and HDAC6.

3. Conclusion

In summary, thirty-four 6-substituted 1*H*-benzimidazole and forty-two N-substituted 6-(chloro/nitro)-1*H*-benzimidazole derivatives including twenty-nine new compounds have been designed, synthesized, and evaluated for their antimicrobial and anticancer activities. The microwave-assisted method has contributed to a significant reduction in reaction time and a significant increase in product yield. In addition, compounds **1d**, **2d**, **3s**, **4b**, and **4k** showed potent antibacterial activity against EC, SF, MSSA, and MRSA with MIC ranging between 2 to 16 $\mu\text{g mL}^{-1}$ compared with standard drug Cipro, especially compound **4k** is potent fungal activity against CA and AN with MIC ranging between 8 to 16 $\mu\text{g mL}^{-1}$ compared with standard drug Flu. Moreover, these compounds also exhibited potent anticancer activity with IC $_{50}$ < 10 μM against all tested cell lines (HepG2, MDA-MB-231, MCF7, C26, and RMS) compared with reference drug PTX. From the structure–activity relationship, the presence of the *N*-benzyl/*N*-(4-chlorobenzyl) group and the chloro/*N,N*-dimethylamino moiety in the aromatic ring at position 2 of the 1*H*-benzimidazole scaffold is more desirable for enhanced antibacterial activity as well as antitumor activity in **1d**, **2d**, **3s**, **4b**, and **4k**, and antifungal activity in **4k**. Molecular docking predicted that dihydrofolate reductase protein from *S. aureus* is the most suitable target for antibacterial and anticancer activities, as well as vascular endothelial growth factor receptor 2 and histone deacetylase 6 are the most suitable targets for anticancer activity. Compound **4k** being the most potent antimicrobial and anticancer displayed good

interactions against DHFR-B, VEGFR2, and HDAC6 with the affinity of -9.4 , -9.6 , and -8.6 Kcal mol $^{-1}$, respectively. Especially, this compound showed electrostatic and hydrophobic interactions that resemble the co-crystallization ligand and reference drugs. ADMET profile was evaluated for the five most active compounds in comparison to ciprofloxacin and fluconazole, and paclitaxel as reference drugs. The obtained results predicted that our derivatives may show a good ADMET profile. All compounds show physical–chemical properties of fragment and lead-like compounds which are of great interest for further drug development. This work paved the way for the synthesis of more potent compounds based on *N*-benzyl-1*H*-benzimidazole scaffolds and explore their various and potential biological activities as well as their mechanism of action.

4. Experimental section

4.1. Materials

All chemicals and solvents were purchased from commercial suppliers Merck and Acros. All the reactions were carried out under an inert atmosphere of nitrogen. TLC was performed on pre-coated aluminum sheets of silica (60 F $_{254}$ nm) and visualized by shortwave UV light at λ 254. Column chromatography uses 0.040–0.063 mm granular silica gel (Merck).

The microwave reactor used was the Microwave synthesizer – CEM Discover, USA, fitted with a magnetic stirrer for continuous stirring and an infrared temperature sensor, which enabled and controlled the temperature. Melting points (mp) were determined on a Sanyo-Gallenkamp melting point apparatus. UV-Vis absorption spectra were recorded on a PerkinElmer Lambda 40p spectrometer. IR spectra were recorded on an IRAffinity-1S. NMR spectra were recorded on a Bruker Avance 500 NMR Spectrometer (^1H NMR 500 MHz, ^{13}C NMR 125 MHz). Chemical shifts were measured in δ (ppm). Mass spectrometry was measured on 1100 series LC-MS Trap Agilent.

4.2. Experimental procedures

4.2.1 General procedure for the preparation of 6-substituted 1*H*-benzimidazole derivatives (1a–1q and 2a–q)

The reflux method. A mixture of 4-chlorobenzene-1,2-diamine or 4-chlorobenzene-1,2-diamine (5 mmol), the substituted aromatic aldehydes (5 mmol), and Na $_2$ S $_2$ O $_5$ (20 mmol) was dissolved in a mixture of absolute alcohol and water at a ratio of 9 : 1 (v/v, 30 mL) and refluxed for 6–12 h at 80 °C. After cooling, the reaction crude was poured on a mixture of ice/water to give a solid that was filtered off in a Büchner funnel. The resulting solid was purified by column chromatography on silica gel using hexane/ethyl acetate as eluent. Reaction yields ranged within 70–91%.

The microwave-assisted method. A mixture of 4-chlorobenzene-1,2-diamine or 4-chlorobenzene-1,2-diamine (5 mmol), the substituted aromatic aldehydes (5 mmol), Na $_2$ S $_2$ O $_5$ (20 mmol), and a mixture of absolute alcohol and water at a ratio of 9 : 1 (v/v, 10 mL) was placed in a microwave oven and irradiated at a power of 300 W for 10–15 min at 80 °C. After cooling, the reaction crude was poured on a mixture of ice/water to give



a solid that was filtered off in a Büchner funnel. The resulting solid was purified by column chromatography on silica gel using hexane/ethyl acetate as eluent. Reaction yields ranged within 90–99%.

6-Chloro-2-(2-chlorophenyl)-1H-benzo[d]imidazole (1a). White solid, mp 122–123 °C. ¹H NMR (500 MHz, DMSO-*d*₆, δ ppm): 12.92 (1H, s, -NH-), 7.91 (1H, dd, *J* = 7.5, 2.0 Hz, H_{Ar}), 7.78–7.70 (1H, m, H_{Ar}), 7.65 (1H, dd, *J* = 7.0, 1.5 Hz, H_{Ar}), 7.60–7.52 (3H, m, H_{Ar}), 7.27 (1H, d, *J* = 4.0 Hz, H_{Ar}). ¹³C NMR (125 MHz, DMSO-*d*₆, δ ppm): 150.4, 144.0, 133.5, 132.1, 131.6, 130.4, 129.4, 127.5, 122.8, 120.5, 118.5, 113.1, 111.3. LC-MS (*m/z*) [M - H]⁻ calcd for C₁₃H₇Cl₂N₂ 260.9992, found 260.9912; [M + H]⁺ calcd for C₁₃H₉Cl₂N₂ 263.0137, found 263.0160.

6-Chloro-2-(4-chlorophenyl)-1H-benzo[d]imidazole (1b). White solid, mp 227–228 °C. ¹H NMR (500 MHz, DMSO-*d*₆, δ ppm): 13.14 (1H, s, -NH-), 8.19 (2H, d, *J* = 8.5 Hz, H_{Ar}), 7.64–7.61 (2H, m, H_{Ar}), 7.40 (2H, d, *J* = 8.5 Hz, H_{Ar}), 7.23 (2H, d, *J* = 8.0 Hz, H_{Ar}). ¹³C NMR (125 MHz, DMSO-*d*₆, δ ppm): 151.6, 134.9 (2C), 129.1 (2C), 128.5 (2C), 128.3 (2C), 126.6 (2C), 122.6 (2C). LC-MS (*m/z*) [M - H]⁻ calcd for C₁₃H₇Cl₂N₂ 260.9992, found 260.9881; [M + H]⁺ calcd for C₁₃H₉Cl₂N₂ 263.0137, found 263.0148.

6-Chloro-2-(2,4-dichlorophenyl)-1H-benzo[d]imidazole (1c). White solid, mp 245–246 °C. ¹H NMR (500 MHz, DMSO-*d*₆, δ ppm): 12.97 (1H, s, -NH-), 7.94 (1H, d, *J* = 8.5 Hz, H_{Ar}), 7.84 (1H, d, *J* = 2.0 Hz, H_{Ar}), 7.77–7.68 (1H, m, H_{Ar}), 7.67–7.59 (2H, m, H_{Ar}), 7.30–7.26 (1H, m, H_{Ar}). ¹³C NMR (125 MHz, DMSO-*d*₆, δ ppm): 149.4, 135.3, 133.2, 132.6 (2C), 129.9 (2C), 128.3 (2C), 127.8 (2C), 122.8 (2C). LC-MS (*m/z*) [M - H]⁻ calcd for C₁₃H₆Cl₃N₂ 294.9602, found 294.9624; [M + H]⁺ calcd for C₁₃H₈Cl₃N₂ 296.9748, found 296.9725.

6-Chloro-2-(3,4-dichlorophenyl)-1H-benzo[d]imidazole (1d). White solid, mp 233–234 °C. ¹H NMR (500 MHz, DMSO-*d*₆, δ ppm): 13.26 (1H, s, -NH-), 8.37 (1H, d, *J* = 2.0 Hz, H_{Ar}), 8.13 (1H, dd, *J* = 8.5, 2.0 Hz, H_{Ar}), 7.83 (1H, d, *J* = 8.5 Hz, H_{Ar}), 7.74–7.55 (2H, m, H_{Ar}), 7.25 (1H, d, *J* = 8.5 Hz, H_{Ar}). ¹³C NMR (125 MHz, DMSO-*d*₆, δ ppm): 150.2, 132.7, 131.9, 131.3 (2C), 130.2 (2C), 128.1 (2C), 126.6 (2C), 122.9 (2C). LC-MS (*m/z*) [M - H]⁻ calcd for C₁₃H₆Cl₃N₂ 294.9602, found 294.9566; [M + H]⁺ calcd for C₁₃H₈Cl₃N₂ 296.9748, found 296.9752.

6-Chloro-2-(2-chloro-6-fluorophenyl)-1H-benzo[d]imidazole (1e). White solid, mp 177–178 °C. ¹H NMR (500 MHz, DMSO-*d*₆, δ ppm): 12.87 (1H, s, -NH-), 7.68 (1H, q, *J* = 8.5 Hz, H_{Ar}), 7.65–7.60 (1H, m, H_{Ar}), 7.56 (1H, d, *J* = 8.0 Hz, H_{Ar}), 7.51 (1H, t, *J* = 8.5 Hz, H_{Ar}), 7.46 (1H, d, *J* = 9.0 Hz, H_{Ar}), 7.15 (1H, t, *J* = 8.5 Hz, H_{Ar}). ¹³C NMR (125 MHz, DMSO-*d*₆, δ ppm): 161.4, 159.2, 148.5, 136.8, 134.3, 134.2, 133.5, 133.6, 126.0, 125.97, 118.9, 118.7, 118.3, 115.3, 115.2. LC-MS (*m/z*) [M - H]⁻ calcd for C₁₃H₆Cl₂FN₂ 278.9898, found 278.9682; [M + H]⁺ calcd for C₁₃H₈Cl₂FN₂ 281.0043, found 281.0109.

6-Chloro-2-(3,4-dimethoxyphenyl)-1H-benzo[d]imidazole (1f). White solid, mp 215–218 °C. ¹H NMR (500 MHz, DMSO-*d*₆, δ ppm): 12.93 (1H, s, -NH-), 7.75–7.73 (2H, m, H_{Ar}), 7.53–7.51 (2H, m, H_{Ar}), 7.19 (1H, d, *J* = 8.0 Hz, H_{Ar}), 7.13 (1H, d, *J* = 8.5 Hz, H_{Ar}), 3.88 (3H, s, -OCH₃), 3.84 (3H, s, -OCH₃). ¹³C NMR (125 MHz, DMSO-*d*₆, δ ppm): 153.1, 150.6, 144.8, 142.7, 135.7, 126.4, 122.2, 121.8, 119.6, 118.1, 112.3, 110.7, 109.8, 55.62, 55.60. LC-MS (*m/z*) [M - H]⁻ calcd for C₁₅H₁₂ClN₂O₂ 287.0593, found

287.0522; [M + H]⁺ calcd for C₁₅H₁₄ClN₂O₂ 289.0738, found 289.0718.

6-Chloro-2-(4-ethoxyphenyl)-1H-benzo[d]imidazole (1g). White solid, mp 253–254 °C. ¹H NMR (500 MHz, DMSO-*d*₆, δ ppm): 12.91 (1H, s, -NH-), 8.09 (2H, d, *J* = 8.5 Hz, H_{Ar}), 7.66–7.61 (1H, m, H_{Ar}), 7.49 (1H, d, *J* = 9.0 Hz, H_{Ar}), 7.18 (1H, t, *J* = 8.5 Hz, H_{Ar}), 7.09 (2H, d, *J* = 9.0 Hz, H_{Ar}), 4.12 (2H, q, *J* = 7.0 Hz, -CH₂-), 1.36 (3H, t, *J* = 7.0 Hz, -CH₃). ¹³C NMR (125 MHz, DMSO-*d*₆, δ ppm): 160.2, 128.2, 122.0 (2C), 119.7, 117.8 (2C), 114.8 (2C), 111.3 (2C), 110.7 (2C), 63.3, 14.6. LC-MS (*m/z*) [M - H]⁻ calcd for C₁₅H₁₂ClN₂O 271.0644, found 271.0628; [M + H]⁺ calcd for C₁₅H₁₄ClN₂O 273.0789, found 273.0771.

4-(6-Chloro-1H-benzo[d]imidazole-2-yl)-2-ethoxyphenol (1h). White solid, mp 215–217 °C. ¹H NMR (500 MHz, DMSO-*d*₆, δ ppm): 12.82 (1H, s, -NH-), 9.51 (1H, s, -OH), 7.71 (1H, s, H_{Ar}), 7.68–7.40 (3H, m, H_{Ar}), 7.17 (1H, dd, *J* = 8.5, 1.5 Hz, H_{Ar}), 6.93 (1H, d, *J* = 8.0 Hz, H_{Ar}), 4.14 (2H, q, *J* = 7.0 Hz, -CH₂-), 1.39 (3H, t, *J* = 7.0 Hz, -CH₃). ¹³C NMR (125 MHz, DMSO-*d*₆, δ ppm): 153.2, 149.1, 147.0, 125.9 (2C), 121.8 (2C), 120.8 (2C), 119.9 (2C), 115.8, 111.7, 64.0, 14.7. LC-MS (*m/z*) [M - H]⁻ calcd for C₁₅H₁₂ClN₂O₂ 287.0593, found 287.0478; [M + H]⁺ calcd for C₁₅H₁₄ClN₂O₂ 289.0738, found 289.0708.

6-Chloro-2-(4-fluorophenyl)-1H-benzo[d]imidazole (1i). White solid, mp 219–221 °C. ¹H NMR (500 MHz, DMSO-*d*₆, δ ppm): 13.18 (1H, s, -NH-), 8.18 (2H, d, *J* = 8.5 Hz, H_{Ar}), 7.67–7.73 (1H, m, H_{Ar}), 7.64 (2H, d, *J* = 8.5 Hz, H_{Ar}), 7.57 (1H, s, H_{Ar}), 7.24 (1H, s, H_{Ar}). ¹³C NMR (125 MHz, DMSO-*d*₆, δ ppm): 151.1, 148.7, 147.8, 124.2 (2C), 120.8 (2C), 108.7 (2C), 106.4 (2C), 101.5 (2C). LC-MS (*m/z*) [M - H]⁻ calcd for C₁₃H₇ClFN₂ 245.0287, found 245.0210; [M + H]⁺ calcd for C₁₃H₉ClFN₂ 247.0433, found 247.0277.

3-(6-Chloro-1H-benzo[d]imidazole-2-yl)phenol (1j). Brown solid, mp 289–290 °C. ¹H NMR (500 MHz, DMSO-*d*₆, δ ppm): 13.01 (1H, s, -NH-), 9.76 (1H, s, -OH), 7.71–7.52 (4H, m, H_{Ar}), 7.35 (1H, t, *J* = 8.0 Hz, H_{Ar}), 7.21 (1H, d, *J* = 7.0 Hz, H_{Ar}), 6.92 (1H, dd, *J* = 8.0, 1.5 Hz, H_{Ar}). ¹³C NMR (125 MHz, DMSO-*d*₆, δ ppm): 157.8, 152.9, 144.7, 142.6, 135.7, 133.8, 130.9, 126.7, 122.5, 120.0, 118.2, 113.4, 110.9. LC-MS (*m/z*) [M - H]⁻ calcd for C₁₃H₈ClN₂O 243.0331, found 243.0196; [M + H]⁺ calcd for C₁₃H₁₀ClN₂O 245.0476, found 245.0427.

6-Chloro-2-(3-methoxyphenyl)-1H-benzo[d]imidazole (1k). White solid, mp 179–181 °C. ¹H NMR (500 MHz, DMSO-*d*₆, δ ppm): 13.07 (1H, s, -NH-), 7.75–7.73 (2H, m, H_{Ar}), 7.70–7.52 (2H, m, H_{Ar}), 7.47 (1H, t, *J* = 8.0 Hz, H_{Ar}), 7.23 (1H, d, *J* = 6.5 Hz, H_{Ar}), 7.08 (1H, dd, *J* = 8.5, 1.5 Hz, H_{Ar}), 3.86 (3H, s, -OCH₃). ¹³C NMR (125 MHz, DMSO-*d*₆, δ ppm): 159.6, 152.1, 144.6, 142.5, 135.7, 130.9, 126.9, 122.6, 120.1, 118.9, 116.2, 112.6, 111.5, 55.3. LC-MS (*m/z*) [M - H]⁻ calcd for C₁₄H₁₀ClN₂O 257.0487, found 257.0487; [M + H]⁺ calcd for C₁₄H₁₂ClN₂O 259.0633, found 259.0684.

5-(6-Chloro-1H-benzo[d]imidazole-2-yl)-2-methoxyphenol (1l). White solid, mp 253–254 °C. IR (ν, cm⁻¹): 1605.2 (C=N), 1439.0 (C=C), 1340.5 (N=O). ¹H NMR (500 MHz, DMSO-*d*₆, δ ppm): 7.66–7.60 (3H, m, H_{Ar}), 7.53 (1H, d, *J* = 9.0 Hz, H_{Ar}), 7.21 (1H, t, *J* = 8.5 Hz, H_{Ar}), 7.14 (1H, d, *J* = 8.5 Hz, H_{Ar}), 3.96 (3H, s, -OCH₃). ¹³C NMR (125 MHz, DMSO-*d*₆, δ ppm): 155.6, 149.8, 147.4, 138.8, 126.3 (2C), 122.1 (2C), 121.2 (2C), 120.1, 115.8, 112.7,



56.9. LC-MS (m/z) $[M + H]^+$ calcd for $C_{14}H_{12}ClN_2O_2$ 275.0582, found 275.0665.

6-Chloro-2-(3-nitrophenyl)-1H-benzodimidazole (1m). Yellow solid, mp 243–244 °C. 1H NMR (500 MHz, DMSO- d_6 , δ ppm): 13.46 (1H, s, -NH-), 8.99 (1H, s, H_{Ar}), 8.59 (1H, d, $J = 7.5$ Hz, H_{Ar}), 8.34 (1H, dd, $J = 8.5, 1.5$ Hz, H_{Ar}), 7.86 (1H, t, $J = 8.0$ Hz, H_{Ar}), 7.70 (1H, s, H_{Ar}), 7.66 (1H, d, $J = 8.5$ Hz, H_{Ar}), 7.27 (1H, dd, $J = 8.5, 1.5$ Hz, H_{Ar}). ^{13}C NMR (125 MHz, DMSO- d_6 , δ ppm): 150.4, 148.3, 132.6, 131.2, 130.7, 127.0 (2C), 124.5 (2C), 123.0 (2C), 121.0 (2C). LC-MS (m/z) $[M - H]^-$ calcd for $C_{13}H_7ClN_3O_2$ 272.0232, found 272.0206; $[M + H]^+$ calcd for $C_{13}H_9ClN_3O_2$ 274.0378, found 274.0318.

6-Chloro-2-(4-nitrophenyl)-1H-benzodimidazole (1n). Yellow solid, mp 260–262 °C. 1H NMR (500 MHz, DMSO- d_6 , δ ppm): 13.47 (1H, s, -NH-), 8.50–8.40 (4H, m, H_{Ar}), 7.72–7.68 (2H, m, H_{Ar}), 7.30 (1H, d, $J = 8.5$ Hz, H_{Ar}). ^{13}C NMR (125 MHz, DMSO- d_6 , δ ppm): 148.1, 135.5, 134.0 (2C), 127.6 (2C), 124.3 (2C), 123.8 (2C), 118.8, 113.2, 111.5. LC-MS (m/z) $[M - H]^-$ calcd for $C_{13}H_7ClN_3O_2$ 272.0232, found 272.0104; $[M + H]^+$ calcd for $C_{13}H_9ClN_3O_2$ 274.0378, found 273.9934.

4-(6-Chloro-1H-benzodimidazole-2-yl)-N,N-dimethylaniline (1o). White solid, mp 246–248 °C. 1H NMR (500 MHz, DMSO- d_6 , δ ppm): 12.71 (1H, s, -NH-), 7.99 (2H, d, $J = 9.0$ Hz, H_{Ar}), 7.54–7.49 (2H, m, H_{Ar}), 7.15 (1H, dd, $J = 8.5, 1.5$ Hz, H_{Ar}), 6.84 (2H, d, $J = 9.0$ Hz, H_{Ar}), 3.00 (6H, s, -N(CH $_3$) $_2$). ^{13}C NMR (125 MHz, DMSO- d_6 , δ ppm): 153.7, 151.4, 134.9 (2C), 127.7 (2C), 125.6 (2C), 121.4 (2C), 116.7 (2C), 111.8, 39.7. LC-MS (m/z) $[M - H]^-$ calcd for $C_{15}H_{13}ClN_3$ 270.0803, found 270.0948; $[M + H]^+$ calcd for $C_{15}H_{15}ClN_3$ 272.0949, found 272.0909.

2-(Benzodimidazole[1,3]dioxol-5-yl)-6-chloro-1H-benzodimidazole (1p). White solid, mp 211–213 °C. 1H NMR (500 MHz, DMSO- d_6 , δ ppm): 12.92 (1H, s, -NH-), 7.71 (1H, d, $J = 8.0$ Hz, H_{Ar}), 7.66 (1H, s, H_{Ar}), 7.65–7.50 (2H, m, H_{Ar}), 7.20 (1H, d, $J = 8.5$ Hz, H_{Ar}), 7.10 (1H, d, $J = 8.0$ Hz, H_{Ar}), 6.13 (2H, s, -CH $_2$ -). ^{13}C NMR (125 MHz, DMSO- d_6 , δ ppm): 149.1, 147.9 (2C), 123.7 (3C), 121.2 (2C), 108.8 (2C), 106.6 (2C), 101.7, 89.2. LC-MS (m/z) $[M - H]^-$ calcd for $C_{14}H_8ClN_2O_2$ 271.0280, found 271.0257; $[M + H]^+$ calcd for $C_{14}H_{10}ClN_2O_2$ 273.0425, found 273.0423.

6-Chloro-2-(furan-2-yl)-1H-benzodimidazole (1q). White solid, mp 175–177 °C. 1H NMR (500 MHz, DMSO- d_6 , δ ppm): 13.11 (1H, s, -NH-), 7.96 (1H, d, $J = 1.0$ Hz, H_{Ar}), 7.80–7.40 (2H, m, H_{Ar}), 7.23–7.20 (2H, m, H_{Ar}), 6.74–6.72 (1H, m, H_{Ar}). ^{13}C NMR (125 MHz, DMSO- d_6 , δ ppm): 145.0, 142.4, 135.0, 133.1, 126.8, 122.6, 122.2, 119.9, 118.1, 112.6, 111.1. LC-MS (m/z) $[M - H]^-$ calcd for $C_{11}H_6ClN_2O$ 217.0174, found 217.0118; $[M + H]^+$ calcd for $C_{11}H_8ClN_2O$ 219.0320, found 219.0366.

2-(2-Chlorophenyl)-6-nitro-1H-benzodimidazole (2a). Yellow solid, mp 173–175 °C. IR (ν , cm^{-1}): 1593.2 (C=N), 1435.0 (C=C), 1336.7 (N=O), 737.2 (C-Cl). 1H NMR (500 MHz, DMSO- d_6 , δ ppm): 13.42 (2H, s, -NH-), 8.61 (1H, s, H_{Ar}), 8.46 (1H, s, H_{Ar}), 8.20–8.14 (2H, m, H_{Ar}), 7.98–7.76 (4H, m, H_{Ar}), 7.71–7.70 (2H, d, $J = 8.0$ Hz, H_{Ar}), 7.63–7.60 (2H, m, H_{Ar}), 7.58–7.55 (2H, m, H_{Ar}). ^{13}C NMR (125 MHz, DMSO- d_6 , δ ppm): 151.8, 147.6, 146.2, 140.3, 137.5, 132.9, 130.1, 129.6, 126.4, 121.9, 120.8, 118.7, 114.0. LC-MS (m/z) $[M + H]^+$ calcd for $C_{13}H_9ClN_3O_2$ 274.0378, found 274.0365.

2-(4-Chlorophenyl)-6-nitro-1H-benzodimidazole (2b). Yellow solid, mp 309–311 °C. IR (ν , cm^{-1}): 1597.1 (C=N), 1442.8 (C=C), 1284.6 (N=O), 733.0 (C-Cl). 1H NMR (500 MHz, DMSO- d_6 , δ ppm): 13.66 (1H, s, -NH-), 8.48 (1H, s, H_{Ar}), 8.24–8.21 (2H, m, H_{Ar}), 8.14 (1H, dd, $J = 9.0, 2.0$ Hz, H_{Ar}), 7.78 (1H, d, $J = 8.5$ Hz, H_{Ar}), 7.70–7.68 (2H, m, H_{Ar}). ^{13}C NMR (125 MHz, DMSO- d_6 , δ ppm): 152.1, 146.4, 144.2, 139.7, 138.3, 134.5, 128.5 (2C), 126.2 (2C), 122.8, 119.0, 116.6. LC-MS (m/z) $[M + H]^+$ calcd for $C_{13}H_9ClN_3O_2$ 274.0378, found 274.0344.

2-(2,4-Dichlorophenyl)-6-nitro-1H-benzodimidazole (2c). Yellow solid, mp 245–246 °C. IR (ν , cm^{-1}): 1624.1 (C=N), 1435.0 (C=C), 1339.3 (N=O), 733.0 (C-Cl). 1H NMR (500 MHz, DMSO- d_6 , δ ppm): 13.45 (1H, s, -NH-), 8.54 (1H, s, H_{Ar}), 8.16 (1H, dd, $J = 8.5, 1.5$ Hz, H_{Ar}), 7.97 (1H, d, $J = 8.5$ Hz, H_{Ar}), 7.87 (1H, d, $J = 2.0$ Hz, H_{Ar}), 7.81 (1H, d, $J = 9.0$ Hz, H_{Ar}), 7.65 (1H, dd, $J = 8.5, 2.0$ Hz, H_{Ar}). ^{13}C NMR (125 MHz, DMSO- d_6 , δ ppm): 152.5, 142.9, 135.9, 133.4 (2C), 132.7 (3C), 130.0, 127.9, 127.7, 118.1 (2C). LC-MS (m/z) $[M - H]^-$ calcd for $C_{13}H_6Cl_2N_3O_2$ 305.9843, found 305.9880.

2-(3,4-Dichlorophenyl)-6-nitro-1H-benzodimidazole (2d). Yellow solid, mp 302–304 °C. 1H NMR (500 MHz, DMSO- d_6 , δ ppm): 13.81 (1H, s, -NH-), 8.51 (1H, s, H_{Ar}), 8.44 (1H, d, $J = 2.0$ Hz, H_{Ar}), 8.19 (1H, dd, $J = 8.5, 2.0$ Hz, H_{Ar}), 8.16 (1H, dd, $J = 8.5, 2.0$ Hz, H_{Ar}), 7.89 (1H, d, $J = 8.5$ Hz, H_{Ar}), 7.81 (1H, d, $J = 9.0$ Hz, H_{Ar}). ^{13}C NMR (125 MHz, DMSO- d_6 , δ ppm): 151.4, 148.2, 145.3, 141.5, 136.9, 133.6, 132.5, 129.0, 125.8, 121.6, 120.2, 118.9, 113.8. LC-MS (m/z) $[M - H]^-$ calcd for $C_{13}H_6Cl_2N_3O_2$ 305.9843, found 305.9795.

2-(2-Chloro-6-fluorophenyl)-6-nitro-1H-benzodimidazole (2e). Yellow solid, mp 183–184 °C. 1H NMR (500 MHz, DMSO- d_6 , δ ppm): 8.59 (1H, s, H_{Ar}), 8.19 (1H, dd, $J = 9.0, 2.0$ Hz, H_{Ar}), 7.84 (1H, d, $J = 9.0$ Hz, H_{Ar}), 7.69 (1H, q, $J = 8.5$ Hz, H_{Ar}), 7.58 (1H, d, $J = 8.0$ Hz, H_{Ar}), 7.50 (1H, t, $J = 8.5$ Hz, H_{Ar}). ^{13}C NMR (125 MHz, DMSO- d_6 , δ ppm): 161.5, 159.5, 148.2, 143.0, 134.1, 134.0, 133.3, 133.2, 126.02, 125.99, 118.8, 118.6, 118.1, 115.1, 115.0. LC-MS (m/z) $[M - H]^-$ calcd for $C_{13}H_6ClFN_3O_2$ 290.0138, found 290.0016; $[M + H]^+$ calcd for $C_{13}H_8ClFN_3O_2$ 292.0284, found 292.0235.

2-(3,4-Dimethoxyphenyl)-6-nitro-1H-benzodimidazole (2f). Yellow solid, mp 126–128 °C. 1H NMR (500 MHz, DMSO- d_6 , δ ppm): 8.44 (1H, d, $J = 2.0$ Hz, H_{Ar}), 8.17 (1H, dd, $J = 8.5, 2.0$ Hz, H_{Ar}), 7.73 (1H, d, $J = 2.0$ Hz, H_{Ar}), 7.70 (1H, dd, $J = 8.0, 2.0$ Hz, H_{Ar}), 7.66 (1H, d, $J = 8.5$ Hz, H_{Ar}), 7.13 (1H, d, $J = 8.0$ Hz, H_{Ar}), 3.98 (3H, s, -OCH $_3$), 3.93 (3H, s, -OCH $_3$). ^{13}C NMR (125 MHz, DMSO- d_6 , δ ppm): 157.8, 153.5, 151.0, 145.0, 122.3 (2C), 121.7, 119.5 (2C), 115.2, 112.3 (2C), 111.5, 56.6, 56.5. LC-MS (m/z) $[M - H]^-$ calcd for $C_{15}H_{12}N_3O_4$ 298.0833, found 298.0710.

2-(4-Ethoxyphenyl)-6-nitro-1H-benzodimidazole (2g). Brown solid, mp 283–285 °C. 1H NMR (500 MHz, DMSO- d_6 , δ ppm): 13.30 (1H, s, -NH-), 8.41 (1H, s, H_{Ar}), 8.14 (2H, d, $J = 8.5$ Hz, H_{Ar}), 8.10 (1H, d, $J = 8.5$ Hz, H_{Ar}), 7.71 (1H, d, $J = 8.0$ Hz, H_{Ar}), 7.12 (2H, t, $J = 8.5$ Hz, H_{Ar}), 4.13 (2H, q, $J = 7.0$ Hz, -CH $_2$ -), 1.36 (3H, t, $J = 7.0$ Hz, -CH $_3$). ^{13}C NMR (125 MHz, DMSO- d_6 , δ ppm): 160.8, 142.5 (2C), 128.7 (2C), 121.2 (3C), 117.7 (3C), 115.0 (2C), 63.4, 14.5. LC-MS (m/z) $[M - H]^-$ calcd for $C_{15}H_{12}N_3O_3$ 282.0884,



found 282.0950; $[M + H]^+$ calcd for $C_{15}H_{14}N_3O_3$ 284.1030, found 284.1096.

2-Ethoxy-4-(6-nitro-1H-benzo[d]imidazole-2-yl)phenol (2h).

Yellow solid, mp 170–172 °C. 1H NMR (500 MHz, DMSO- d_6 , δ ppm): 8.46 (1H, d, $J = 2.0$ Hz, H_{Ar}), 8.18 (1H, dd, $J = 8.5, 2.0$ Hz, H_{Ar}), 7.73 (1H, d, $J = 2.0$ Hz, H_{Ar}), 7.66 (1H, d, $J = 8.5$ Hz, H_{Ar}), 7.61 (1H, dd, $J = 8.5, 2.0$ Hz, H_{Ar}), 6.99 (1H, d, $J = 8.0$ Hz, H_{Ar}), 4.25 (2H, q, $J = 7.0$ Hz, $-CH_2-$), 1.51 (3H, t, $J = 7.0$ Hz, $-CH_3$). ^{13}C NMR (125 MHz, DMSO- d_6 , δ ppm): 151.5, 148.8, 144.9, 121.9 (2C), 121.3 (2C), 119.3 (2C), 116.9 (2C), 112.8 (2C), 65.8, 15.1. LC-MS (m/z) $[M - H]^-$ calcd for $C_{15}H_{12}N_3O_4$ 298.0833, found 298.0721.

2-(4-Fluorophenyl)-6-nitro-1H-benzo[d]imidazole (1i).

Yellow solid, mp 219–221 °C. 1H NMR (500 MHz, DMSO- d_6 , δ ppm): 13.60 (1H, s, $-NH-$), 8.47 (1H, s, H_{Ar}), 8.26 (2H, d, $J = 9.0$ Hz, H_{Ar}), 8.13 (1H, dd, $J = 9.0, 1.5$ Hz, H_{Ar}), 7.76 (1H, s, H_{Ar}), 7.45 (2H, t, $J = 9.0$ Hz, H_{Ar}). ^{13}C NMR (125 MHz, DMSO- d_6 , δ ppm): 164.7, 162.7, 142.7 (2C), 129.5 (3C), 129.4, 125.6 (2C), 116.3 (2C), 116.2. LC-MS (m/z) $[M - H]^-$ calcd for $C_{13}H_7FN_3O_2$ 256.0528, found 256.0454; $[M + H]^+$ calcd for $C_{13}H_9FN_3O_2$ 258.0673, found 258.0654.

3-(6-Nitro-1H-benzo[d]imidazole-2-yl)phenol (2j). Red solid, mp 307–309 °C. 1H NMR (500 MHz, DMSO- d_6 , δ ppm): 12.89 (1H, s, $-NH-$), 9.78 (1H, s, $-OH$), 8.11–8.02 (4H, m, H_{Ar}), 7.42 (1H, t, $J = 8.0$ Hz, H_{Ar}), 7.34 (1H, d, $J = 7.0$ Hz, H_{Ar}), 6.97 (1H, dd, $J = 8.0, 1.5$ Hz, H_{Ar}). ^{13}C NMR (125 MHz, DMSO- d_6 , δ ppm): 157.5, 152.9, 144.5, 135.1, 133.9, 130.7, 126.3, 122.9, 119.6, 117.5, 113.5, 112.8, 110.7. LC-MS (m/z) $[M - H]^-$ calcd for $C_{13}H_8N_3O_3$ 254.0571, found 254.0576; $[M + H]^+$ calcd for $C_{13}H_{10}N_3O_3$ 256.0717, found 256.0738.

2-(3-Methoxyphenyl)-6-nitro-1H-benzo[d]imidazole (2k).

Yellow solid, mp 234–236 °C. 1H NMR (500 MHz, DMSO- d_6 , δ ppm): 13.02 (1H, s, $-NH-$), 8.46 (1H, s, H_{Ar}), 8.11 (1H, dd, $J = 9.0, 2.0$ Hz, H_{Ar}), 7.75 (1H, d, $J = 8.5$ Hz, H_{Ar}), 7.72–7.52 (3H, m, H_{Ar}), 7.09 (1H, dd, $J = 8.5, 1.5$ Hz, H_{Ar}), 3.85 (3H, s, $-OCH_3$). ^{13}C NMR (125 MHz, DMSO- d_6 , δ ppm): 159.5, 152.1, 142.1, 135.8, 133.6, 130.6, 126.9, 122.5, 120.2, 118.7, 116.5, 112.9, 111.5, 55.4. LC-MS (m/z) $[M - H]^-$ calcd for $C_{14}H_{10}N_3O_3$ 268.0728, found 268.0814; $[M + H]^+$ calcd for $C_{14}H_{12}N_3O_3$ 270.0873, found 270.0749.

2-Methoxy-5-(6-nitro-1H-benzo[d]imidazole-2-yl)phenol (2l).

Yellow solid, mp 263–265 °C. IR (ν , cm^{-1}): 1600.1 (C=N), 1436.9 (C=C), 1333.7 (N=O). 1H NMR (500 MHz, DMSO- d_6 , δ ppm): 8.50 (1H, s, H_{Ar}), 8.22–8.19 (1H, dd, $J = 9.0, 2.5$ Hz, H_{Ar}), 7.71 (1H, d, $J = 9.0$ Hz, H_{Ar}), 7.65–7.61 (2H, m, H_{Ar}), 7.14 (1H, d, $J = 8.5$ Hz, H_{Ar}), 3.98 (3H, s, $-OCH_3$). ^{13}C NMR (125 MHz, DMSO- d_6 , δ ppm): 153.7, 149.5, 147.6, 144.1, 126.3, 122.0 (2C), 120.9, 120.2 (2C), 115.9, 112.8 (2C), 56.4. LC-MS (m/z) $[M + H]^+$ calcd for $C_{14}H_{12}N_3O_4$ 286.0822, found 286.0871.

6-Nitro-2-(3-nitrophenyl)-1H-benzo[d]imidazole (2m).

Yellow solid, mp 290–292 °C. IR (ν , cm^{-1}): 1518.0 (C=N), 1446.6 (C=C), 1342.5 (N=O). 1H NMR (500 MHz, DMSO- d_6 , δ ppm): 13.92 (1H, s, $-NH-$), 9.00 (1H, t, $J = 2.0$ Hz, H_{Ar}), 8.62 (1H, d, $J = 8.0$ Hz, H_{Ar}), 8.50 (1H, s, H_{Ar}), 8.36 (1H, dd, $J = 8.5, 1.5$ Hz, H_{Ar}), 8.14 (1H, dd, $J = 8.5, 2.0$ Hz, H_{Ar}), 7.88 (1H, t, $J = 8.0$ Hz, H_{Ar}), 7.80 (1H, d, $J = 9.0$ Hz, H_{Ar}). ^{13}C NMR (125 MHz, DMSO- d_6 , δ ppm): 153.5, 148.3 (2C), 143.0, 133.0, 130.9 (2C), 130.5, 125.2, 121.4 (2C), 118.4 (2C). LC-MS (m/z) $[M - H]^-$ calcd for

$C_{13}H_7N_4O_4$ 283.0473, found 283.0440; $[M + H]^+$ calcd for $C_{13}H_9N_4O_4$ 285.0618, found 285.0601.

6-Nitro-2-(4-nitrophenyl)-1H-benzo[d]imidazole (2n). Yellow solid, mp 285–286 °C. 1H NMR (500 MHz, DMSO- d_6 , δ ppm): 13.36 (1H, s, $-NH-$), 8.50 (1H, s, H_{Ar}), 8.43 (2H, d, $J = 8.0$ Hz, H_{Ar}), 8.16 (2H, d, $J = 8.0$ Hz, H_{Ar}), 8.04 (1H, dd, $J = 9.0, 2.0$ Hz, H_{Ar}), 7.71 (1H, d, $J = 8.5$ Hz, H_{Ar}). ^{13}C NMR (125 MHz, DMSO- d_6 , δ ppm): 148.7, 143.6 (2C), 135.8, 134.2, 127.5 (2C), 124.4 (2C), 123.6, 118.9, 113.3, 111.7. LC-MS (m/z) $[M - H]^-$ calcd for $C_{13}H_7N_4O_4$ 283.0473, found 283.0411; $[M + H]^+$ calcd for $C_{13}H_9N_4O_4$ 285.0618, found 285.0670.

***N,N*-Dimethyl-4-(6-nitro-1H-benzo[d]imidazole-2-yl)aniline (2o).**

Red solid, mp 212–214 °C. IR (ν , cm^{-1}): 1606.7 (C=N), 1494.8 (C=C), 1330.9 (N=O). 1H NMR (500 MHz, DMSO- d_6 , δ ppm): 13.19 (1H, s, $-NH-$), 8.42–8.26 (1H, m, H_{Ar}), 8.07 (1H, d, $J = 8.5$ Hz, H_{Ar}), 8.03 (2H, d, $J = 8.5$ Hz, H_{Ar}), 7.69–7.60 (1H, m, H_{Ar}), 6.86 (2H, d, $J = 9.0$ Hz, H_{Ar}), 3.02 (6H, s, $-CH_3$). ^{13}C NMR (125 MHz, DMSO- d_6 , δ ppm): 154.1, 151.3, 127.6 (2C), 126.5 (2C), 122.4, 117.1 (3C), 112.5 (3C), 39.6. LC-MS (m/z) $[M - H]^-$ calcd for $C_{15}H_{13}N_4O_2$ 281.1044, found 281.0968; $[M + H]^+$ calcd for $C_{15}H_{15}N_4O_2$ 283.1190, found 283.1166.

2-(Benzo[d][1,3]dioxol-5-yl)-6-nitro-1H-benzo[d]imidazole (2p).

Yellow solid, mp 208–210 °C. 1H NMR (500 MHz, DMSO- d_6 , δ ppm): 12.85 (1H, s, $-NH-$), 8.41 (1H, s, H_{Ar}), 8.07 (1H, dd, $J = 9.0, 2.0$ Hz, H_{Ar}), 7.68 (1H, d, $J = 8.5$ Hz, H_{Ar}), 7.74 (1H, d, $J = 8.0$ Hz, H_{Ar}), 7.66–7.51 (1H, m, H_{Ar}), 7.10 (1H, d, $J = 8.0$ Hz, H_{Ar}), 6.15 (2H, s, $-CH_2-$). ^{13}C NMR (125 MHz, DMSO- d_6 , δ ppm): 150.2, 148.1 (3C), 143.6, 123.9 (2C), 121.5 (2C), 109.5 (2C), 106.8, 101.9, 89.4. LC-MS (m/z) $[M - H]^-$ calcd for $C_{14}H_8N_3O_4$ 282.0520, found 282.0568; $[M + H]^+$ calcd for $C_{14}H_{10}N_3O_4$ 284.0666, found 284.0653.

2-(Furan-2-yl)-6-nitro-1H-benzo[d]imidazole (2q).

Yellow solid, mp 228–230 °C. 1H NMR (500 MHz, DMSO- d_6 , δ ppm): 13.62 (1H, s, $-NH-$), 8.44 (1H, s, H_{Ar}), 8.13 (1H, dd, $J = 8.5, 2.0$ Hz, H_{Ar}), 8.03 (1H, d, $J = 1.0$ Hz, H_{Ar}), 7.72 (1H, s, H_{Ar}), 7.35 (1H, d, $J = 3.5$ Hz, H_{Ar}), 6.79 (1H, dd, $J = 3.5, 2.0$ Hz, H_{Ar}). ^{13}C NMR (125 MHz, DMSO- d_6 , δ ppm): 146.9, 145.6 (2C), 145.2 (3C), 119.7 (2C), 113.9, 113.6 (2C). LC-MS (m/z) $[M - H]^-$ calcd for $C_{11}H_6N_3O_3$ 228.0415, found 228.0409.

4.2.2 General procedure for the preparation of *N*,6-disubstituted 1H-benzimidazole derivatives (3a–x and 4a–r)

The reflux method. A mixture of 6-substituted 1H-benzimidazole derivatives 1–2 (1 mmol) and potassium carbonate (1 mmol) in acetonitrile (10 mL) was added to substituted halides (1.2 mmol) at 80 °C. The reaction mixture was then heated for 12–24 h and monitored by TLC. After cooling, the reaction crude was poured on a mixture of ice/water to give a solid that was filtered off in a Büchner funnel. The resulting solid was purified by column chromatography on silica gel using hexane/ethyl acetate as eluent. Reaction yields ranged within 26–43%.

The microwave-assisted method. A mixture of 6-substituted 1H-benzimidazole derivatives 1–2 (1 mmol), potassium carbonate (1 mmol), acetonitrile (10 mL), and substituted halides (1.2 mmol) was placed in a microwave oven and irradiated at a power of 300 W for 20–60 min at 80 °C. After cooling, the reaction crude was poured on a mixture of ice/water to give a solid that was filtered off in a Büchner funnel. The resulting



solid was purified by column chromatography on silica gel using hexane/ethyl acetate as eluent. Reaction yields ranged within 40–50%.

1-Allyl-6-chloro-2-(2-chlorophenyl)-1H-benzodimidazole (3a). White solid, mp 91–92 °C. IR (ν , cm^{-1}): 1610.6 (C=N), 1452.4 (C=C), 761.9 (C-Cl). ^1H NMR (500 MHz, DMSO- d_6 , δ ppm): 7.79 (1H, d, $J = 1.5$ Hz, H_{Ar}), 7.73 (1H, d, $J = 8.5$ Hz, H_{Ar}), 7.69 (1H, d, $J = 8.5$ Hz, H_{Ar}), 7.64–7.60 (2H, m, H_{Ar}), 7.53 (1H, d, $J = 8.0$ Hz, H_{Ar}), 7.35 (1H, dd, $J = 8.5, 2.0$ Hz, H_{Ar}), 5.85–5.79 (1H, m, -CH=), 5.09 (1H, d, $J = 10.5$ Hz, =CH₂), 4.87 (1H, d, $J = 17.0$ Hz, =CH₂), 4.70 (2H, s, -CH₂-). ^{13}C NMR (125 MHz, DMSO- d_6 , δ ppm): 151.8, 143.3, 141.2, 135.3, 132.9, 132.1, 129.6, 127.3, 126.5, 122.8, 120.7, 118.8, 117.2, 112.5, 111.0, 46.2. LC-MS (m/z) [$M + H$]⁺ calcd for C₁₆H₁₃Cl₂N₂ 303.0450, found 303.09.

1-Allyl-6-chloro-2-(4-chlorophenyl)-1H-benzodimidazole (3b). White solid, mp 95–97 °C. IR (ν , cm^{-1}): 1608.6 (C=N), 1456.3 (C=C), 790.8 (C-Cl). ^1H NMR (500 MHz, DMSO- d_6 , δ ppm): 7.90 (2H, d, $J = 8.5$ Hz, H_{Ar}), 7.77 (1H, d, $J = 1.5$ Hz, H_{Ar}), 7.71 (1H, d, $J = 8.5$ Hz, H_{Ar}), 7.58 (2H, d, $J = 9.0$ Hz, H_{Ar}), 7.32 (1H, dd, $J = 8.5, 2.0$ Hz, H_{Ar}), 6.08–6.01 (1H, m, -CH=), 5.20 (1H, d, $J = 10.5$ Hz, =CH₂), 4.94 (1H, d, $J = 17.0$ Hz, =CH₂), 4.87 (2H, s, -CH₂-). ^{13}C NMR (125 MHz, DMSO- d_6 , δ ppm): 153.3, 143.3, 141.2, 136.6, 135.0, 133.1, 130.7 (2C), 128.9 (2C), 127.2, 122.8, 120.5, 118.6, 112.4, 46.7. LC-MS (m/z) [$M + H$]⁺ calcd for C₁₆H₁₃Cl₂N₂ 303.0450, found 303.19.

1-Allyl-6-chloro-2-(2,4-dichlorophenyl)-1H-benzodimidazole (3c). White solid, mp 79–81 °C. IR (ν , cm^{-1}): 1609.5 (C=N), 1450.5 (C=C), 790.8 (C-Cl). ^1H NMR (500 MHz, DMSO- d_6 , δ ppm): 7.88 (1H, s, H_{Ar}), 7.79 (1H, d, $J = 1.5$ Hz, H_{Ar}), 7.74–7.70 (3H, m, H_{Ar}), 7.33 (1H, dd, $J = 8.5, 1.5$ Hz, H_{Ar}), 5.85–5.80 (1H, m, -CH=), 5.09 (1H, d, $J = 10.5$ Hz, =CH₂), 4.87 (1H, dd, $J = 17.0, 1.5$ Hz, =CH₂), 4.72 (2H, s, -CH₂-). ^{13}C NMR (125 MHz, DMSO- d_6 , δ ppm): 150.8, 143.2, 141.2, 135.9, 134.2, 133.5, 132.4, 129.4, 128.1, 127.7, 126.7, 123.0, 120.8, 118.9, 112.6, 46.3. LC-MS (m/z) [$M + H$]⁺ calcd for C₁₆H₁₂Cl₃N₂ 337.0061, found 336.17.

1-Allyl-6-chloro-2-(3,4-dichlorophenyl)-1H-benzodimidazole (3d). White solid, mp 96–98 °C. IR (ν , cm^{-1}): 1610.6 (C=N), 1458.2 (C=C), 792.9 (C-Cl). ^1H NMR (500 MHz, DMSO- d_6 , δ ppm): 8.01 (1H, d, $J = 2.0$ Hz, H_{Ar}), 7.85 (1H, d, $J = 8.5$ Hz, H_{Ar}), 7.78 (1H, d, $J = 2.0$ Hz, H_{Ar}), 7.74 (1H, d, $J = 8.5$ Hz, H_{Ar}), 7.62 (1H, d, $J = 8.5$ Hz, H_{Ar}), 7.35 (1H, dd, $J = 8.5, 2.0$ Hz, H_{Ar}), 6.05–6.01 (1H, m, -CH=), 5.21 (1H, d, $J = 10.5$ Hz, =CH₂), 4.98 (1H, dd, $J = 17.0, 1.5$ Hz, =CH₂), 4.88 (2H, s, -CH₂-). ^{13}C NMR (125 MHz, DMSO- d_6 , δ ppm): 151.9, 143.1, 141.1, 136.6, 134.7, 133.1, 131.6, 130.6, 128.9, 127.5, 126.9, 123.1, 120.7, 118.7, 112.5, 46.8. LC-MS (m/z) [$M + H$]⁺ calcd for C₁₆H₁₂Cl₃N₂ 337.0061, found 337.11.

1-Allyl-6-chloro-2-(3,4-dimethoxyphenyl)-1H-benzodimidazole (3e). White solid, mp 108–110 °C. IR (ν , cm^{-1}): 1608.9 (C=N), 1459.3 (C=C), 1248.0 (C-O). ^1H NMR (500 MHz, DMSO- d_6 , δ ppm): 7.74 (1H, d, $J = 1.5$ Hz, H_{Ar}), 7.69 (1H, d, $J = 8.5$ Hz, H_{Ar}), 7.53 (1H, d, $J = 8.5$ Hz, H_{Ar}), 7.33–7.25 (2H, m, H_{Ar}), 7.14 (1H, d, $J = 8.5$ Hz, H_{Ar}), 6.13–6.07 (1H, m, -CH=), 5.24 (1H, d, $J = 10.0$ Hz, =CH₂), 4.92 (1H, dd, $J = 17.0, 1.5$ Hz, =CH₂), 4.90 (2H, s, -CH₂-), 3.85 (3H, s, -CH₃), 3.82 (3H, s, -CH₃). ^{13}C NMR (125 MHz, DMSO- d_6 , δ ppm): 154.5, 150.4, 148.7, 143.4, 141.3, 136.7, 134.7, 133.3, 126.7, 122.3, 121.8, 120.2, 118.3, 112.3,

111.6, 55.6, 55.3, 46.8. LC-MS (m/z) [$M + H$]⁺ calcd for C₁₈H₁₈ClN₂O₂ 329.1051, found 329.22.

1-Allyl-6-chloro-2-(4-ethoxyphenyl)-1H-benzodimidazole (3f). White solid, mp 92–94 °C. IR (ν , cm^{-1}): 1610.5 (C=N), 1462.0 (C=C), 1244.1 (C-O), 790.8 (C-Cl). ^1H NMR (500 MHz, DMSO- d_6 , δ ppm): 7.72 (1H, d, $J = 1.5$ Hz, H_{Ar}), 7.70 (2H, d, $J = 8.5$ Hz, H_{Ar}), 7.53 (1H, d, $J = 8.5$ Hz, H_{Ar}), 7.28 (1H, dd, $J = 8.5, 2.0$ Hz, H_{Ar}), 7.10 (2H, d, $J = 9.0$ Hz, H_{Ar}), 6.11–6.03 (1H, m, -CH=), 5.20 (1H, d, $J = 10.5$ Hz, =CH₂), 4.92 (2H, s, -CH₂-), 4.88 (1H, d, $J = 17.0$ Hz, =CH₂), 4.12 (2H, q, $J = 7.0$ Hz, -CH₂-), 1.37 (3H, t, $J = 7.0$ Hz, -CH₃). ^{13}C NMR (125 MHz, DMSO- d_6 , δ ppm): 159.9, 154.5, 143.4, 134.7, 133.2, 130.4 (2C), 126.5, 122.3, 121.6, 118.3, 116.7, 114.7 (2C), 112.2, 63.3, 46.8, 14.5. LC-MS (m/z) [$M + H$]⁺ calcd for C₁₈H₁₈ClN₂O 313.1102, found 313.24.

1-Allyl-6-chloro-2-(4-fluorophenyl)-1H-benzodimidazole (3g). White solid, mp 106–108 °C. IR (ν , cm^{-1}): 1606.7 (C=N), 1458.4 (C=C), 1224.8 (C-F), 736.8 (C-Cl). ^1H NMR (500 MHz, DMSO- d_6 , δ ppm): 7.82 (2H, d, $J = 8.5$ Hz, H_{Ar}), 7.76 (1H, d, $J = 2.0$ Hz, H_{Ar}), 7.70 (1H, d, $J = 8.5$ Hz, H_{Ar}), 7.41 (2H, d, $J = 8.5$ Hz, H_{Ar}), 7.32 (1H, dd, $J = 8.5, 2.0$ Hz, H_{Ar}), 6.08–6.00 (1H, m, -CH=), 5.20 (1H, d, $J = 10.5$ Hz, =CH₂), 4.92 (1H, dd, $J = 17.0, 1.5$ Hz, =CH₂), 4.87 (2H, s, -CH₂-). ^{13}C NMR (125 MHz, DMSO- d_6 , δ ppm): 164.0, 153.5, 143.3, 136.5, 133.1, 131.4, 127.0 (2C), 122.7, 120.4, 118.5, 116.7 (2C), 115.9, 112.4, 46.7. LC-MS (m/z) [$M + H$]⁺ calcd for C₁₆H₁₃ClFN₂ 287.0746, found 287.0679.

1-Allyl-6-chloro-2-(3-nitrophenyl)-1H-benzodimidazole (3h). Yellow solid, mp 130–132 °C. IR (ν , cm^{-1}): 1612.5 (C=N), 1533.4 (C=C), 1350.2 (N=O), 707.9 (C-Cl). ^1H NMR (500 MHz, DMSO- d_6 , δ ppm): 8.58 (1H, t, $J = 2.0$ Hz, H_{Ar}), 8.41 (1H, d, $J = 9.0$ Hz, H_{Ar}), 8.24 (1H, d, $J = 9.0$ Hz, H_{Ar}), 7.90–7.86 (1H, m, H_{Ar}), 7.83 (1H, d, $J = 2.0$ Hz, H_{Ar}), 7.77 (1H, d, $J = 9.0$ Hz, H_{Ar}), 7.37 (1H, dd, $J = 9.0, 2.0$ Hz, H_{Ar}), 6.14–6.06 (1H, m, -CH=), 5.25 (1H, dd, $J = 10.5, 1.0$ Hz, =CH₂), 5.02 (2H, s, -CH₂-), 4.93 (1H, dd, $J = 17.0, 1.0$ Hz, =CH₂). ^{13}C NMR (125 MHz, DMSO- d_6 , δ ppm): 152.0, 147.9, 143.2, 141.1, 136.7, 135.1, 133.0, 131.0, 127.7, 124.6, 123.5, 122.9, 120.8, 118.8, 112.6, 46.9. LC-MS (m/z) [$M + H$]⁺ calcd for C₁₆H₁₃ClN₃O₂ 314.0691, found 314.18.

1-Allyl-6-chloro-2-(4-nitrophenyl)-1H-benzodimidazole (3i). Yellow solid, mp 140–142 °C. IR (ν , cm^{-1}): 1600.9 (C=N), 1460.1 (C=C), 1347.6 (N=O), 707.9 (C-Cl). ^1H NMR (500 MHz, DMSO- d_6 , δ ppm): 8.41 (2H, d, $J = 9.0$ Hz, H_{Ar}), 8.07 (2H, d, $J = 9.0$ Hz, H_{Ar}), 7.83 (1H, d, $J = 2.0$ Hz, H_{Ar}), 7.65 (1H, d, $J = 8.5$ Hz, H_{Ar}), 7.37 (1H, dd, $J = 8.5, 2.0$ Hz, H_{Ar}), 6.09–6.02 (1H, m, -CH=), 5.30 (1H, dd, $J = 10.5, 1.0$ Hz, =CH₂), 5.01 (2H, s, -CH₂-), 4.89 (1H, dd, $J = 17.0, 1.5$ Hz, =CH₂). ^{13}C NMR (125 MHz, DMSO- d_6 , δ ppm): 152.2, 148.1, 143.3, 141.2, 136.8, 135.6, 133.0, 130.3, 127.8 (2C), 123.9 (2C), 120.9, 118.9, 112.7, 46.9. LC-MS (m/z) [$M + H$]⁺ calcd for C₁₆H₁₃ClN₃O₂ 314.0691, found 314.16.

1-Benzyl-6-chloro-2-(2-chlorophenyl)-1H-benzodimidazole (3j). White solid, mp 83–84 °C. IR (ν , cm^{-1}): 1606.9 (C=N), 1454.3 (C=C), 723.3 (C-Cl). ^1H NMR (500 MHz, DMSO- d_6 , δ ppm): 7.79 (1H, d, $J = 1.5$ Hz, H_{Ar}), 7.74 (1H, d, $J = 9.0$ Hz, H_{Ar}), 7.67 (1H, d, $J = 8.5$ Hz, H_{Ar}), 7.62–7.57 (2H, m, H_{Ar}), 7.55 (1H, d, $J = 9.0$ Hz, H_{Ar}), 7.30 (1H, dd, $J = 8.5, 2.0$ Hz, H_{Ar}), 7.24–7.21 (3H, m, H_{Ar}), 6.93 (2H, dd, $J = 8.5, 2.0$ Hz, H_{Ar}), 5.32 (2H, s, -CH₂-). ^{13}C NMR (125 MHz, DMSO- d_6 , δ ppm): 152.2, 141.3, 136.0, 135.5, 133.6, 133.1, 132.3, 129.8, 129.1, 128.6 (2C), 127.7, 126.7 (2C), 123.1,



122.7, 120.9, 119.0, 112.7, 47.4. LC-MS (m/z) $[M + H]^+$ calcd for $C_{20}H_{15}Cl_2N_2$ 353.0607, found 353.03.

1-Benzyl-6-chloro-2-(4-chlorophenyl)-1H-benzodimidazole (3k).

White solid, mp 98–101 °C. IR (ν , cm^{-1}): 1606.8 (C=N), 1454.5 (C=C), 723.3 (C-Cl). 1H NMR (500 MHz, DMSO- d_6 , δ ppm): 7.80 (1H, d, $J = 2.0$ Hz, H_{Ar}), 7.76–7.73 (3H, m, H_{Ar}), 7.59 (2H, d, $J = 8.5$ Hz, H_{Ar}), 7.31 (1H, dd, $J = 8.5, 2.0$ Hz, H_{Ar}), 7.29–7.24 (3H, m, H_{Ar}), 6.97 (2H, dd, $J = 8.5, 2.0$ Hz, H_{Ar}), 5.61 (2H, s, $-CH_2-$). ^{13}C NMR (125 MHz, DMSO- d_6 , δ ppm): 153.6, 143.4, 141.3, 136.7, 135.0, 134.9, 130.8, 128.9 (2C), 128.5 (2C), 127.6 (2C), 126.8 (2C), 123.0, 120.6, 118.7, 112.6, 47.6. LC-MS (m/z) $[M + H]^+$ calcd for $C_{20}H_{15}Cl_2N_2$ 353.0607, found 353.08.

1-Benzyl-6-chloro-2-(2,4-dichlorophenyl)-1H-benzodimidazole (3l).

White solid, mp 119–121 °C. IR (ν , cm^{-1}): 1645.3 (C=N), 1452.4 (C=C), 794.6 (C-Cl). 1H NMR (500 MHz, DMSO- d_6 , δ ppm): 7.85 (1H, d, $J = 2.0$ Hz, H_{Ar}), 7.81 (1H, d, $J = 1.5$ Hz, H_{Ar}), 7.75 (1H, d, $J = 8.5$ Hz, H_{Ar}), 7.63 (1H, dd, $J = 8.5$ Hz, H_{Ar}), 7.58 (1H, dd, $J = 8.5, 1.5$ Hz, H_{Ar}), 7.31 (1H, dd, $J = 8.5, 2.0$ Hz, H_{Ar}), 7.26–7.21 (3H, m, H_{Ar}), 6.95 (2H, dd, $J = 8.5, 2.0$ Hz, H_{Ar}), 5.35 (2H, s, $-CH_2-$). ^{13}C NMR (125 MHz, DMSO- d_6 , δ ppm): 151.1, 143.4, 141.3, 136.0, 135.9, 135.6, 134.3, 133.6, 129.4 (2C), 128.3, 127.7, 126.8 (2C), 123.2, 122.7, 120.9, 119.0, 112.7, 47.4. LC-MS (m/z) $[M + H]^+$ calcd for $C_{20}H_{14}Cl_3N_2$ 387.0217, found 386.98.

1-Benzyl-6-chloro-2-(3,4-dichlorophenyl)-1H-benzodimidazole (3m).

White solid, mp 143–145 °C. IR (ν , cm^{-1}): 1601.8 (C=N), 1452.4 (C=C), 702.5 (C-Cl). 1H NMR (500 MHz, DMSO- d_6 , δ ppm): 7.80–7.74 (2H, m, H_{Ar}), 7.70–7.69 (2H, m, H_{Ar}), 7.56 (1H, d, $J = 9.0$ Hz, H_{Ar}), 7.30 (1H, dd, $J = 8.5, 2.0$ Hz, H_{Ar}), 7.28–7.24 (3H, m, H_{Ar}), 6.99 (2H, d, $J = 7.5$ Hz, H_{Ar}), 5.61 (2H, s, $-CH_2-$). ^{13}C NMR (125 MHz, DMSO- d_6 , δ ppm): 152.3, 143.3, 141.2, 136.9, 134.9, 133.1, 131.7, 130.8, 130.2, 129.1 (2C), 127.7, 127.1 (2C), 126.1, 123.4, 120.8, 118.9, 112.7, 47.7. LC-MS (m/z) $[M + H]^+$ calcd for $C_{20}H_{14}Cl_3N_2$ 387.0217, found 386.89.

1-Benzyl-6-chloro-2-(3,4-dimethoxyphenyl)-1H-benzodimidazole (3n).

White solid, mp 157–159 °C. IR (ν , cm^{-1}): 1610.6 (C=N), 1494.8 (C=C), 1253.7 (C-O), 815.9 (C-Cl). 1H NMR (500 MHz, DMSO- d_6 , δ ppm): 7.71 (1H, d, $J = 8.5$ Hz, H_{Ar}), 7.62 (1H, d, $J = 2.0$ Hz, H_{Ar}), 7.34–7.31 (2H, m, H_{Ar}), 7.28–7.25 (3H, m, H_{Ar}), 7.23 (1H, d, $J = 2.0$ Hz, H_{Ar}), 7.08 (1H, d, $J = 8.5$ Hz, H_{Ar}), 7.02 (2H, d, $J = 7.0$ Hz, H_{Ar}), 5.61 (2H, s, $-CH_2-$), 3.81 (3H, s, $-OCH_3$), 3.65 (3H, s, $-OCH_3$). ^{13}C NMR (125 MHz, DMSO- d_6 , δ ppm): 154.4, 150.3, 148.6, 141.3, 136.9, 136.8, 128.8 (2C), 127.5, 126.9 (2C), 125.9, 122.5, 121.8, 121.7, 120.3, 112.3, 111.7, 110.8, 55.6, 55.3, 47.6. The NOESY correlation including: δ_H 7.71 with δ_H 7.28–7.25; δ_H 7.62 with δ_H 5.61; δ_H 7.34–7.31 with δ_H 7.02; δ_H 7.28–7.25 with δ_H 7.08, 5.61 and 3.81–3.65; δ_H 7.08 with δ_H 3.81; δ_H 7.02 with δ_H 5.61. LC-MS (m/z) $[M + H]^+$ calcd for $C_{22}H_{20}ClN_2O_2$ 379.1208, found 379.13.

1-Benzyl-6-chloro-2-(4-ethoxyphenyl)-1H-benzodimidazole (3o).

White solid, mp 128–129 °C. IR (ν , cm^{-1}): 1611.4 (C=N), 1462.0 (C=C), 1249.9 (C-O), 794.7 (C-Cl). 1H NMR (500 MHz, DMSO- d_6 , δ ppm): 7.75 (1H, d, $J = 1.5$ Hz, H_{Ar}), 7.70 (1H, d, $J = 8.5$ Hz, H_{Ar}), 7.65 (2H, d, $J = 8.5$ Hz, H_{Ar}), 7.32 (1H, d, $J = 9.0$ Hz, H_{Ar}), 7.29–7.23 (3H, m, H_{Ar}), 7.05 (2H, d, $J = 8.5$ Hz, H_{Ar}), 6.99 (2H, d, $J = 7.5$ Hz, H_{Ar}), 5.58 (2H, s, $-CH_2-$), 4.09 (2H, q, $J = 7.0$ Hz, $-CH_2-$), 1.35 (3H, t, $J = 7.0$ Hz, $-CH_3$). ^{13}C NMR (125 MHz, DMSO- d_6 , δ ppm): 159.9, 154.8, 143.5, 136.7, 134.7, 130.5

(2C), 128.8 (2C), 127.5, 126.8 (2C), 122.4, 121.6, 120.3, 118.4, 114.7 (2C), 112.3, 63.3, 47.6, 14.5. LC-MS (m/z) $[M + H]^+$ calcd for $C_{22}H_{20}ClN_2O$ 363.1259, found 363.18.

1-Benzyl-6-chloro-2-(4-fluorophenyl)-1H-benzodimidazole (3p).

White solid, mp 117–118 °C. IR (ν , cm^{-1}): 1606.7 (C=N), 1475.2 (C=C), 1226.7 (C-F), 794.7 (C-Cl). 1H NMR (500 MHz, DMSO- d_6 , δ ppm): 7.73 (2H, d, $J = 8.5$ Hz, H_{Ar}), 7.66 (1H, d, $J = 2.0$ Hz, H_{Ar}), 7.52 (1H, d, $J = 8.5$ Hz, H_{Ar}), 7.37 (2H, d, $J = 8.5$ Hz, H_{Ar}), 7.30 (1H, d, $J = 8.5$ Hz, H_{Ar}), 7.28–7.24 (3H, m, H_{Ar}), 6.98 (2H, d, $J = 8.0$ Hz, H_{Ar}), 5.59 (2H, s, $-CH_2-$). ^{13}C NMR (125 MHz, DMSO- d_6 , δ ppm): 171.5, 162.9, 152.9, 146.2, 145.9, 144.1, 140.9, 138.3, 137.0, 136.2, 135.7, 132.3, 130.0 (2C), 128.1 (2C), 125.5 (2C), 122.0, 120.5 (2C), 57.1. LC-MS (m/z) $[M + H]^+$ calcd for $C_{20}H_{15}ClFN_2$ 337.0902, found 337.0900.

1-Benzyl-6-chloro-2-(3-nitrophenyl)-1H-benzodimidazole (3q).

Yellow solid, mp 143–145 °C. IR (ν , cm^{-1}): 1603.6 (C=N), 1510.3 (C=C), 727.2 (C-Cl). 1H NMR (500 MHz, DMSO- d_6 , δ ppm): 8.50 (1H, d, $J = 2.0$ Hz, H_{Ar}), 8.36 (1H, d, $J = 9.0$ Hz, H_{Ar}), 8.17 (1H, d, $J = 9.0$ Hz, H_{Ar}), 7.86–7.79 (1H, m, H_{Ar}), 7.75 (1H, d, $J = 2.0$ Hz, H_{Ar}), 7.61 (1H, d, $J = 9.0$ Hz, H_{Ar}), 7.35 (1H, d, $J = 8.5$ Hz, H_{Ar}), 7.30–7.23 (3H, m, H_{Ar}), 7.01 (2H, d, $J = 8.0$ Hz, H_{Ar}), 5.67 (2H, s, $-CH_2-$). ^{13}C NMR (125 MHz, DMSO- d_6 , δ ppm): 152.3, 147.9, 143.3, 141.2, 137.0, 135.2, 131.1, 130.5, 128.8 (2C), 127.8, 127.1 (2C), 126.1, 124.6, 123.7, 120.9, 119.0, 112.8, 47.8. LC-MS (m/z) $[M + H]^+$ calcd for $C_{20}H_{15}ClN_3O_2$ 364.0847, found 364.14.

1-Benzyl-6-chloro-2-(4-nitrophenyl)-1H-benzodimidazole (3r).

Yellow solid, mp 186–188 °C. IR (ν , cm^{-1}): 1601.4 (C=C), 1518.9 (C=N), 1348.1 (N=O), 732.7 (C-Cl). 1H NMR (500 MHz, DMSO- d_6 , δ ppm): 8.36 (2H, d, $J = 8.0$ Hz, H_{Ar}), 8.04 (2H, d, $J = 8.0$ Hz, H_{Ar}), 7.76 (1H, s, H_{Ar}), 7.61 (1H, d, $J = 9.0$ Hz, H_{Ar}), 7.34 (1H, t, $J = 8.5$ Hz, H_{Ar}), 7.29–7.22 (3H, m, H_{Ar}), 6.98 (2H, d, $J = 8.5$ Hz, H_{Ar}), 5.68 (2H, s, $-CH_2-$). ^{13}C NMR (125 MHz, DMSO- d_6 , δ ppm): 152.5, 148.1, 143.4, 137.7, 136.3, 135.8, 130.4, 128.8 (2C), 127.9 (2C), 126.1 (2C), 123.9 (2C), 123.1, 121.0, 119.0, 112.9, 47.6. LC-MS (m/z) $[M + H]^+$ calcd for $C_{20}H_{15}ClN_3O_2$ 364.0847, found 364.0811.

4-(1-Benzyl-6-chloro-1H-benzodimidazole-2-yl)-N,N-dimethylaniline (3s).

White solid, mp 184–186 °C. IR (ν , cm^{-1}): 1607.6 (C=N), 1456.3 (C=C), 796.8 (C-Cl). 1H NMR (500 MHz, DMSO- d_6 , δ ppm): 7.66–7.50 (4H, m, H_{Ar}), 7.33 (1H, t, $J = 8.5$ Hz, H_{Ar}), 7.30–7.21 (3H, m, H_{Ar}), 7.01 (2H, d, $J = 7.5$ Hz, H_{Ar}), 6.78 (2H, d, $J = 8.5$ Hz, H_{Ar}), 5.58 (2H, s, $-CH_2-$), 2.96 (6H, s, $-CH_3$). ^{13}C NMR (125 MHz, DMSO- d_6 , δ ppm): 154.8, 150.3, 148.6, 143.5, 136.8, 134.9, 128.8 (2C), 127.5 (2C), 126.6 (2C), 125.9, 122.5, 121.8, 118.4, 112.3 (2C), 111.7, 47.7, 39.0 (2C). LC-MS (m/z) $[M + H]^+$ calcd for $C_{22}H_{21}ClN_3$ 362.1419, found 361.19.

6-Chloro-1-(2-chlorobenzyl)-2-(4-chlorophenyl)-1H-benzodimidazole (3t). White solid, mp 140–142 °C. IR (ν , cm^{-1}): 1610.6 (C=N), 1465.9 (C=C), 752.2 (C-Cl). 1H NMR (500 MHz, DMSO- d_6 , δ ppm): 7.80 (1H, d, $J = 2.0$ Hz, H_{Ar}), 7.76 (1H, d, $J = 8.5$ Hz, H_{Ar}), 7.67 (2H, d, $J = 8.5$ Hz, H_{Ar}), 7.60 (2H, d, $J = 8.5$ Hz, H_{Ar}), 7.48 (1H, dd, $J = 8.0, 1.5$ Hz, H_{Ar}), 7.32–7.27 (2H, m, H_{Ar}), 7.20 (1H, d, $J = 8.5$ Hz, H_{Ar}), 6.65 (1H, d, $J = 8.0$ Hz, H_{Ar}), 5.61 (2H, s, $-CH_2-$). ^{13}C NMR (125 MHz, DMSO- d_6 , δ ppm): 153.8, 143.4, 135.1, 134.8, 133.6, 131.5, 130.7, 130.6, 129.8, 129.5 (2C), 129.0 (2C), 127.8, 127.3, 123.2, 120.8, 118.9, 112.5, 46.1. LC-MS (m/z) $[M + H]^+$ calcd for $C_{20}H_{14}Cl_3N_2$ 387.0217, found 386.90.



6-Chloro-1-(4-chlorobenzyl)-2-(3,4-dichlorophenyl)-1H-benzodimidazole (3u). White solid, mp 168–169 °C. IR (ν , cm^{-1}): 1610.3 (C=N), 1458.7 (C=C), 754.1 (C-Cl). ^1H NMR (500 MHz, DMSO- d_6 , δ ppm): 7.94 (1H, d, $J = 2.0$ Hz, H_{Ar}), 7.82–7.66 (3H, m, H_{Ar}), 7.57 (1H, d, $J = 9.0$ Hz, H_{Ar}), 7.37–7.30 (3H, m, H_{Ar}), 7.02–6.99 (2H, m, H_{Ar}), 5.62 (2H, s, $-\text{CH}_2-$). ^{13}C NMR (125 MHz, DMSO- d_6 , δ ppm): 153.5, 142.9, 135.3, 134.9, 133.4, 131.7, 130.8, 129.9, 129.6, 129.2 (2C), 128.7 (2C), 127.6, 127.0, 123.1, 120.6, 118.5, 112.4, 46.8. LC-MS (m/z) [$\text{M} + \text{H}$] $^+$ calcd for $\text{C}_{20}\text{H}_{12}\text{Cl}_4\text{N}_2$ 420.9827, found 420.9731.

6-Chloro-1-(4-chlorobenzyl)-2-(furan-2-yl)-1H-benzodimidazole (3v). White solid, mp 129–131 °C. IR (ν , cm^{-1}): 1612.4 (C=N), 1459.3 (C=C), 753.2 (C-Cl). ^1H NMR (500 MHz, DMSO- d_6 , δ ppm): 7.94 (1H, d, $J = 2.0$ Hz, H_{Ar}), 7.75 (1H, d, $J = 2.0$ Hz, H_{Ar}), 7.63 (1H, d, $J = 8.5$ Hz, H_{Ar}), 7.36 (2H, d, $J = 8.5$ Hz, H_{Ar}), 7.30 (1H, dd, $J = 8.5, 2.0$ Hz, H_{Ar}), 7.19 (1H, d, $J = 3.0$ Hz, H_{Ar}), 7.11 (2H, d, $J = 8.5$ Hz, H_{Ar}), 6.73 (1H, dd, $J = 4.0, 1.5$ Hz, H_{Ar}), 5.80 (2H, s, $-\text{CH}_2-$). ^{13}C NMR (125 MHz, DMSO- d_6 , δ ppm): 151.8, 148.3, 143.6, 141.0, 136.8, 135.6, 134.9, 132.9, 130.2 (2C), 127.0 (2C), 123.4, 123.0, 120.9, 116.9, 111.2, 46.7. LC-MS (m/z) [$\text{M} - \text{H}$] $^-$ calcd for $\text{C}_{18}\text{H}_{11}\text{Cl}_2\text{N}_2\text{O}$ 341.0254, found 341.0219; [$\text{M} + \text{H}$] $^+$ calcd for $\text{C}_{18}\text{H}_{13}\text{Cl}_2\text{N}_2\text{O}$ 343.0399, found 343.0349.

5-Chloro-1-(4-chlorobenzyl)-2-(4-chlorophenyl)-1H-benzodimidazole (3w). White solid, mp 165–167 °C. IR (ν , cm^{-1}): 1600.9 (C=N), 1465.9 (C=C), 796.6 (C-Cl). ^1H NMR (500 MHz, DMSO- d_6 , δ ppm): 7.80 (1H, d, $J = 2.0$ Hz, H_{Ar}), 7.73 (2H, d, $J = 9.0$ Hz, H_{Ar}), 7.60 (2H, d, $J = 8.5$ Hz, H_{Ar}), 7.53 (1H, d, $J = 9.0$ Hz, H_{Ar}), 7.35 (2H, d, $J = 8.5$ Hz, H_{Ar}), 7.30 (1H, dd, $J = 8.5, 2.0$ Hz, H_{Ar}), 7.00 (2H, d, $J = 9.0$ Hz, H_{Ar}), 5.60 (2H, s, $-\text{CH}_2-$). ^{13}C NMR (125 MHz, DMSO- d_6 , δ ppm): 153.5, 143.4, 135.5, 135.0, 134.7, 132.2, 130.8, 128.9 (2C), 128.8 (2C), 128.4 (2C), 128.0 (2C), 126.9, 123.1, 118.8, 112.5, 48.0. The NOESY correlation including: δ_{H} 7.73 with δ_{H} 7.60 and 5.60; δ_{H} 7.53 with δ_{H} 7.30 and 5.60; δ_{H} 7.35 with δ_{H} 7.00; δ_{H} 7.00 with δ_{H} 5.60. LC-MS (m/z) [$\text{M} + \text{H}$] $^+$ calcd for $\text{C}_{20}\text{H}_{14}\text{Cl}_3\text{N}_2$ 387.0217, found 386.92.

1-Benzyl-5-chloro-2-(3,4-dimethoxyphenyl)-1H-benzodimidazole (3x). White solid, mp 146–148 °C. IR (ν , cm^{-1}): 1604.8 (C=N), 1487.1 (C=C), 1222.9 (C-O), 790.8 (C-Cl). ^1H NMR (500 MHz, DMSO- d_6 , δ ppm): 7.74 (1H, d, $J = 2.0$ Hz, H_{Ar}), 7.49 (1H, d, $J = 8.5$ Hz, H_{Ar}), 7.33–7.23 (6H, m, H_{Ar}), 7.09 (1H, d, $J = 8.5$ Hz, H_{Ar}), 7.02 (2H, d, $J = 7.0$ Hz, H_{Ar}), 5.61 (2H, s, $-\text{CH}_2-$), 3.81–3.66 (6H, s, $-\text{CH}_3$). ^{13}C NMR (125 MHz, DMSO- d_6 , δ ppm): 154.8, 150.3, 148.6, 143.5, 136.8, 134.9, 128.8 (2C), 127.5 (2C), 126.6, 125.9, 122.5, 121.8, 121.7, 118.4, 112.3, 112.2, 111.7, 55.6, 55.3, 47.7. The NOESY correlation including: δ_{H} 7.49 with δ_{H} 7.28–7.23 and 5.61; δ_{H} 7.33–7.30 with δ_{H} 7.02; δ_{H} 7.28–7.23 with δ_{H} 7.09, 5.61 and 3.81–3.66; δ_{H} 7.09 with δ_{H} 3.81–3.66; δ_{H} 7.02 with δ_{H} 5.61. LC-MS (m/z) [$\text{M} + \text{H}$] $^+$ calcd for $\text{C}_{22}\text{H}_{20}\text{ClN}_2\text{O}_2$ 379.1208, found 379.14.

1-Allyl-2-(2,4-dichlorophenyl)-6-nitro-1H-benzodimidazole (4a). Yellow solid, mp 150–152 °C. IR (ν , cm^{-1}): 1516.1 (C=N), 1438.9 (C=C), 1332.8 (N=O), 734.9 (C-Cl). ^1H NMR (500 MHz, DMSO- d_6 , δ ppm): 8.62 (1H, d, $J = 2.0$ Hz, H_{Ar}), 8.24 (1H, d, $J = 9.0, 2.5$ Hz, H_{Ar}), 8.07 (1H, d, $J = 2.0$ Hz, H_{Ar}), 7.92 (1H, d, $J = 9.0$ Hz, H_{Ar}), 7.88 (1H, dd, $J = 8.5, 1.0$ Hz, H_{Ar}), 7.81 (1H, d, $J = 8.5$ Hz, H_{Ar}), 6.13–6.04 (1H, m, $-\text{CH}=\text{CH}_2$), 5.23 (1H, d, $J = 9.5$ Hz,

$=\text{CH}_2$), 5.06 (2H, s, $-\text{CH}_2-$), 4.92 (1H, d, $J = 17.5$ Hz, $=\text{CH}_2$). ^{13}C NMR (125 MHz, DMSO- d_6 , δ ppm): 155.5, 146.7, 143.3, 141.5, 140.2, 135.3, 133.6, 131.7, 130.9, 129.5, 119.8, 118.5, 117.1, 115.5, 111.8, 47.1. LC-MS (m/z) [$\text{M} + \text{H}$] $^+$ calcd for $\text{C}_{16}\text{H}_{12}\text{Cl}_2\text{N}_3\text{O}_2$ 348.0301, found 348.0136.

1-Allyl-2-(3,4-dichlorophenyl)-6-nitro-1H-benzodimidazole (4b). Yellow solid, mp 190–192 °C. IR (ν , cm^{-1}): 1518.0 (C=N), 1438.9 (C=C), 1334.7 (N=O), 742.6 (C-Cl). ^1H NMR (500 MHz, DMSO- d_6 , δ ppm): 8.61 (1H, d, $J = 2.0$ Hz, H_{Ar}), 8.23 (1H, dd, $J = 9.0, 2.5$ Hz, H_{Ar}), 8.07 (1H, d, $J = 2.0$ Hz, H_{Ar}), 7.92 (1H, d, $J = 9.0$ Hz, H_{Ar}), 7.88 (1H, d, $J = 8.5$ Hz, H_{Ar}), 7.80 (1H, d, $J = 8.5$ Hz, H_{Ar}), 6.13–6.04 (1H, m, $-\text{CH}=\text{CH}_2$), 5.23 (1H, d, $J = 10.5$ Hz, $=\text{CH}_2$), 5.10 (2H, s, $-\text{CH}_2-$), 4.90 (1H, d, $J = 17.5$ Hz, $=\text{CH}_2$). ^{13}C NMR (125 MHz, DMSO- d_6 , δ ppm): 155.5, 146.7, 143.3, 141.5, 140.2, 135.3, 133.7, 131.8, 130.9, 129.5, 119.8, 118.5, 117.1, 115.5, 111.9, 47.1. LC-MS (m/z) [$\text{M} + \text{H}$] $^+$ calcd for $\text{C}_{16}\text{H}_{12}\text{Cl}_2\text{N}_3\text{O}_2$ 348.0301, found 348.0306.

1-Allyl-2-(3,4-dimethoxyphenyl)-6-nitro-1H-benzodimidazole (4c). Yellow solid, mp 144–146 °C. IR (ν , cm^{-1}): 1516.2 (C=N), 1437.0 (C=C), 1332.8 (N=O). ^1H NMR (500 MHz, DMSO- d_6 , δ ppm): 8.57 (1H, d, $J = 2.0$ Hz, H_{Ar}), 8.20 (1H, dd, $J = 9.0, 2.0$ Hz, H_{Ar}), 7.92 (1H, d, $J = 9.0$ Hz, H_{Ar}), 7.87 (1H, d, $J = 8.5$ Hz, H_{Ar}), 7.40 (1H, d, $J = 2.0$ Hz, H_{Ar}), 7.17 (1H, dd, $J = 8.5, 2.0$ Hz, H_{Ar}), 6.19–6.09 (1H, m, $-\text{CH}=\text{CH}_2$), 5.27 (1H, d, $J = 10.5$ Hz, $=\text{CH}_2$), 5.10 (2H, s, $-\text{CH}_2-$), 4.92 (1H, d, $J = 17.0$ Hz, $=\text{CH}_2$), 3.86 (3H, s, $-\text{OCH}_3$), 3.83 (3H, s, $-\text{OCH}_3$). ^{13}C NMR (125 MHz, DMSO- d_6 , δ ppm): 158.1, 150.8, 150.7, 148.7, 143.0, 140.4, 135.3, 133.2, 122.0, 121.1, 119.1, 117.9, 114.9, 112.3, 111.3, 55.6, 55.3, 47.1. LC-MS (m/z) [$\text{M} + \text{H}$] $^+$ calcd for $\text{C}_{18}\text{H}_{18}\text{N}_3\text{O}_4$ 340.1292, found 340.1264.

1-Allyl-2-(4-ethoxyphenyl)-6-nitro-1H-benzodimidazole (4d). Yellow solid, mp 129–131 °C. IR (ν , cm^{-1}): 1610.6 (C=N), 1510.3 (C=C), 1330.9 (N=O), 1253.7 (C-O). ^1H NMR (500 MHz, DMSO- d_6 , δ ppm): 8.55 (1H, d, $J = 2.5$ Hz, H_{Ar}), 8.18 (1H, dd, $J = 9.0, 2.5$ Hz, H_{Ar}), 7.85 (1H, d, $J = 9.0$ Hz, H_{Ar}), 7.75 (2H, d, $J = 8.5$ Hz, H_{Ar}), 7.12 (2H, d, $J = 8.5$ Hz, H_{Ar}), 6.15–6.06 (1H, m, $-\text{CH}=\text{CH}_2$), 5.24 (1H, d, $J = 10.5$ Hz, $=\text{CH}_2$), 5.09 (2H, s, $-\text{CH}_2-$), 4.90 (1H, d, $J = 17.5$ Hz, $=\text{CH}_2$), 4.13 (2H, q, $J = 7.0$ Hz, $-\text{CH}_2-$), 1.38 (3H, t, $J = 7.0$ Hz, $-\text{CH}_3$). ^{13}C NMR (125 MHz, DMSO- d_6 , δ ppm): 160.4, 158.0, 147.2, 142.5, 140.3, 133.1, 130.7 (2C), 120.9, 119.1, 117.9, 116.8, 114.9 (2C), 111.3, 63.4, 47.0, 14.5. LC-MS (m/z) [$\text{M} + \text{H}$] $^+$ calcd for $\text{C}_{18}\text{H}_{18}\text{N}_3\text{O}_3$ 324.1343, found 324.1301.

1-Allyl-2-(4-fluorophenyl)-6-nitro-1H-benzodimidazole (4e). Yellow solid, mp 211–213 °C. IR (ν , cm^{-1}): 1506.4 (C=N), 1448.5 (C=C), 1331.6 (N=O). ^1H NMR (500 MHz, DMSO- d_6 , δ ppm): 8.59 (1H, d, $J = 1.5$ Hz, H_{Ar}), 8.21 (1H, dd, $J = 9.0, 2.0$ Hz, H_{Ar}), 7.88 (2H, d, $J = 8.5$ Hz, H_{Ar}), 7.78 (1H, d, $J = 8.5$ Hz, H_{Ar}), 7.44 (2H, d, $J = 8.5$ Hz, H_{Ar}), 6.12–6.04 (1H, m, $-\text{CH}=\text{CH}_2$), 5.23 (1H, d, $J = 10.5$ Hz, $=\text{CH}_2$), 5.05 (2H, s, $-\text{CH}_2-$), 4.90 (1H, d, $J = 17.5$ Hz, $=\text{CH}_2$). ^{13}C NMR (125 MHz, DMSO- d_6 , δ ppm): 162.4, 157.1, 146.9, 142.9, 135.2, 133.0, 131.7 (2C), 125.5, 119.5, 118.2, 117.0, 116.9, 116.2 (2C), 115.3, 111.7, 47.0. LC-MS (m/z) [$\text{M} + \text{H}$] $^+$ calcd for $\text{C}_{16}\text{H}_{13}\text{FN}_3\text{O}_2$ 298.0986, found 298.0972.

4-(1-Allyl-6-nitro-1H-benzodimidazole-2-yl)-N,N-dimethylamine (4f). Red solid, mp 170–172 °C. IR (ν , cm^{-1}): 1611.7 (C=N), 1458.2 (C=C), 1323.2 (N=O). ^1H NMR (500 MHz, DMSO- d_6 , δ ppm): 8.51 (1H, d, $J = 2.0$ Hz, H_{Ar}), 8.14 (1H, dd, $J = 9.0, 2.5$ Hz,



H_{Ar}), 7.80 (1H, d, $J = 9.0$ Hz, H_{Ar}), 7.67 (2H, d, $J = 8.5$ Hz, H_{Ar}), 6.86 (2H, d, $J = 8.5$ Hz, H_{Ar}), 6.18–6.09 (1H, m, $-CH=$), 5.24 (1H, d, $J = 10.5$ Hz, $=CH_2$), 5.04 (2H, m, $-CH_2-$), 4.93 (1H, d, $J = 17.0$ Hz, $=CH_2$), 3.01 (6H, s, $-CH_3$). ^{13}C NMR (125 MHz, DMSO- d_6 , δ ppm): 158.9, 151.6, 147.6, 142.9, 140.6, 135.5, 130.1 (2C), 118.5, 116.7, 115.3, 114.4, 111.7 (2C), 111.0, 47.1, 41.5 (2C). LC-MS (m/z) [$M + H$] $^+$ calcd for $C_{18}H_{19}N_4O_2$ 323.1503, found 323.1437.

1-(4-Chlorobenzyl)-2-(3,4-dichlorophenyl)-6-nitro-1H-benzimidazole (4g). Yellow solid, mp 190–192 °C. IR (ν , cm^{-1}): 1516.1 (C=N), 1438.9 (C=C), 1332.8 (N=O), 734.9 (C-Cl). 1H NMR (500 MHz, DMSO- d_6 , δ ppm): 8.61 (1H, d, $J = 2.5$ Hz, H_{Ar}), 8.20 (1H, dd, $J = 9.0, 2.5$ Hz, H_{Ar}), 8.00 (1H, d, $J = 2.0$ Hz, H_{Ar}), 7.96 (1H, d, $J = 9.0$ Hz, H_{Ar}), 7.83 (1H, d, $J = 8.5$ Hz, H_{Ar}), 7.73 (1H, dd, $J = 8.5, 2.0$ Hz, H_{Ar}), 7.37–7.35 (2H, m, H_{Ar}), 7.04 (2H, d, $J = 8.5$ Hz, H_{Ar}), 5.78 (2H, s, $-CH_2-$). ^{13}C NMR (125 MHz, DMSO- d_6 , δ ppm): 152.9, 142.4, 135.8, 134.2, 133.0, 130.7, 129.4, 131.1, 129.5, 129.0 (2C), 128.2 (2C), 126.6, 127.1, 122.8, 120.5, 118.2, 112.1, 46.9. LC-MS (m/z) [$M - H$] $^-$ calcd for $C_{20}H_{11}Cl_3N_3O_2$ 429.9922, found 429.9852.

1-(4-Chlorobenzyl)-2-(3,4-dimethoxyphenyl)-6-nitro-1H-benzimidazole (4h). Yellow solid, mp 145–146 °C. IR (ν , cm^{-1}): 1517.8 (C=N), 1450.4 (C=C), 1334.7 (N=O), 740.2 (C-Cl). 1H NMR (500 MHz, DMSO- d_6 , δ ppm): 8.60 (1H, d, $J = 2.0$ Hz, H_{Ar}), 8.17 (1H, dd, $J = 9.0, 2.5$ Hz, H_{Ar}), 7.72 (1H, d, $J = 9.0$ Hz, H_{Ar}), 7.39–7.37 (2H, m, H_{Ar}), 7.29 (2H, m, H_{Ar}), 7.12 (1H, d, $J = 9.0$ Hz, H_{Ar}), 7.06 (2H, d, $J = 8.5$ Hz, H_{Ar}), 5.69 (2H, s, $-CH_2-$), 3.82 (3H, s, $-OCH_3$), 3.70 (3H, s, $-OCH_3$). ^{13}C NMR (125 MHz, DMSO- d_6 , δ ppm): 154.7, 150.4, 148.9, 142.1, 137.2, 136.5, 128.9 (2C), 127.6 (2C), 127.0, 126.1, 123.5, 122.5, 121.4, 120.8, 112.9, 111.6, 110.5, 55.7, 55.5, 47.8. LC-MS (m/z) [$M - H$] $^-$ calcd for $C_{22}H_{17}ClN_3O_4$ 422.0913, found 422.0811; [$M + H$] $^+$ calcd for $C_{22}H_{19}ClN_3O_4$ 424.1059, found 424.1087.

4-(1-(4-Chlorobenzyl)-6-nitro-1H-benzimidazole-2-yl)-2-ethoxyphenol (4i). Yellow solid, mp 150–152 °C. IR (ν , cm^{-1}): 1519.0 (C=N), 1451.6 (C=C), 1334.5 (N=O), 739.5 (C-Cl). 1H NMR (500 MHz, DMSO- d_6 , δ ppm): 8.66 (1H, d, $J = 2.0$ Hz, H_{Ar}), 8.18 (1H, dd, $J = 8.0, 2.5$ Hz, H_{Ar}), 7.75 (1H, d, $J = 8.0$ Hz, H_{Ar}), 7.46 (1H, dd, $J = 9.0, 2.0$ Hz, H_{Ar}), 7.37 (2H, d, $J = 8.5$ Hz, H_{Ar}), 7.26 (1H, d, $J = 2.0$ Hz, H_{Ar}), 7.18 (1H, d, $J = 9.0$ Hz, H_{Ar}), 7.03 (2H, d, $J = 8.5$ Hz, H_{Ar}), 5.68 (2H, s, $-CH_2-$), 3.95 (2H, q, $J = 7.0$ Hz, $-CH_2-$), 1.27 (3H, t, $J = 7.0$ Hz, $-CH_3$). ^{13}C NMR (125 MHz, DMSO- d_6 , δ ppm): 153.6, 151.2, 149.1, 143.6, 137.4, 136.3, 129.1, 127.8 (2C), 127.0 (2C), 126.5, 123.2, 122.7, 121.6, 120.4, 112.5, 111.8, 110.9, 55.6, 47.7, 14.8. LC-MS (m/z) [$M - H$] $^-$ calcd for $C_{22}H_{17}ClN_3O_4$ 422.0913, found 422.0915.

3-(1-(4-Chlorobenzyl)-6-nitro-1H-benzimidazole-2-yl)phenol (4j). Yellow solid, mp 212–213 °C. IR (ν , cm^{-1}): 1522.4 (C=N), 1454.8 (C=C), 1351.7 (N=O), 737.1 (C-Cl). 1H NMR (500 MHz, DMSO- d_6 , δ ppm): 9.86 (1H, s, $-OH$), 8.62 (1H, d, $J = 2.0$ Hz, H_{Ar}), 8.18 (1H, dd, $J = 9.0, 2.0$ Hz, H_{Ar}), 7.70 (1H, d, $J = 9.0$ Hz, H_{Ar}), 7.37 (2H, d, $J = 8.5$ Hz, H_{Ar}), 7.35 (1H, d, $J = 8.0$ Hz, H_{Ar}), 7.14 (1H, d, $J = 1.5$ Hz, H_{Ar}), 7.13 (1H, d, $J = 8.0$ Hz, H_{Ar}), 7.03 (2H, d, $J = 8.5$ Hz, H_{Ar}), 6.98 (1H, dd, $J = 9.0, 1.5$ Hz, H_{Ar}), 5.66 (2H, s, $-CH_2-$). ^{13}C NMR (125 MHz, DMSO- d_6 , δ ppm): 157.9, 152.7, 142.5, 135.6, 134.5, 133.1, 131.3, 130.6, 129.8, 129.1, 128.5 (2C),

127.5 (2C), 126.8, 123.2, 120.8, 118.4, 111.7, 46.8. LC-MS (m/z) [$M - H$] $^-$ calcd for $C_{20}H_{13}ClN_3O_3$ 378.0651, found 378.0595.

4-(1-(4-Chlorobenzyl)-6-nitro-1H-benzimidazole-2-yl)-N,N-dimethylaniline (4k). Red solid, mp 169–171 °C. IR (ν , cm^{-1}): 1536.9 (C=N), 1457.3 (C=C), 1352.5 (N=O), 740.6 (C-Cl). 1H NMR (500 MHz, DMSO- d_6 , δ ppm): 8.54 (1H, d, $J = 2.5$ Hz, H_{Ar}), 8.12 (1H, dd, $J = 9.0, 2.0$ Hz, H_{Ar}), 7.64 (1H, d, $J = 9.0$ Hz, H_{Ar}), 7.60 (2H, d, $J = 9.0$ Hz, H_{Ar}), 7.39 (2H, d, $J = 9.0$ Hz, H_{Ar}), 7.05 (2H, d, $J = 8.5$ Hz, H_{Ar}), 6.81 (2H, d, $J = 9.0$ Hz, H_{Ar}), 5.68 (2H, s, $-CH_2-$), 2.98 (6H, s, $-CH_3$). ^{13}C NMR (125 MHz, DMSO- d_6 , δ ppm): 155.0, 150.9, 141.5, 136.6, 126.4, 129.5 (2C), 128.4 (2C), 127.1 (2C), 126.0, 125.6, 121.8, 119.5, 116.2, 111.4 (2C), 110.1, 47.4, 39.3 (2C). LC-MS (m/z) [$M + H$] $^+$ calcd for $C_{22}H_{20}ClN_4O_2$ 407.1269, found 407.1198.

Ethyl 2-(2-(4-chlorophenyl)-6-nitro-1H-benzimidazole-1-yl)acetate (4l). Yellow solid, mp 272–274 °C. IR (ν , cm^{-1}): 1737.9 (C=O), 1518.0 (C=N), 1448.5 (C=C), 1329.0 (N=O), 733.0 (C-Cl). 1H NMR (500 MHz, DMSO- d_6 , δ ppm): 8.78 (1H, d, $J = 2.0$ Hz, H_{Ar}), 8.25 (1H, dd, $J = 9.0, 2.5$ Hz, H_{Ar}), 7.92 (1H, d, $J = 9.0$ Hz, H_{Ar}), 7.78 (2H, d, $J = 8.5$ Hz, H_{Ar}), 7.68 (2H, d, $J = 8.5$ Hz, H_{Ar}), 5.44 (2H, s, $-CH_2-$), 4.11 (2H, q, $J = 7.0$ Hz, $-CH_2-$), 1.12 (3H, t, $J = 7.0$ Hz, $-CH_3$). ^{13}C NMR (125 MHz, DMSO- d_6 , δ ppm): 166.8, 152.3, 145.9, 144.5, 139.6, 138.4, 133.8, 128.7 (2C), 126.1 (2C), 122.6, 119.1, 116.5, 62.5, 47.8, 14.6. LC-MS (m/z) [$M + H$] $^+$ calcd for $C_{17}H_{15}ClN_3O_4$ 360.0746, found 360.0747.

Ethyl 2-(2-(4-(dimethylamino)phenyl)-6-nitro-1H-benzimidazole-1-yl)acetate (4m). Yellow solid, mp 162–163 °C. IR (ν , cm^{-1}): 1741.7 (C=O), 1606.7 (C=N), 1434.6 (C=C), 1325.1 (N=O). 1H NMR (500 MHz, DMSO- d_6 , δ ppm): 8.78 (1H, d, $J = 2.0$ Hz, H_{Ar}), 8.24 (1H, dd, $J = 9.0, 2.5$ Hz, H_{Ar}), 7.91 (1H, d, $J = 9.0$ Hz, H_{Ar}), 7.77 (2H, d, $J = 8.5$ Hz, H_{Ar}), 7.69 (2H, d, $J = 8.5$ Hz, H_{Ar}), 5.38 (2H, s, $-CH_2-$), 4.12 (2H, q, $J = 7.0$ Hz, $-CH_2-$), 1.12 (3H, t, $J = 7.0$ Hz, $-CH_3$). ^{13}C NMR (125 MHz, DMSO- d_6 , δ ppm): 167.0, 152.7, 150.8, 143.2, 139.5, 138.1, 132.6, 127.5 (2C), 124.9, 121.6, 117.2, 112.4 (2C), 62.3, 47.6, 39.5 (2C), 14.5. LC-MS (m/z) [$M - H$] $^-$ calcd for $C_{19}H_{19}N_4O_4$ 367.1412, found 367.1332; [$M + H$] $^+$ calcd for $C_{19}H_{21}N_4O_4$ 369.1557, found 369.1457.

Ethyl 2-(2-(4-fluorophenyl)-6-nitro-1H-benzimidazole-1-yl)acetate (4n). Yellow solid, mp 178–179 °C. IR (ν , cm^{-1}): 1737.9 (C=O), 1519.9 (C=N), 1375.3 (C=C), 1217.1 (N=O), 1153.4 (C-F). 1H NMR (500 MHz, DMSO- d_6 , δ ppm): 8.80 (1H, d, $J = 2.5$ Hz, H_{Ar}), 8.25 (1H, dd, $J = 9.0, 2.5$ Hz, H_{Ar}), 7.93 (1H, d, $J = 9.0$ Hz, H_{Ar}), 7.82 (2H, d, $J = 8.5$ Hz, H_{Ar}), 7.46 (2H, d, $J = 8.5$ Hz, H_{Ar}), 5.45 (2H, s, $-CH_2-$), 4.11 (2H, q, $J = 7.0$ Hz, $-CH_2-$), 1.12 (3H, t, $J = 7.0$ Hz, $-CH_3$). ^{13}C NMR (125 MHz, DMSO- d_6 , δ ppm): 166.9, 164.6, 162.5, 146.8, 142.5, 129.7, 129.2 (2C), 125.5, 119.6, 118.0, 117.2, 116.5, 116.4 (2C), 115.2, 62.2, 47.3, 14.6. LC-MS (m/z) [$M - H$] $^-$ calcd for $C_{17}H_{13}FN_3O_4$ 342.0896, found 342.0811; [$M + H$] $^+$ calcd for $C_{17}H_{15}FN_3O_4$ 344.1041, found 344.0937.

Ethyl 2-(2-(3-(2-ethoxy-2-oxoethoxy)-4-methoxyphenyl)-6-nitro-1H-benzimidazole-1-yl)acetate (4o). Yellow solid, mp 117–118 °C. IR (ν , cm^{-1}): 1766.8 and 1737.9 (C=O), 1603.2 (C=N), 1439.8 (C=C), 1330.9 (N=O), 1251.8 (C-O). 1H NMR (500 MHz, DMSO- d_6 , δ ppm): 8.75 (1H, d, $J = 2.0$ Hz, H_{Ar}), 8.22 (1H, dd, $J = 9.0, 2.0$ Hz, H_{Ar}), 7.88 (1H, d, $J = 9.0$ Hz, H_{Ar}), 7.37 (1H, dd, $J = 8.0, 2.0$ Hz, H_{Ar}), 7.28 (1H, d, $J = 2.0$ Hz, H_{Ar}), 7.23 (1H, d, $J = 8.0$ Hz, H_{Ar}), 5.42 (2H, s, $-CH_2-$), 5.34 (2H, s, $-CH_2-$), 4.20–4.12



(4H, m, $-\text{CH}_2-$), 3.89 (3H, s, $-\text{OCH}_3$), 1.24–1.15 (6H, m, $-\text{CH}_3$). ^{13}C NMR (125 MHz, $\text{DMSO}-d_6$, δ ppm): 169.1, 166.8, 153.8, 149.6, 147.5, 144.3, 135.5, 129.5, 126.4, 122.1, 121.0, 120.3, 118.2, 115.8, 112.5, 65.6, 61.3, 61.0, 56.5, 47.4, 14.5, 14.3. LC-MS (m/z) $[\text{M} - \text{H}]^-$ calcd for $\text{C}_{22}\text{H}_{22}\text{N}_3\text{O}_8$ 456.1412, found 456.1298; $[\text{M} + \text{H}]^+$ calcd for $\text{C}_{22}\text{H}_{24}\text{N}_3\text{O}_8$ 458.1558, found 458.1457.

1-Allyl-2-(furan-2-yl)-6-nitro-1H-benzofurazolidine (4p). Brown solid, mp 168–170 °C. IR (ν , cm^{-1}): 1606.7 (C=N), 1510.3 (C=C), 1351.8 (N=O), 1282.6 (C-O). ^1H NMR (500 MHz, $\text{DMSO}-d_6$, δ ppm): 8.60 (1H, d, $J = 2.0$ Hz, H_{Ar}), 8.19 (1H, dd, $J = 9.0, 2.0$ Hz, H_{Ar}), 8.06 (1H, d, $J = 1.0$ Hz, H_{Ar}), 7.83 (1H, d, $J = 9.0$ Hz, H_{Ar}), 7.37 (1H, d, $J = 3.5$ Hz, H_{Ar}), 6.81 (1H, d, $J = 3.0$ Hz, H_{Ar}), 6.13–6.07 (1H, m, $-\text{CH}=\text{CH}_2$), 5.30 (2H, s, $-\text{CH}_2-$), 5.18 (1H, d, $J = 10.0$ Hz, $=\text{CH}_2$), 4.93 (1H, d, $J = 17.0$ Hz, $=\text{CH}_2$). ^{13}C NMR (125 MHz, $\text{DMSO}-d_6$, δ ppm): 148.2, 147.2, 143.7, 141.7, 134.9, 132.9, 119.2, 116.9, 115.0, 114.4, 112.5, 111.2, 107.6, 47.0. LC-MS (m/z) $[\text{M} + \text{H}]^+$ calcd for $\text{C}_{14}\text{H}_{12}\text{N}_3\text{O}_3$ 270.0873, found 270.0815.

1-(4-Chlorobenzyl)-2-(furan-2-yl)-6-nitro-1H-benzofurazolidine (4q). Yellow solid, mp 168–170 °C. IR (ν , cm^{-1}): 1532.4 (C=N), 1455.7 (C=C), 1349.8 (N=O), 742.0 (C-Cl). ^1H NMR (500 MHz, $\text{DMSO}-d_6$, δ ppm): 8.57 (1H, d, $J = 2.0$ Hz, H_{Ar}), 8.19 (1H, dd, $J = 8.5, 2.0$ Hz, H_{Ar}), 7.99 (1H, d, $J = 1.5$ Hz, H_{Ar}), 7.85 (1H, d, $J = 9.0$ Hz, H_{Ar}), 7.37 (2H, d, $J = 8.5$ Hz, H_{Ar}), 7.30 (1H, dd, $J = 4.0, 1.0$ Hz, H_{Ar}), 7.13 (2H, d, $J = 8.5$ Hz, H_{Ar}), 6.76 (1H, dd, $J = 3.5, 2.0$ Hz, H_{Ar}), 5.90 (2H, s, $-\text{CH}_2-$). ^{13}C NMR (125 MHz, $\text{DMSO}-d_6$, δ ppm): 152.2, 148.5, 143.8, 141.3, 136.7, 135.8, 135.0, 133.2, 130.4 (2C), 127.2 (2C), 123.5, 123.1, 121.2, 116.8, 111.5, 46.8. LC-MS (m/z) $[\text{M} - \text{H}]^-$ calcd for $\text{C}_{18}\text{H}_{11}\text{ClN}_3\text{O}_3$ 352.0494, found 352.0427; $[\text{M} + \text{H}]^+$ calcd for $\text{C}_{18}\text{H}_{13}\text{ClN}_3\text{O}_3$ 354.0640, found 354.0699.

Ethyl 2-(2-(furan-2-yl)-6-nitro-1H-benzofurazolidine-1-yl)acetate (4r). Brown solid, mp 136–137 °C. IR (ν , cm^{-1}): 1745.6 (C=O), 1508.3 (C=N), 1435.0 (C=C), 1329.0 (N=O). ^1H NMR (500 MHz, $\text{DMSO}-d_6$, δ ppm): 8.54 (1H, d, $J = 1.5$ Hz, H_{Ar}), 8.21 (1H, dd, $J = 9.0, 2.5$ Hz, H_{Ar}), 8.02 (1H, s, H_{Ar}), 7.95 (1H, d, $J = 9.0$ Hz, H_{Ar}), 7.36 (1H, d, $J = 3.5$ Hz, H_{Ar}), 6.80 (1H, d, $J = 2.0$ Hz, H_{Ar}), 5.56 (2H, s, $-\text{CH}_2-$), 4.18 (2H, q, $J = 7.0$ Hz, $-\text{CH}_2-$), 1.19 (3H, t, $J = 7.0$ Hz, $-\text{CH}_3$). ^{13}C NMR (125 MHz, $\text{DMSO}-d_6$, δ ppm): 166.5, 147.5, 145.8, 144.9, 135.6, 133.4, 130.5, 127.3, 122.2, 119.8, 113.7, 113.5, 61.6, 47.8, 14.5. LC-MS (m/z) $[\text{M} + \text{H}]^+$ calcd for $\text{C}_{15}\text{H}_{14}\text{N}_3\text{O}_5$ 316.0928, found 316.0814.

4.3. *In vitro* antibacterial and antifungal activities

The minimum inhibitory concentration of the test compounds (MIC) was determined by the micro-broth dilution technique using nutrient broth.²⁸ All bacterial strains were maintained on nutrient agar medium at ± 37 °C, and fungal strains were maintained on potato dextrose agar at ± 25 °C. Serial twofold dilutions ranging from 1024 to 2 $\mu\text{g mL}^{-1}$ were prepared in media. The inoculum was prepared using a 4–6 h old broth culture of each bacteria and fungi and diluted in broth media to give a final concentration of 5×10^5 CFU mL^{-1} in the test tray. The trays were covered and placed in plastic bags to prevent evaporation and are incubated at 35 °C for 18–20 h with the bacteria, and the fungal culture was incubated at 25 °C for 72 h. All determinations were done in triplicates. Ciprofloxacin and

fluconazole were used as the positive control for antibacterial and antifungal activities, respectively. The MIC was defined as the lowest concentration of the compound giving complete inhibition of visible growth.

4.4. *In vitro* anticancer activity

The cytotoxic activity of the synthesized compounds was evaluated against the human hepatocyte carcinoma cell line (HepG2), human breast adenocarcinoma cell line (MDA-MB-231), human breast cancer cell line (MCF7), human rhabdomyosarcoma cell line (RMS), and colon carcinoma cell line (C26) using the methyl thiazolyl tetrazolium (MTT) method conducted according to the MTT assay protocol. Paclitaxel was used as the positive control. The assay detects the reduction of yellow tetrazolium (MTT) by metabolically active cells to be purple formazan measured using spectrophotometry.³⁴

The cells lines were seeded into 96-well plates at a density of 5000 cells per well, replenished with growth media consisting of Eagle's Minimum Essential Medium (EMEM), 10% Fetal Calf Serum (FCS), 2 mM L-glutamine, 100 IU mL^{-1} penicillin, 100 $\mu\text{g mL}^{-1}$ streptomycin. The cells were incubated at 37 °C in 5% CO_2 for 24 h. Then, a series of concentrations of the tested compounds and paclitaxel in DMSO was added to each well of the plate and incubated for 48 h. After that, 10 μL fresh solution of MTT reagent was added to each well, and the plate was incubated in a CO_2 incubator at 37 °C for 4 h. After the purple precipitate was obtained, the cells were dissolved in ethanol and their optical density was recorded at 570 nm. The experiment was performed on 6 wells for a concentration of the test sample and conducted in parallel with the control DMSO at the same concentration. The percent of proliferation inhibition was calculated using the following formula:

$$\text{Viability cells inhibition}(\%) = 100 - \left[\frac{(A_t - A_b)}{(A_c - A_b)} \right] \times 100\%$$

A_t = absorption of test compound, A_b = absorption of blank, A_c = absorption of control.

4.5. ADME-Tox predictions

The physicochemical properties were calculated using ChemBio3D (ChemBioOffice Ultra 18.0 suite). *In silico* prediction of the ADME properties (absorption, distribution, metabolism, and excretion) and the toxicity risks (mutagenicity, tumorigenicity, irritation, and reproduction) was performed using ADMETlab 2.0 descriptors algorithm protocol and SwissADME web tool.⁴⁵

4.6. *In silico* molecular docking studies

The structure of ligand molecules and the standards were drawn in ChemBioDraw Ultra 19.0. The energy of each molecule was minimized using ChemBio3D Ultra 19.0. The ligand molecules with minimized energy were then used as input for AutoDock Vina, in order to carry out the docking simulation. The ligand molecules with minimized energy were then used as input for AutoDock Vina, in order to carry out the docking



Table 6 Targets for *in silico* molecular docking studies

Entry	Target	Symbol	PDB ID	Organism	Expression system
1	Dihydrofolate reductase	DHFR-B	3FYV	<i>Staphylococcus aureus</i>	<i>Escherichia coli</i>
2	Dihydrofolate reductase	DHFR-F	4HOF	<i>Candida albicans</i>	<i>Escherichia coli</i> BL21 (DE3)
3	<i>N</i> -Myristoyl transferase	NMT	1IYL	<i>Candida albicans</i>	<i>Escherichia coli</i>
4	Gyrase B	GyrB	4URM	<i>Staphylococcus aureus</i>	<i>Escherichia coli</i> BL21 (DE3)
5	Vascular endothelial growth factor receptor 2	VEGFR-2	5EW3	<i>Homo sapiens</i>	<i>Spodoptera frugiperda</i>
6	Fibroblast growth factor receptor 1	FGFR-1	5A46	<i>Homo sapiens</i>	<i>Escherichia coli</i>
7	Histone deacetylase 6	HDAC6	5EEF	<i>Danio rerio</i>	<i>Escherichia coli</i> BL21 (DE3)

simulation.²⁹ Protein molecules of dihydrofolate reductase, *N*-myristoyl transferase, gyrase B, vascular endothelial growth factor receptor 2, fibroblast growth factor receptor 1, and histone deacetylase 6 were retrieved from the protein data bank (Table 6). These protein molecules were retrieved from the protein data bank. The receptors were removed all the water molecules and added only polar hydrogen and Kollman charges. The Graphical User Interface program BMGL Tools was used to set the grid box for docking simulations. The compounds or commercial drugs were docked with the target in order to determine the docking parameters with the help of Grid-based ligand docking. Auto Dock Vina was compiled and run under Windows 10.0 Professional operating system. Discovery Studio 2021 was used to deduce the pictorial representation of the interaction between the ligands and the target protein.

4.7. Statistical analysis

All values are expressed in Mean \pm SEM (Standard Error of Mean). The difference in IC₅₀ value between tested compounds and paclitaxel was analyzed by one-way analysis of variance (ANOVA) with Tukey's Honestly Significant Difference (Tukey HSD) post hoc test using Minitab 18.0 software. The results were considered statistically significant if $p < 0.05$. The chart is drawn using Microsoft Excel 2019 software.

Author contributions

Em Canh Pham: conceptualization, methodology, investigation, data curation, supervision, writing-original draft preparation, writing – review & editing. Tuong Vi Thi Le: investigation, software. Tuyen Ngoc Truong: data curation, supervision, writing-original draft preparation, writing – review & editing.

Conflicts of interest

The authors declare that they have no known competing financial interests or personal relationships that could have appeared to influence the work reported in this paper.

References

- M. F. Brana, J. M. Castellano, G. Keilhauer, A. Machuca, Y. Martin, C. Redondo, E. Schlick and N. Walker, *Anticancer Drug Des.*, 1994, **9**, 527–538.

- H. M. Refaat, *Eur. J. Med. Chem.*, 2010, **45**, 2949–2956.
- B. T. Buu Hue, H. T. Kim Quy, W. K. Oh, V. D. Duy, C. N. Tram Yen, T. T. Kim Cuc, P. C. Em, T. P. Thao, T. T. Loan and M. V. Hieu, *Tetrahedron Lett.*, 2016, **57**, 887–891.
- T. H. Kim Chi, T. N. Hong An, T. N. Cam Thu and T. H. Kim Dung, *RSC Adv.*, 2020, **10**, 20543.
- M. Tunçbilek, T. Kiper and N. Altanlar, *Eur. J. Med. Chem.*, 2009, **44**, 1024–1033.
- H. Z. Zhang, G. L. Damu, G. X. Cai and C. H. Zhou, *Eur. J. Med. Chem.*, 2013, **64**, 329–344.
- S. Malasala, M. N. Ahmad, R. Akunuri, M. Shukla, G. Kaul, A. Dasgupta, Y. V. Madhavi, S. Chopra and S. Nanduri, *Eur. J. Med. Chem.*, 2021, **212**, 112996.
- K. C. Achar, K. M. Hosamani and H. R. Seetharamareddy, *Eur. J. Med. Chem.*, 2010, **45**, 2048–2054.
- N. Pribut, A. E. Basson, W. A. L. van Otterlo, D. C. Liotta and S. C. Pelly, *ACS Med. Chem. Lett.*, 2019, **10**, 196–202.
- M. C. Sharma, D. V. Kohli and S. Sharma, *Int. J. Drug Delivery*, 2010, **2**, 228–237.
- D. C. Cole, J. L. Gross, T. A. Comery, S. Aschmies, W. D. Hirst, C. Kelley, J. I. Kim, K. Kubek, X. Ning, B. J. Platt, A. J. Robichaud, W. R. Solvibile, J. R. Stock, G. Tawa, M. J. Williams and J. W. Ellingboe, *Bioorg. Med. Chem. Lett.*, 2010, **20**, 1237–1240.
- G. Surineni, Y. Gao, M. Hussain, Z. Liu, Z. Lu, C. Chhotaray, M. M. Islam, H. M. A. Hameed and T. Zhang, *Medchemcomm*, 2019, **10**, 49–60.
- L. Welage and R. Berardi, *J. Am. Pharm. Assoc.*, 2000, **40**, 52.
- B. G. Mohamed, A. A. Abdel-Alim and M. A. Hussein, *Acta Pharm.*, 2006, **56**, 31–48.
- M. Ouattara, D. Sissouma, M. W. Koné, H. E. Menan, S. A. Touré and L. Ouattara, *Trop. J. Pharm. Res.*, 2011, **10**, 767–775.
- D. Valdez-Padilla, S. Rodriguez-Morales, A. Hernandez-Campos, F. Hernandez-Luis, L. Yépez-Mulia, A. Tapia-Contreras and R. Castillo, *Bioorg. Med. Chem.*, 2009, **17**, 1724–1730.
- N. Bharti, M. T. Shailendra, G. Garza, D. E. Cruz-Vega, J. Catro-Garza, K. Saleem, F. Naqvi, M. R. Maurya and A. Azam, *Bioorg. Med. Chem. Lett.*, 2002, **12**, 869–871.
- B. Bhriugu, N. Siddiqui, D. Pathak, M. S. Alam, R. Ali and B. Azad, *Acta Pol. Pharm.*, 2012, **69**, 53–62.
- J. Valdez, R. Cedillo, A. Hernández-Campos, L. Yépez, F. Hernández-Luis, G. Navarrete-Vázquez, A. Tapia,



- R. Cortés, M. Hernández and R. Castillo, *Bioorg. Med. Chem. Lett.*, 2002, **12**, 2221–2224.
- 20 S. Tahlan, K. Ramasamy, S. M. Lim, S. A. A. Shah, V. Mani and B. Narasimhan, *BMC Chem.*, 2019, **13**, 12.
- 21 D. Hao, J. D. Rizzo, S. Stringer, R. V. Moore, J. Marty, D. L. Dexter, G. L. Mangold, J. B. Camden, D. D. Von Hoff and S. D. Weitman, *Invest. New Drugs*, 2002, **20**, 261–270.
- 22 H. Joensuu, J. Y. Blay, A. Comandone, J. Martin-Broto, E. Fumagalli, G. Grignani, X. G. Del Muro, A. Adenis, C. Valverde, A. L. Pousa, O. Bouché, A. Italiano, S. Bauer, C. Barone, C. Weiss, S. Crippa, M. Camozzi, R. Castellana and A. Le Cesne, *Br. J. Cancer*, 2017, **117**, 1278–1285.
- 23 C. Y. Hsieh, P. W. Ko, Y. J. Chang, M. Kapoor, Y. C. Liang, H. H. Lin, J. C. Horng and M. H. Hsu, *Molecules*, 2019, **24**, 3259.
- 24 G. Mariappan, R. Hazarika, F. Alam, R. Karki, U. Patangia and S. Nath, *Arabian J. Chem.*, 2015, **8**, 715–719.
- 25 P. Boggu, E. Venkateswararao, M. Manickam, D. Kwak, Y. Kim and S. H. Jung, *Bioorg. Med. Chem.*, 2016, **24**, 1872–1878.
- 26 D. R. Gund, A. P. Tripathi and S. D. Vaidya, *Eur. J. Chem.*, 2017, **8**, 149–154.
- 27 E. M. E. Dokla, N. S. Abutaleb, S. N. Milik, D. Li, K. El-Baz, M. W. Shalaby, R. Al-Karaki, M. Nasr, C. D. Klein, K. A. M. Abouzid and M. N. Seleem, *Eur. J. Med. Chem.*, 2020, **186**, 111850.
- 28 P. C. Em, L. T. Tuong Vi, T. P. Long, T. N. Huong-Giang, N. B. L. Khanh and N. T. Tuyen, *Arabian J. Chem.*, 2022, **15**, 103682.
- 29 P. C. Em, V. V. Lenh, V. N. Cuong, N. D. Ngoc Thoi, L. T. Tuong Vi and N. T. Tuyen, *Biomed. Pharmacother.*, 2022, **146**, 112611.
- 30 P. Singla, V. Luxami and K. Paul, *J. Photochem. Photobiol., B*, 2017, **168**, 156–164.
- 31 S. B. Nabuurs, M. Wagener and J. de Vlieg, *J. Med. Chem.*, 2007, **50**, 6507–6518.
- 32 S. M. Rizvi, S. Shakil and M. Haneef, *EXCLI J.*, 2013, **12**, 831–857.
- 33 N. El-Hachem, B. Haibe-Kains, A. Khalil, F. H. Kobeissy and G. Nemer, *Methods Mol. Biol.*, 2017, **1598**, 391–403.
- 34 P. C. Em, T. N. Tuyen, D. H. Nguyen, V. D. Duy and D. T. Hong Tuoi, *Med. Chem.*, 2022, **18**, 558–573.
- 35 M. Congreve, R. Carr, C. Murray and H. Jhoti, *Drug Discovery Today*, 2003, **8**, 876–877.
- 36 C. A. Lipinski, *Drug Discovery Today: Technol.*, 2004, **1**, 337–341.
- 37 M. M. Morcoss, E. S. M. N. Abdelhafez, R. A. Ibrahim, H. M. Abdel-Rahman, M. Abdel-Aziz and D. A. Abou El-Ella, *Bioorg. Chem.*, 2020, **101**, 103956.
- 38 Y. Keng Yoon, M. Ashraf Ali, T. S. Choon, R. Ismail, A. Chee Wei, R. Suresh Kumar, H. Osman and F. Beevi, *BioMed Res. Int.*, 2013, **2013**, 926309.
- 39 L. Shi, T. T. Wu, Z. Wang, J. Y. Xue and Y. G. Xu, *Bioorg. Med. Chem.*, 2014, **22**, 4735–4744.
- 40 L. V. Nayak, B. Nagaseshadri, M. V. P. S. Vishnuvardhan and A. Kamal, *Bioorg. Med. Chem. Lett.*, 2016, **26**, 3313–3317.
- 41 Y. K. Yoon, M. A. Ali, A. C. Wei, A. N. Shirazi, K. Parang and T. S. Choon, *Eur. J. Med. Chem.*, 2014, **83**, 448–454.
- 42 J. Zhang, D. Yao, Y. Jiang, J. Huang, S. Yang and J. Wang, *Bioorg. Chem.*, 2017, **72**, 168–181.
- 43 N. S. Goud, S. M. Ghouse, J. Vishnu, D. Komal, V. Talla, R. Alvala, J. Pranay, J. Kumar, I. A. Qureshi and M. Alvala, *Bioorg. Chem.*, 2019, **89**, 103016.
- 44 U. Das, S. Kumar, J. R. Dimmock and R. K. Sharma, *Curr. Cancer Drug Targets*, 2012, **12**, 667–692.
- 45 G. Xiong, Z. Wu, J. Yi, L. Fu, Z. Yang, C. Hsieh, M. Yin, X. Zeng, C. Wu, A. Lu, X. Chen, T. Hou and D. Cao, *Nucleic Acids Res.*, 2021, **49**, W5–W14.

